University of Stavanger

Faculty of Science and Technology

BACHELOR`S THESIS

Study program/Specialization: Civil Engineering - Bachelor's Degree Programme	Spring semester, 2021 Open access
Writer: Daniel kvamme Yousef Bassam Tayyem	*Daniel Kvamme* .... (Writer's signature)
Faculty supervisor: Yanyan Sha External supervisor(s): Yanyan Sha	
Thesis title: Investigation on The Mechanical Properties of CO_2 Cured Concrete with Natural Aggregates.	
Credits (ECTS): 20	
Keywords: Accelerated carbonation curing; Different Water-Cement Ratio; Mechanical Properties; CO_2 Uptake; Density; Porosity; pH.	Pages: ………83… + enclosure: …...26… Stavanger, …14.05.2021… Date/year

Frontpage for bachelor thesis
Faculty of Science and Technology
Decision made by the Dean October 30th 2009

Abstract

Concrete production is one of the leading industry emitters of CO_2 in the world. A small reduction in CO_2 released into the atmosphere during production could therefore be highly beneficial in reducing the carbon footprint from the industry in general. Accelerated carbonation curing (ACC) is a new technique of concrete curing that forcibly diffuses CO_2 gas into freshly prepared concrete. This permits the CO_2 to be captured and stored in the concrete thus reducing the carbon footprint. It may also lead to economic benefits in terms of reduced a carbon tax. Previous researches in this field have found that ACC improved the mechanical properties and durability characteristics of CO_2 cured concrete, when compared to traditional methods such as water curing.

The main goal of this research is to investigate the mechanical properties and durability characteristics of CO_2 cured concrete with two different water-cement ratios of 0.4 and 0.6 of a total of 8 mixtures. ACC specimens are placed in a climate chamber for five to six hours of initial air pre-curing at a temperature of 25°C and a relative humidity of 60%, followed by 3 and 4 hours of CO_2 carbonation curing with respectively 4 and 6 bar CO_2 gas pressure with a 99% purity in an airtight carbonation chamber. ACC specimens are subjected to further water curing for 1 and 28 days, while reference specimens undergo the same initial pre-curing and the same water curing conditions as ACC specimens, without exposing them to CO_2 gas. The performance of ACC and water cured concrete specimens are evaluated in terms of compressive strength, density, porosity, pH level and weight gain.

Based on the results of this study, ACC specimens have shown an increase in compressive strength after 1 day of curing and a slight difference after 28 days of curing compared to their references. Such curing without any adverse impact on the properties of concrete can therefor be recommended for pre-casted concrete production, as an effective method to capture CO_2 during cement production and store it in the concrete rather than emitting it into the atmosphere.

Contents

List of Figures

List of Tables

List of Notations

$°C$ Degree celsius

μ Micro

A_c Cross-sectional area

ACC Accelerated Carbonation Curing

atm Atmospheric pressure

cm Centimeter

FA Fly ash

g Gram

$GGBS$ Ground granulated blast furnace slag

Kg Kilogram

kPa kilopascal

m Meter

m^3 Cubic meter

MK Metakaolin

mm Millimeter

mm^2 Square millimeter

MPa Megapascal

nm Nanometer

Npc	Normal portland cement
ppm	Parts Per Million
psi	Pounds per square inch
R/F	Reinforcement
RH	Relative humidity
RHA	Rice husk ash
SEM	Scanning electron microscopy
SF	Silica fume
V	Volume
w/c	Water to cement ratio
XDR	X-ray diffraction

Chapter 1

Introduction

1.1 Introduction

Global warming is the product of greenhouse gas pollution/emissions, especially CO_2 gas, which is a global issue and responsible for climate change. It is important to limit the increase in global temperature in order to preserve the planet. This can be done by limiting the amount of greenhouse gases caused by various human activities since the beginning of the Industrial Revolution. Global atmospheric carbon dioxide emissions have an annual increasing rate of about 100 times faster than the rate at the end of the last ice age. The levels of carbon dioxide in the atmosphere in 2019 was 409.8 ± 0.1 ppm which is an increase of 2.5 ± 0.1 ppm from 2018, when the global growth rate of CO_2 in the 1960s was approx. 0.6 ± 0.1 ppm per year (Lindsey 2020). Figure 1.1 shows that the amount of carbon dioxide in the atmosphere (raspberry line) has increased along with human emissions (blue line) since the start of the Industrial Revolution in 1750.
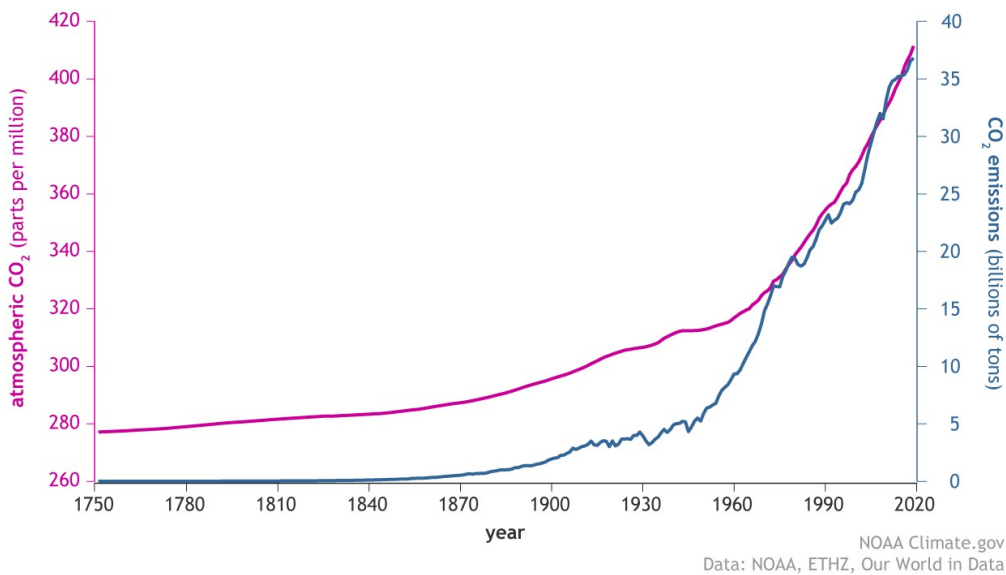
Figure 1.1: CO_2 in the atmosphere and annual emissions (1750-2019). Figure from Lindsey (2020)

Reducing CO_2 emissions requires (in theory) a complete stop of emissions resulting from human activities such as agriculture, industry, various means of transportation, etc., or the removal of greenhouse gases accumulated in the Earth's atmosphere. Studies indicate that limiting the rise in global temperature to about 1.5 - 2°C requires the removal of about hundreds of gigatons of carbon dioxide during the current century (Rogelj et al. 2018). This means disposing of tens of gigatons of this gas annually and storing them safely to neutralize the effects of harmful carbon gas in the atmosphere. Removing carbon dioxide from the atmosphere requires the use of several methods and techniques, some natural and others industrial, whose goal is to reduce the proportion of carbon dioxide in the atmosphere to what it was before the beginning of the Industrial Revolution in the mid-1700s, which amounted to 280 ppm, as it can be seen in Figure 1.1.

Several methods have been proposed, some of which have now been applied and are being tested to find out the extent of their efficacy and effects on the planet's ecosystem, taking into account their applicability, material costs and feasibility of their application, while studying the long-term effects of large-scale carbon removal. These methods include:

Afforestation and energy crops

Trees naturally capture a high amount of CO_2, and increasing the amount of forests on our planet would allow for a reduction in the CO_2 present in the atmosphere. Cultivation of energy crops for the production of biofuels is one of the most important methods of removing carbon dioxide from the air, as is planting trees. Agricultural crops and herbs work to remove carbon gas from the atmosphere, and when they are burned to produce energy the carbon is captured from the resulting gases and converted into a liquid state and stored in the core of the earth.

On the other hand, the removal of large areas of forests has led to the accumulation of huge amounts of carbon dioxide in the atmosphere, and planting trees and increasing the area of land covered by forests is one of the important ways to absorb carbon gas from the atmosphere and store it in wood and soil.

Direct air capture

Is a technology to capture CO_2 from the atmosphere. Capturing carbon dioxide from the atmosphere and storing it in the ground is one of the most promising technologies to get rid of millions of tons of carbon in the atmosphere. Several oil and gas companies have adopted this technique to reduce the resulting carbon dioxide emissions occurring during oil and gas extraction from subsurface reservoirs. There are several government regulations which promote this capture, both environmental and economic requirements such as reducing the amount of carbon emission tax. Equinor is one of the largest energy companies in Norway and it is one of the first companies to adopt such technology. In 1996 Equinor started to inject produced CO_2 from the Sleipner field back into the reservoir. This resulted in decreased emissions and economic benefits as they were able to extract more oil and gas from the reservoir. The Sleipner field is at a depth of about 790 meters below the seabed in the Norwegian sector of the North Sea and the CO_2 is then safely stored inside the reservoir. The direct capture gas carbon technology is based on passing the gases emitted from power plants operating on fossil fuels in special absorption towers in which there are chemicals that absorb carbon dioxide from the smoke emitted from these stations, where it is removed and converted into a liquid to be transported in special tubes under high pressure to be buried in the ground. Northern Lights is a project which aims to store the captured CO_2 in underground reservoirs in the North Sea. The project originated from Equinor and is currently in early stages. Figure 1.2 illustrates the main idea.
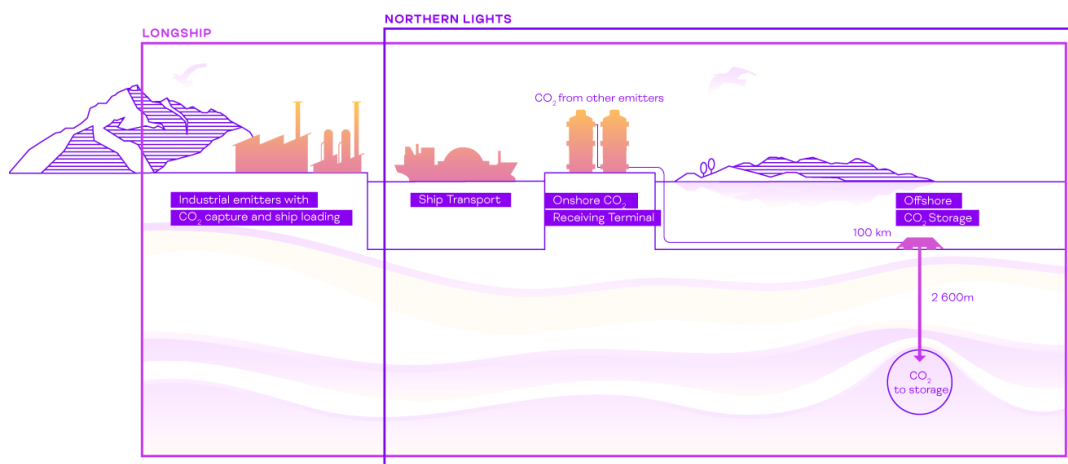
Figure 1.2: Industrial decarbonisation, CO_2 storage for Europe. Figure modified from Northern lights (2021)

Plankton and seaweeds

In the last decade of the twentieth century, a number of researchers proposed a technique for fertilizing the world's oceans to get rid of large amounts of carbon dioxide in the air, and this technique depends on increasing the growth of phytoplankton in the oceans by providing them with nutrients necessary for their growth, such as iron and other materials and elements. However, this method has been met with global rejection due to its environmental risks, as it has been shown that it could lead to a major disruption in the ocean ecosystem, as it will result in a shortage of dissolved oxygen in the water and this may negatively affect the fish health. The decomposition of the plankton as they die may also lead to the captured CO_2 to be emitted back into the atmosphere.

Carbonation curing of concrete

Concrete is the second most commonly used substance on earth after water. If the cement industry were to be combined into a nation, this nation would be the world's third largest CO_2 emitter with an estimated production of up to 2.8 billion tonnes (Watts 2019). Reducing the carbon footprint from the cement industry can therefore lead to a significant reduction in CO_2 emissions. One method to reduce greenhouse gas emissions caused by concrete productions is to use CO_2 as a compound for curing.

Carbonation is a mechanism in which CO_2 penetrates the concrete and forms carbonic acid, in the presence of humidity. Hydrated cement $Ca(OH)_2$ interacts with the carbonic acid that forms Calcium Carbonate $CaCO_3$ and Water (Rostami et al. 2012). Carbonation results in several modifications in the microstructure of hardened concrete in the long-term phase such as:

- Significant decrease of pH due to alkalinity depletion. The drop in pH may lead to increased corrosion (Ahmad 2003).

- Carbonation shrinkage is when concrete contracts and shrinks because of the reduction in hydration materials volumes. Therefore, the long-term carbonation process is consequently known to be harmful to the durability of the concrete.

Bertos et al. (2004) investigated how short-term carbonation can be used as an alternative approach for concrete curing (i.e., exposure of concrete to CO_2 pressure for short periods). This

carbonation method is known as accelerated carbonation curing (ACC). Concrete subjected to short-term carbonation shows enhancements to its physico-mechanical properties, durability characteristics and longevity, such as increasing the strength, density, chloride ions penetration and reducing water absorption (Jerga 2004, Monkman and Shao 2010, Rostami et al. 2012). Rostami et al. (2011) reported that the pH decrease occurs primarily on the concrete surface, not at the core. The reinforcement steel bars are also not exposed to dealkalization corrosion. By adding incorporating mineral admixtures such as slag can further reduce the carbonation shrinkage caused by ACC. Carbonated and hydrated cement concrete demonstrate considerable resistance to shrinkage and reduction of shrinkage by carbonation treatment (Monkman and Shao 2010).

Kashef-Haghighi and Ghoshal (2013) reported that around 1.5 of 16.4 million tons of CO_2 can be stored in products made from concrete cement in 2004 in the United States. This is approximately 9 % of CO_2 by mass of cement to be absorbed by US concrete products. Storing CO_2 in concrete can therefore reduce greenhouse gas emissions and could potentially open up new possibilites in terms of CO_2 capture methods.

1.2 Objectives

The objective of this thesis is to investigate whether accelerated carbonation curing (ACC) enhances rapid strength development of concrete. This is done by first comparing the mechanical properties of carbon dioxide (CO_2) cured concrete with a water cured concrete used as reference. Natural aggregates are used in the concrete mix for all samples when mixing the concrete for both cases.

Chapter 2

Literature Review

The objective of this chapter is to show the theory behind ACC and its advantages. Important factors such as mechanical and chemical properties are shown for both ACC and traditional curing methods. The most important factors impacting the efficiency of ACC and the testing procedures used by previous studies to assess the performance of concrete subjected to ACC is shown.

2.1   Mechanism of accelerated carbonation curing

When concrete solidifies in a standard environment, carbon dioxide (CO_2) penetrates the concrete through natural paths and pores in the concrete formed during the hydration process. The carbon dioxide (CO_2) penetration depth (also called natural carbonation depth) is a function of concrete strength, and Table 2.1 shows the penetration depth after 20 years for different concrete strengths (Lee et al. 2013). This process is quite slow because the amount of carbon dioxide in air is approximately 0,03%. Accelerated carbonation curing is designed to accelerate this process by increasing the concentration of carbon dioxide (CO_2) in a controlled environment such as a pressurized chamber.

Table 2.1: Carbonated depth after 20 years for different types of concrete. Increasing the design strength reduces the carbonated depth.

Design strength (MPa)	24	27	30	35
Carbonated depth (mm)	16.88	12.76	9.66	5.54

Generally, the carbon dioxide (CO_2) absorbed in the early stages of concrete hydration interacts with calcium carbonates from cement ($CaCO_3$) (Bertos et al. 2004, Jerga 2004, Mo and Panesar 2013, Rostami et al. 2012). When water is added to the cement, a chemical reaction occurs between the four clinker minerals in the cement and the water. This results in hydration.

Calcium silicate hydrate (C-S-H) and calcium hydroxide (C-H) are formed when tricalcium silicate () and dicalcium silicate (C_2S) are hydrated. This reaction is shown in Equations 2.1 and 2.2 (Liang et al. 2020). Further, any calcium hydroxide (C-H) present in the cement paste will react with carbon dioxide (CO_2) and water (H_2O) resulting in the formation of calcium carbonate, as shown in Equation 2.3 (Moorehead 1986).

$$3CaO \cdot SiO_2 + 3CO_2 + \mu H_2O \rightarrow SiO_2 \cdot \mu H_2O + 3CaCO_3 \tag{2.1}$$

$$2CaO \cdot SiO_2 + 2CO_2 + \mu H_2O \rightarrow SiO_2 \cdot \mu H_2O + 2CaCO_3 \tag{2.2}$$

$$Ca(OH)_2 + CO_2 \rightarrow CaCO_3 + H_2O \tag{2.3}$$
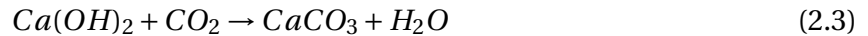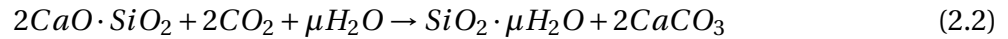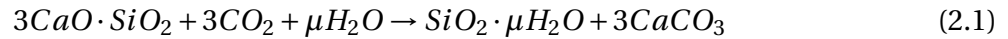
According to Berger et al. (1972), the water in concrete is carbonized first before reacting with the two clinker minerals tricalcium silicate () and dicalcium silicate (C_2S). This is shown in equations 2.4 and 2.5. These reactions result in the formation of calcium silicate hydrate (C-S-H) and calcium carbonate ($CaCO_3$).

$$3CaO \cdot SiO_2 + (3-x)CO_2 + \mu H_2O \rightarrow xCaO \cdot SiO_2 \cdot \mu H_2O + (3-x)CaCO_3 \tag{2.4}$$

$$2CaO \cdot SiO_2 + (2-x)CO_2 + \mu H_2O \rightarrow xCaO \cdot SiO_2 \cdot \mu H_2O + (2-x)CaCO_3 \tag{2.5}$$
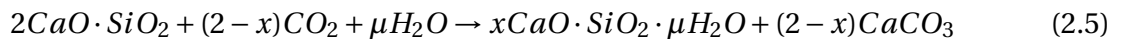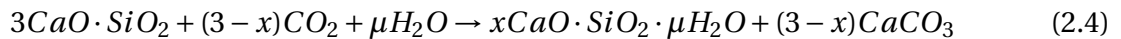
Equation 2.4 and 2.5 show that higher amounts of carbon dioxide (CO_2) will prevent the formation of calcium silicate hydrate (C-S-H) so that the reaction between tricalcium silicate (), dicalcium silicate (C_2S) and carbon dioxide (CO_2) leads to the formation of silicate hydrate (S-H) and calcium carbonate ($CaCO_3$). This is shown in Equation 2.1 and 2.2. According to Maries (1992), the following steps are a summary of what is occurring when carbon dioxide (CO_2) reacts with a hydrating cementitious material.

- CO_2 gas diffuses through the air to the surface of the fresh concrete.

- Permeation of CO_2 through the fresh concrete.

- Dissolution of CO_2(g) to CO_2(aq).

- CO_2 (aq) reacts with H_2O resulting H_2CO_3.

- Ionisation of H_2CO_3 to H^+, H_2CO_3 and CO_3^{2-}. The pH is lowered locally due to the presence of H^+ ions, before rising later as the microstructure matures.

- Tricalcium silicate (3CaO · SiO_2) and dicalcium silicate (2CaO · SiO_2) dissolve, and a thin layer of C-S-H forms around the cement grains. This layer will dissolve rapidly, resulting in the release of Ca^{2+} and SiO_4^{4-} ions.

- Formation of conventional C-S-H gel and thermodynamically stable $CaCO_3$.

- Calcite is formed when $CaCO_3$ solidifies.

- Secondary carbonation occurs when CO_2 reacts with C-S-H gel, causing C-S-H to decalcify, resulting in S-H and $CaCO_3$ formation.

The reaction between C-H, CO_2 and H_2O in fresh concrete, as shown in Equation 2.3, is considered negligible when adding CO_2 to fresh concrete, as limited amounts of C-H are formed early in the hydration process (Kashef-Haghighi and Ghoshal 2010). At the same time, the reaction between C_3S, C_2S and CO_2 will reduce the formation of C-H. It is therefore assumed that available CO_2 will only react with C_3S and C_2S (Kashef-Haghighi and Ghoshal 2010).

Calcium carbonate formed by the reaction between C_2S and CO_2 is of the crystalline calcite type (Goto et al. 1995), which is 1-100 nm in size and homogeneously distributed in the cement paste (Monkman et al. 2018). Whereas, particles with a size smaller than 100 nm are classified as nanomaterials (Silvestre et al. 2016).

It has been discovered that by directly adding nano-calcium carbonate, which has a larger specific surface area, to fresh concrete it then acts as growth areas for the formation of C-S-H. It has been demonstrated that because nano-calcium carbonate facilitates the formation of C-S-H, it results in a faster hydration process, a higher degree of hydration, and increased early strength, this process is shown in Figure 2.1 (Sato and Diallo 2010). Nano-calcium carbonate has also been found to have a filler effect in the matrix, which helps to increase the density of the concrete (Guhua 2006).

By adding CO_2 to young age concrete, the goal is to achieve the same effects as by direct addition of nano-calcium carbonate, while binding CO_2 in the concrete.
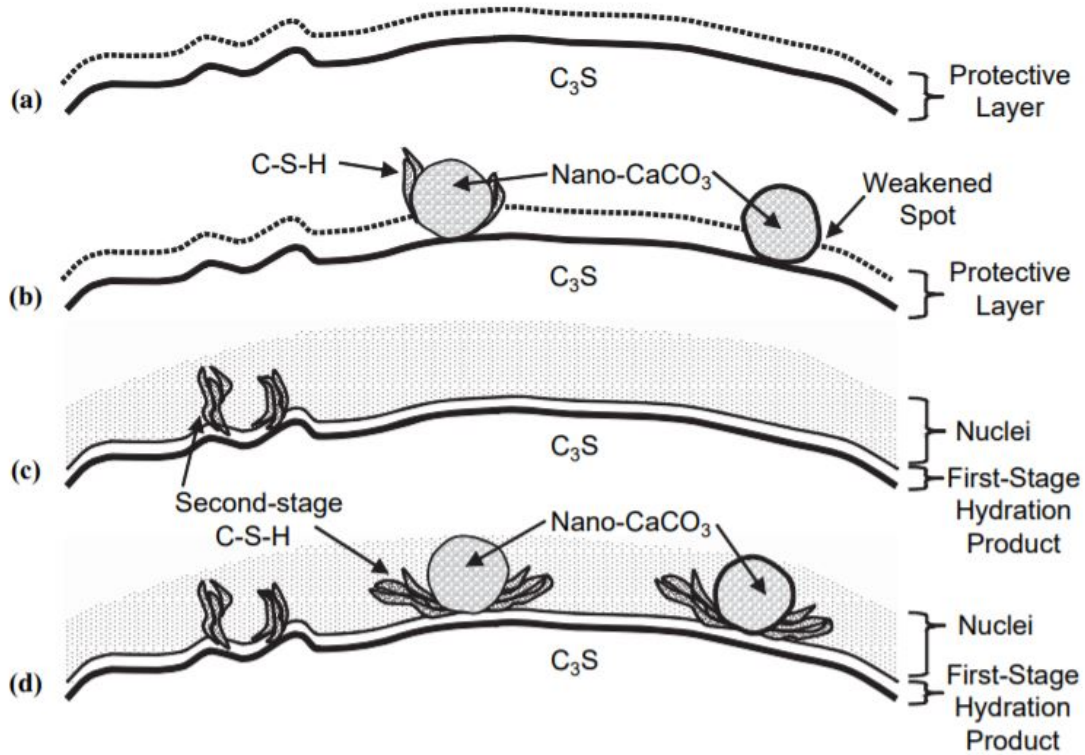
Figure 2.1: Schematic description of accelerating effect of addition of nano-$CaCO_3$ on hydration of C_3S. Figure from (Sato and Diallo 2010)

The cement particles before and after reaction with CO_2 is illustrated in Figure 2.2 (Shi et al. 2012b).

(a) an original cement particle   (b) a cement particle at curing time t
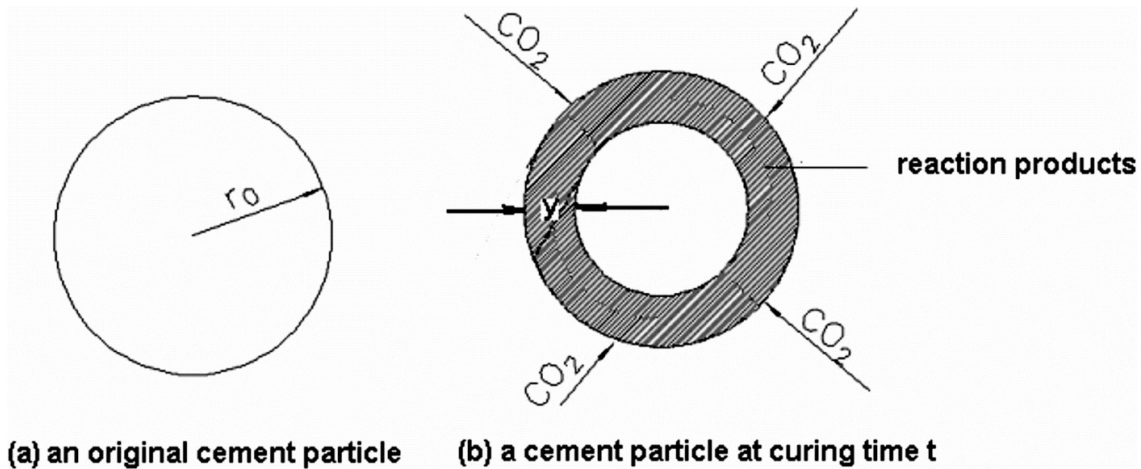
Figure 2.2: Illustration of original and CO_2 cured cement particles. Figure from (Shi et al. 2012b).

2.2 Benefits and advantages

When ACC is done correctly, it has the potential of being an important factor in reducing greenhouse gas emissions. Since the CO_2 is permanently stored in the concrete materials it therefore has the ability to reduce the carbon footprint of the concrete industry. ACC also introduces improvements in the mineralogy, microstructure and morphology of concrete. It increases the density of concrete and creates greater strength and durability (Jerga 2004, Mo and Panesar 2013, Rostami et al. 2012). In addition, it reduces curing time, cost and increases the overall productivity. A recent study suggests that 4-8 hours of CO_2 curing can develop the same strength as obtained after 18-24h of conventional steam curing (Shi et al. 2012a). Another study on the beneficial use of carbon dioxide in precast concrete production shows that the durability improvement is more significant than the strength gain. It also shows improved resistance to freeze-thaw cycles, ettringite sulfate attacks and thaumasite sulfate attacks. This improvement is because of increased density of the cement matrix and a reduction in pore size (Shao 2014). Carbonation-cured, steam-cured and sealed-hydrate concrete blocks after 10, 15 and 20 freeze-thaw cycles can be seen in Figure 2.3 and indicates an improvement in freeze-thaw resistance to carbonation-cured blocks relative to steam-cured blocks. The pH value of concrete should be held above the R/F corrosion value because the pH can be reduced by using ACC due to the reduction of the available amount of $Ca(OH)_2$ in the reaction. Furthermore, due to the reduced amount of $Ca(OH)_2$ available, the sulfate and acid resistance of concrete can be improved. Further, ACC can also be used for the treatment of plain cement and reinforced precast concrete components (Rostami et al. 2011; 2012, Shao et al. 2014).

	Carbonation-cured	Steam cured	Sealed-hydrated
Before F-T cycles			
After 10 cycles			
After 15 cycles			
After 20 cycles			
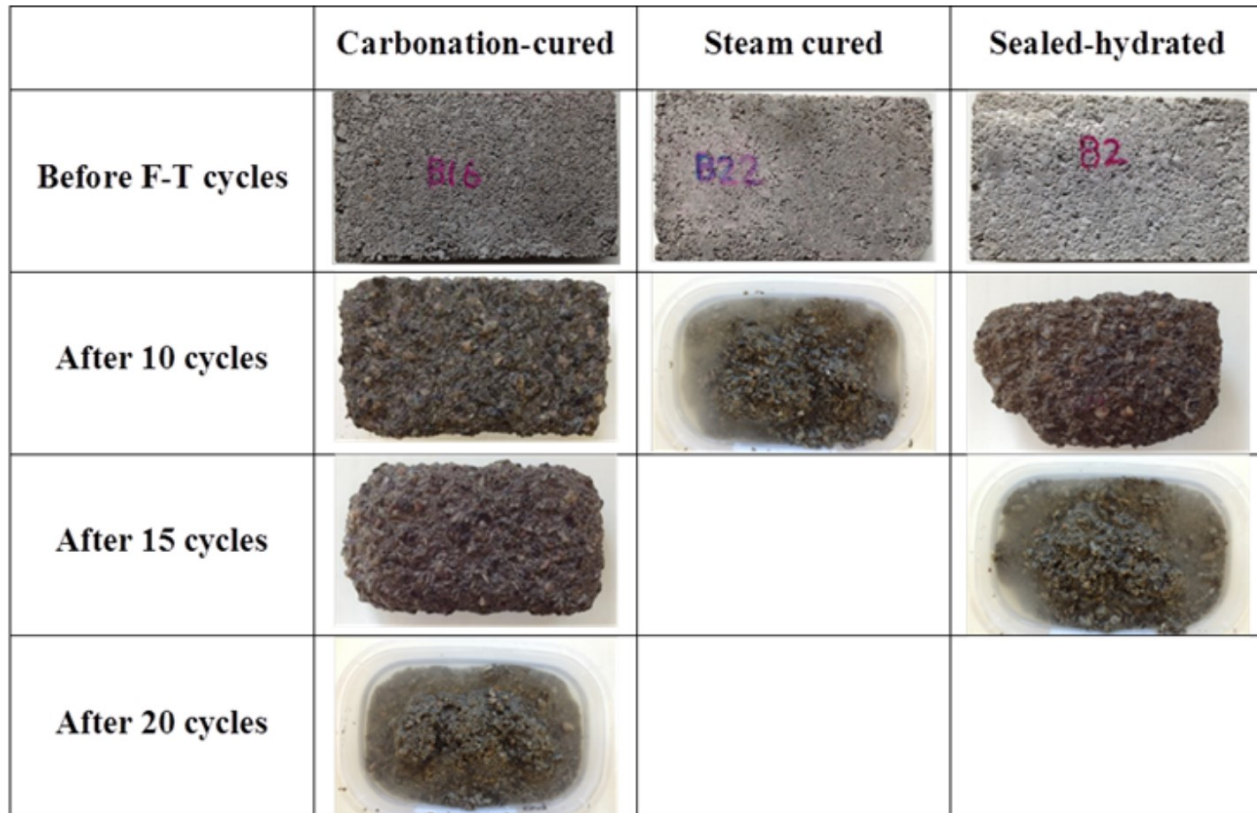
Figure 2.3: Concrete blocks after freeze-thaw exposure. Carbonation-cured concrete shows increased durability to freezing cycles compared to steam-cured and sealed-hydrated concrete. Figure from (Shao 2014)

2.3 Factors influencing the result of ACC

The result of ACC is influenced by several factors, reported in various studies. The main factors can be divided into two categories, before and during the carbonation curing process.

2.3.1 Before carbonation curing

- **The water-cement ratio**

  The concrete age at demoulding, the type and amount of binders and the moisture content are all factors influencing the result of the ACC. Jerga (2004) stated that a lower water to cement ratio and a higher cement content make the carbonation curing more efficient. ZOU et al. (2008) investigated the impact of concrete moisture content on carbonation curing and discovered that when concrete has a lower moisture content, the degree of car-

bonation is higher. Furthermore, as the degree of CO_2 curing increases, concrete strength increases, and can be very similar to that of conventional steam curing.

- **Pre-conditioning** can be performed with either the use of a climate chamber, or wrapped in plastic and left in room temperature. This is performed directly after casting in moulds to obtain adequate strength before demoulding. After this process the specimens can be placed in water for reference or inside the CO_2 chamber for further curing without damaging the specimens. A studie performed by Shi et al. (2011) suggests that in order to obtain a proper CO_2 curing degree, the duration and relative humidity for pre-conditioning in climate chamber should be at least 3 hours at 60-70% RH. When pre-curing is performed at a low relative humidity, the level of CO_2-curing degree shows an significant improvment. However, this is not beneficial for the later strength development. Another studie performed by Rostami et al. (2012) suggests that pre-curing the specimens in the air for a period of time before exposing them to CO_2 gas is critical for improved CO_2 diffusion into the concrete and thus noticeable early strength gain. The CO_2 uptake was 8% and 23 % for ACC done after casting and for ACC done after 18 hours air curing, respectively (El-Hassan et al. 2013)

- **Cement replacement** A study was done by Atiş (2003) on the accelerated carbonation curing of concrete made with 0%, 50% and 70% replacement of normal Portland cement, NPC, with fly ash, FA. He found that up to 50% FA replacement concrete showed lower or similar improvement in carbonation to NPC concrete. However, 70% FA replacement showed higher carbonation compared to normal Portland cement.

  Monkman and Shao (2010) found that using slag as a partial substitute for cement had a positive effect. Their research, which looked at the performance of ACC made with cement partially replaced by 15%, 25%, and 50% slag, found that using slag can be beneficial in strength gain, shrinkage reduction, as well as resistance to de-icing salt. Mo and Panesar (2012; 2013) found that using reactive MgO as a partial substitute for NPC improved the efficiency of ACC.

2.3.2 During carbonation curing

- **Relative humidity:** carbonation is more rapid at a relative humidity of 50–70% and decreases at higher and lower relative humidity levels (Fattuhi 1988, Walton et al. 1997).

- **Temperature:** high temperature up to 60°C increases the uptake of CO_2 (Liu et al. 2001). However, higher temperatures above 60°C reduce the solubility of CO_2 in water and thus reduce the carbonation rate. On the other hand, tests have shown that more calcite is formed when very cold carbonic acid is used for carbonation purposes. The heat of the carbonation reaction promotes the formation of meta-stable forms of $CaCO_3$ and the process should be maintained at low temperatures in the range 0–10 °C (Asavapisit et al. 1997). Therefore, an optimal temperature value is required.

- ***CO_2 Concentration***: The higher the amount of carbon dioxide phase gas, the higher the rate of carbonation. Nevertheless, the strength of carbonated products stops at some point, no matter the CO_2 overflow pressure (Sorochkin et al. 1975). This implies that the CO_2 concentration inside the chamber is a significant factor.

- **Pressure:** a slight increase in CO_2 pressure increases the rate of reaction and influences the strength development. In spite of that, carbonation pressure does not have a significant impact between 10 kPa and 500 kPa (1.45 and 72.51 psi) (Tam et al. 2020). Researchers have used various pressure inside the chamber between 1,45 and 72,5 psi. Some researchers have vacuumed the curing chamber before injecting CO_2 gas and after inserting the specimens in the chamber to achieve a better accuracy. To avoid affecting the porosity of concrete, this procedure should be carried out under low pressure and for only a few seconds. (El-Hassan et al. 2013, Monkman and Shao 2010, Zhan et al. 2013).

- **Carbonation duration in the chamber:** compressive strength various with curing time under different CO_2 concentrations. The lower the concentration, the lower the compressive strength is for a given curing time. Lower CO_2 concentrations result in slower reaction rates and less reaction products. However, when the curing time is longer than 4 hours, the increase in strength at a low CO_2 concentration is higher than at a high CO_2 concentration (Shi et al. 2011). Furthermore, researchers used different durations of exposure to CO_2 gas. Monkman and Shao (2010) reported CO_2 uptake between 8 to 10% by the

mass of binder and they found that after 2 hours of carbonation curing, the strength was equivalent to 80% of the strength after 24 hours of conventional curing. Zhan et al. (2013) performed a study on ACC using 100% concentration of CO_2 at a pressure of 1 bar, a temperature of 26 to 30°C, and a relative humidity of 82 to 95% for various durations of 6, 12, and 24 hours. They discovered that increasing the duration of ACC resulted an increase in CO_2 absorption and strength, as well as a reduction in drying shrinkage.

- **Surface area of carbonated materials:** the larger the surface area of the carbonated material, the faster it can be carbonated (Haselbach and Thomle 2014, Tam et al. 2016). Kashef-Haghighi and Ghoshal (2010; 2013) discovered that the formation of $CaCO_3$ during the carbonation process has a negative impact on the CO_2 uptake, and that the formed layer of calcium carbonate reduces the cement reactive surface area. Kashef-Haghighi and Ghoshal (2013) found that increasing the amount of reactive mineral and fineness in the cements could increase CO_2 absorption by a small amount, which would lead to a larger reactive surface area.

2.4 Test methods of accelerated carbonation cured concrete

As stated by different researchers, the test methods used to evaluate the performance of CO_2 cured concrete are presented as follows:

2.4.1 Degree of carbonation curing and CO_2 uptake

The efficacy of accelerated carbonation cured concrete is measured in either CO_2 uptake as percentage of the binder mass or the actual CO_2 curing degree. The change in the specimens obtained net mass, is due to the CO_2 reaction with cement clinker minerals and hydration materials, which is sequestered. As a result, the mass-change of the specimen and the curing chamber with silica gel is measured before and after the CO_2 curing phase to determine the amount of captured CO_2, M_{CO2} (Zhan et al. 2013):

$$M_{CO2} = \Delta M_{specimen} + \Delta M_{water} \tag{2.6}$$

where $\Delta M_{specimen}$ and ΔM_{water} represent the net mass gain of the specimens and the moisture loss. The CO_2 curing degree (D_{cc}) is defined as the ratio of the actual captured CO_2 amount, M_{CO_2}, to the maximum theoretical CO_2 amount, $M_c\ CO_{2\,\%max}$, captured by cement in the specimens:

$$D_{cc} = \frac{M_{CO_2}}{M_c\ CO_{2\,\%max}} \tag{2.7}$$

where M_c represents the cement mass in the specimens, while the maximum theoretical CO_2 $CO_{2\%max}$ captured by Portland cement can be calculated based on the metal oxide content by the following formula as given by Zhan et al. (2013):

$$CO_{2\,\%max} = 0.785\,(CaO - 0.7\,SO_3) + 1.091\,MgO + 1.42\,Na_2O + 0.935\,K_2O \tag{2.8}$$

Where the expression for theoretical CO_2 as given by Kashef-Haghighi and Ghoshal (2013)

$$CO_{2\,\%\,max\,total} = 0.785\,(CaO - 0.56\,CaCO_3 - 0.7\,SO_3) + 1.091\,MgO + 1.42\,Na_2O + 0.935\,K_2O \tag{2.9}$$

Whereas the actual CO_2 uptake expression is given by Rostami et al. (2011; 2012) as follows:

$$CO_2\,uptake\,(\%) = \frac{\text{(Mass after carbonation + Water lost) - Mass before carbonation}}{Mass_{cement}} \tag{2.10}$$

2.4.2 Physico-Chemical Properties

Researchers Kashef-Haghighi and Ghoshal (2013), Mo and Panesar (2012; 2013), Panesar and Mo (2013), Rostami et al. (2011; 2012), Shao et al. (2006) have investigated the morphology of carbonates, as well as the pH and microstructure of concrete, which are the principle physico-chemical properties of concrete, in order to evaluate the performance of accelerated carbonation curing using a variety of methods, such as:

- **X-ray diffraction (XRD):** By crushing slices at different depths from the carbonated concrete surface, this method can detect the presence of strong calcite peaks and the absence of $Ca(OH)_2$

- **Scanning electron microscopy (SEM):** The morphology of carbonates on concrete slices

taken at various depths from the carbonated concrete surface is investigated using this method. It depicts the spatial distribution of CaCO$_3$ (s) precipitates that formed during the accelerated carbonation curing process.

- **pH test** on crushed samples taken at different depths from the carbonated concrete surface is used to establish the carbonation front.

- **Porosity Measurements (PF):** This test is used to determine how porous carbonated concrete is.

2.4.3   Physico-Chemical Properties and Durability Characteristics

Researchers Mo and Panesar (2013), Monkman and Shao (2006), Panesar and Mo (2013), Pizzol et al. (2014), Rostami et al. (2011) have identified compressive strength, water permeability, shrinkage, stress-strain behavior, acid and sulfate tolerance, density, modulus of elasticity, and chloride resistance as indicators for evaluating the effectiveness of accelerated concrete curing.

Chapter 3

Research Methodology

Various details on the materials required for the experimental work, preparation and testing of specimens are presented in this chapter.

3.1 Experimental Work Plan

The experimental workflow for ACC is illustrated in Figure 3.1. The test is performed using industrial cement with two different w/c ratios of 0.4 and 0.6 and carbonation time of three and four hours, respectively. Four mixtures of each of these water to cement ratios are created. Each set of ACC samples are compared with reference samples of the same mixture, which had the same initial pre-conditioning curing. After casting, the ACC specimens and the reference specimens are pre-cured in a climate chamber for five to six hours. After pre-curing, ACC specimens are placed in a carbonation chamber for CO_2 curing then placed in water for further water curing. In the same way, reference specimens are placed in water for further water curing, but not in the carbonation chamber. All specimens are tested for compressive strength,porosity, pH, density and CO_2 uptake after 1 and 28 days from casting.
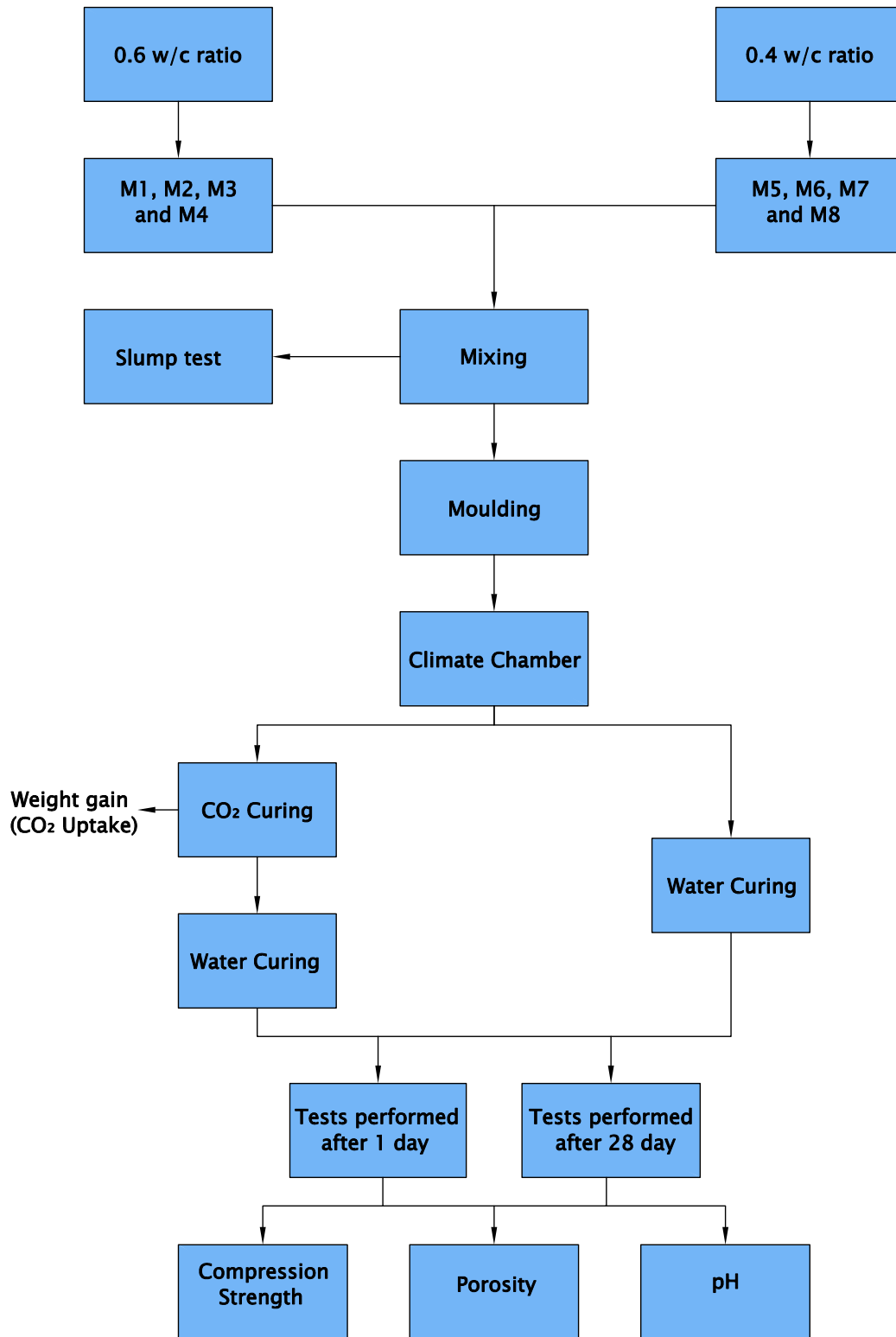
Figure 3.1: The entire workflow for the experiment is shown in this diagram.

3.2 Materials

3.2.1 Portland Cement

Norcem industrial cement CEM I 52,5 R is used in this study . Norcem Industrial is a cement designed for construction at winter time. The cement has a high early strength, and is also well designed for production of concrete elements and concrete products (Norcem 2016). Table 3.1 shows the chemical composition of industrial cement and appendix A.1 shows cement's data sheet.

Table 3.1: Chemical composition of Norcem industrial cement CEM I 52,5 R. Data from Norcem (2016)

Component	Declared data
Sulfate (% SO_3)	≤ 4.0
Chloride (% Cl-)	≤ 0.085
Chromium (ppm Cr)	≤ 2
Alkali (% Na_2O)	1.3
Clinker (%)	96
Secondary constituents (%)	4

3.2.2 Aggregates

Aggregates are a common term for sand, gravel and stone used in concrete production. Concrete usually consists of 60-70% aggregates and have a major impact on the quality of the end result (Gjerp et al. 2004). Aggregates are divided into two distinct categories, fine aggregate and coarse aggregate. For a good concrete mix, it is important to have a well-composed aggregates, where all the grain sizes are represented and evenly distributed. This helps to give a good grain grading so that smaller grains always fill the gaps between larger grains (Gjerp et al. 2004). In this study, two types of aggregates are used in all concrete mixtures:

- Fine aggregates 0-8mm (sand). Local sand from Velde Pukk AS with 1.0% water absorption capability.

- Coarse aggregates 8-16mm. Local crashed aggregates from Velde Pukk AS with 0.4% water absorption capability.

Figure 3.2 shows the two different types of aggregates. Their particle-size distribution curves can be seen in appendix A.2 and A.3. For data sheets A.4 and A.5 for both types of aggregates.
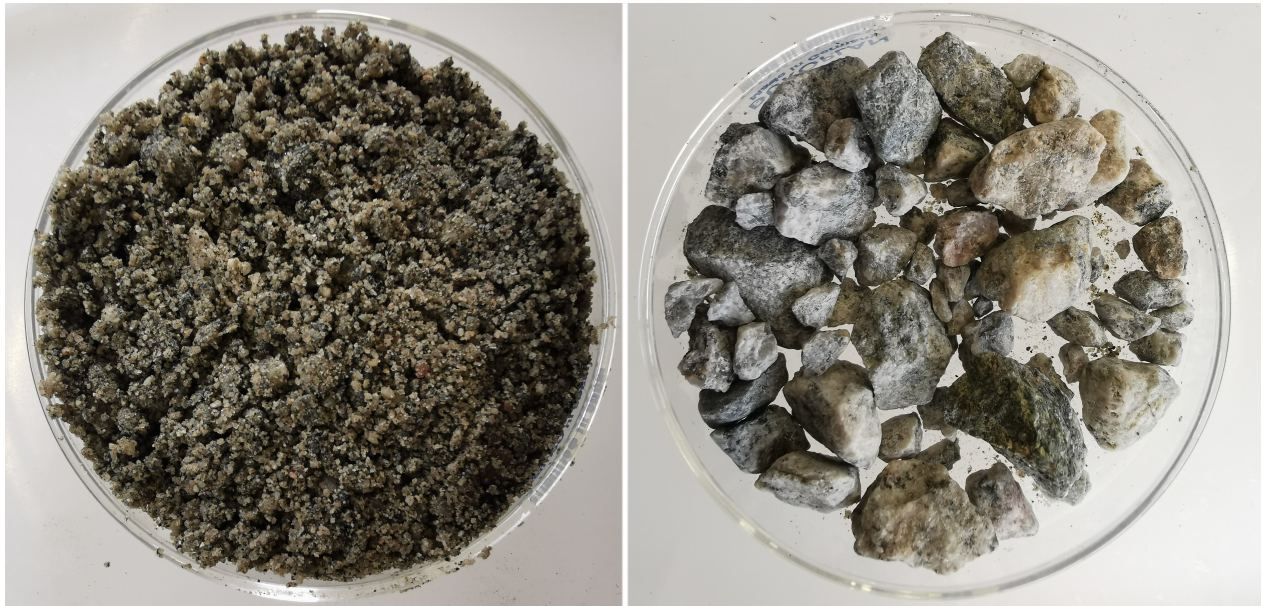
Figure 3.2: 0-8mm fine aggregates to the left and 8-16mm coarse aggregates to the right

A sieve analysis should be performed to ensure a good distribution of different grain sizes. In the laboratory, a set of sieves in a sieve shaker can be used to conduct the test, with the following decreasing sieve mesh sizes from top to bottom: 22.4 mm - 16 mm - 11.2 mm - 8 mm - 4 mm - 2 mm - 1 mm - 0.500 mm - 0.250 mm - 0.125 mm and a pan at the bottom.

The aggregates must be dry so that the grains do not stick together and can pass through the meshes more easily. In the top sieve mesh, 1 kg of aggregates is placed. Then the sieve is vigorously shaken until the aggregates are separated into fractions. Each fraction must be weighed and recorded in the sieve meshes. These weights are then used to create a particle-size distribution.

Particle jump may occur if a specific size in the aggregates is missing or is very underrepresented. It results in a higher void percentage and it needs a larger amount of water, cement or additives such as fly ash or silica dust to fill the voids (Gjerp et al. 2004).

3.2.3 Carbon Dioxide (CO_2) Gas

The high-pressure carbon dioxide cylinder is provided by Nippon gases and is used during the carbonation curing process. Table 3.2 shows the contents of CO_2 cylinder, provided by Nippon gases. See the attachment A.6 in Appendix A, for the gas data sheet.

Table 3.2: Carbon dioxide specification. Data from appendix A.6

Carbon dioxide (CO_2) Standard quality			
Compound	**Formula**	**Conc.**	**Unit**
Humidity	H_2O	< 40	Vol-ppm
Purity	CO_2	> 99.7	Vol. %

3.2.4 Superplasticizer (SP)

Superplasticizer is used in all types of concrete to improve the workability and/or reduce the amount of water needed. Dynamon SX-N, superplasticising admixture shown in Figure 3.3, is a product from Mapei company and it is used in all concrete mixtures in small dosages. Dynamon SX-N was added after mixing all dry materials with water. Table 3.3 shows the technical data of Dynamon SX-N, as provided by Mapei. See the attachment A.7 in Appendix A, for data sheet.

Table 3.3: Technical data of Dynamon SX-N. The Alkali content is Na_2O-equivalents. Data from appendix A.7

Product identity	**Dynamo SX**
Appearance	Liquid
Colour	Yellowish brown
Viscosity	Easy flowing < 30 mPa $\cdot$ s
Solids content [%]	18.5 ± 1.0
Density [g/cm^3]	1.06 ± 0.02
pH:	6.5 ± 1
Chloride content [%]	< 0.05
Alkali content % [%]	< 2.0
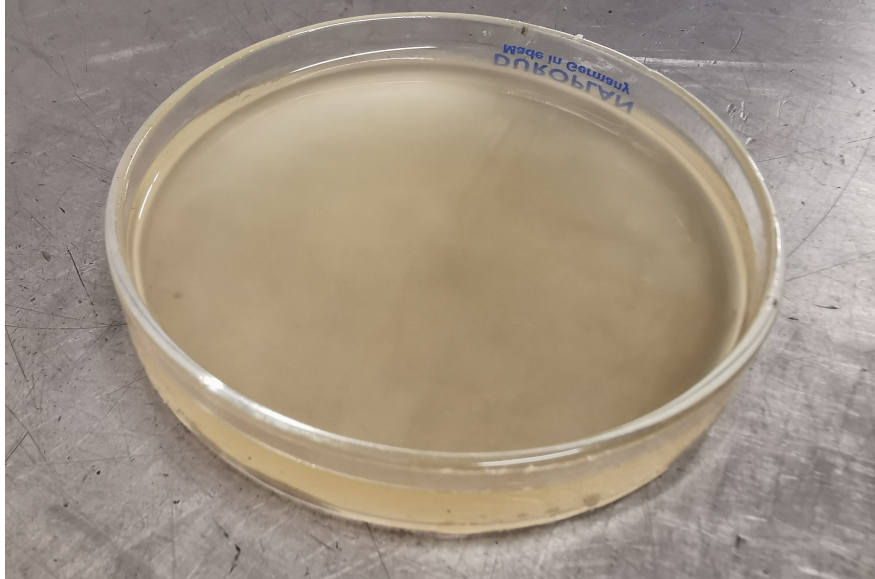
Figure 3.3: Superplasticizer is used in all types of concrete to improve the workability and/or reduce the amount of water needed.

3.2.5 Mixing Water

Water is an important factor in the production of cement-based materials. When water is mixed with cement, it forms a paste that binds the aggregates together. Through a process known as hydration, water causes concrete to harden. Hydration is a chemical reaction between water molecules and cement compounds that become hydration products. Water must be pure to prevent weakness occurring in the concrete. Fresh potable water of acceptable quality is used for the experiment.

3.2.6 Silica Gel

Silica gel is a product that absorbs water and is used to calculate how much water has evaporated during the hydration process inside the CO_2 curing chamber. This is done by weighing the silica before and after the CO_2 curing according to the weight gain method 3.15. Figure 3.4 shows the Chameleon® C 2 - 6 mm drying agent before and after it is used in the CO_2 curing process. The figure also shows the color change of the silica after it absorbs water. See attachment A.8 in Appendix A, for silica gel data sheet.
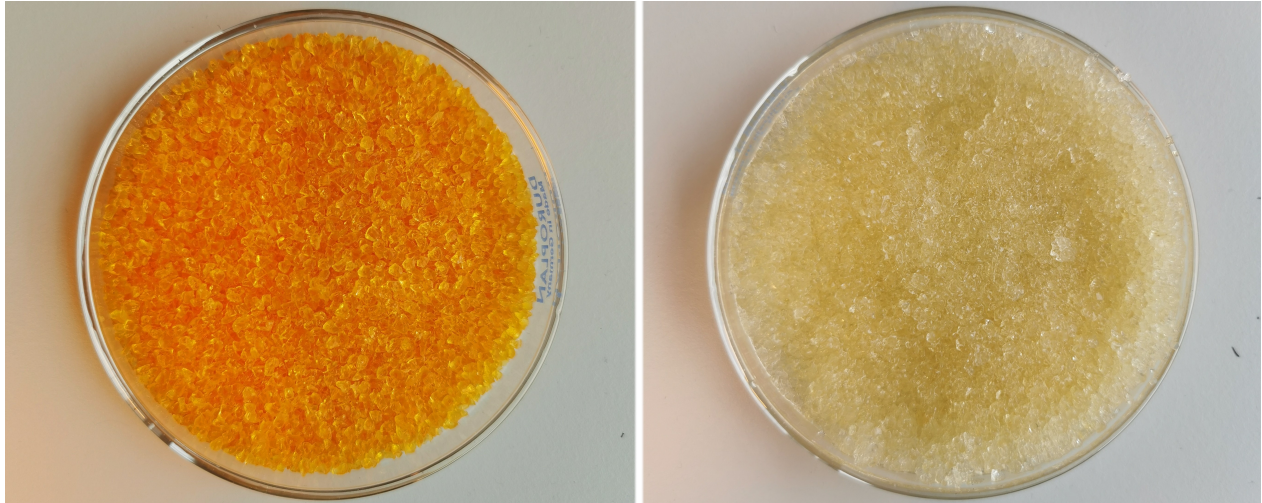
Figure 3.4: Dry Silica gel to the left and wet Silica gel to the right. The silica gel absorbs water vapour in the curing chamber.

3.3 Carbonation Chamber Set Up

Figure 3.5 shows the setup in the lab and Figure 3.6 gives a schematic overview of the setup. The carbonation chamber is constructed with stainless steel with a wall thickness of 8 mm for safety reasons. A clear diameter of 29 cm and a clear height of 16 cm define the cylindrical shape. The chamber's wall features two circular openings; inlet and outlet. The inlet is used to connect the chamber to a CO_2 gas cylinder via a pressure gauge in order to measure and maintain constant pressure inside the chamber. The outlet is used to connect the chamber to an air compressor with a rubber hose. There are no more than four specimens in the pressure chamber at the same time.

The ACC specimens are placed over a metal net sheet which is then placed over plastic spacers inside the chamber. The plastic spacers are used in order to obtain 3-4 cm gap under the ACC specimens so that the CO_2 gas can easily reach the specimens' bottom surface. Silica gel is evenly distributed over the chamber's bottom surface, between plastic spacers and under the metal net.
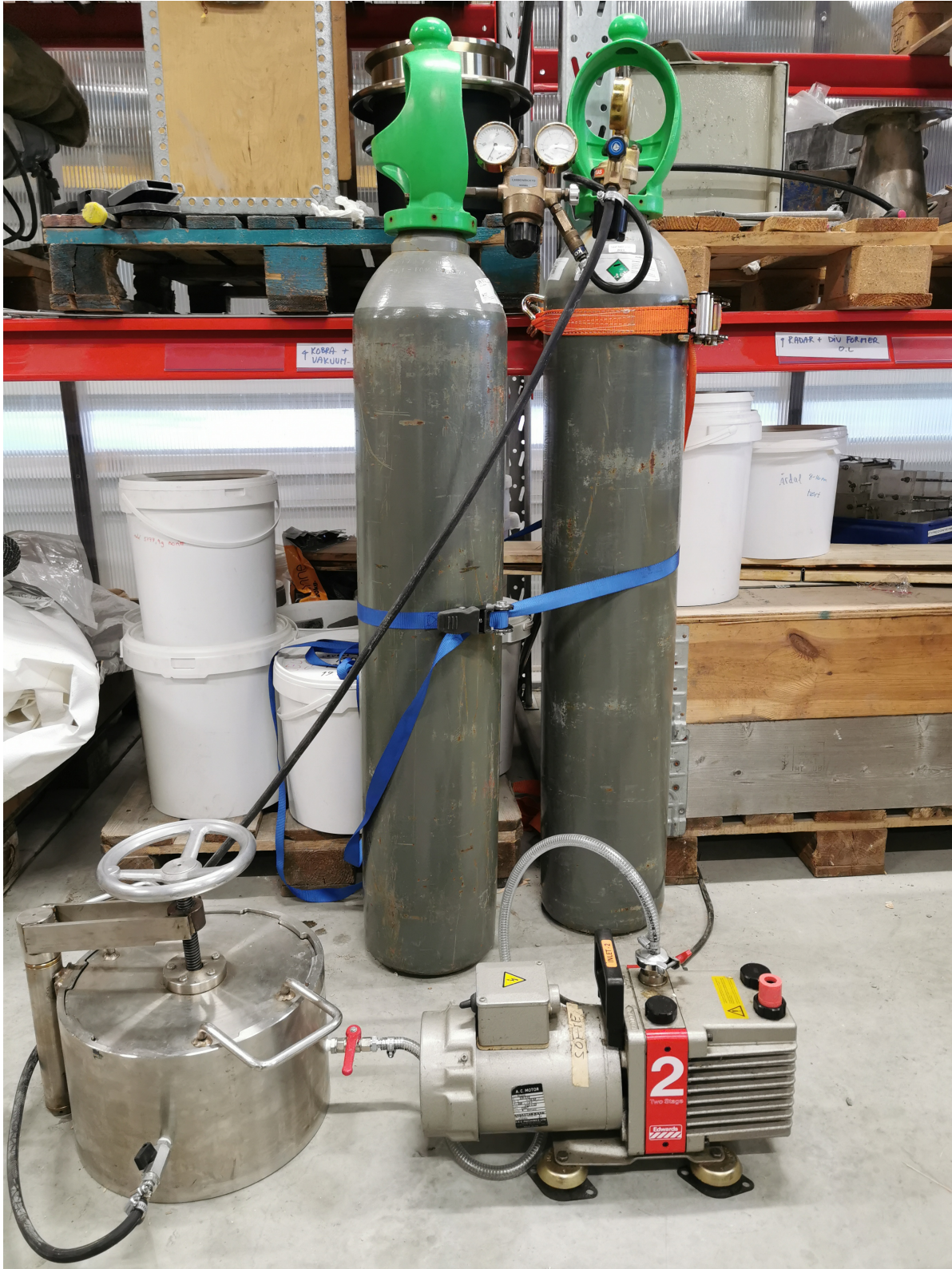
Figure 3.5: Carbonation curing setup. The chamber is shown on the lower left side and the air compressor is shown on the lower right. The tanks containing CO_2 gas are visible in the background.

Pressure Gauge

CO2 Gas 99.9%
Purity

Outlet valve

Specimens

Metal net

AIR COMPRESSOR

Plastic spacer

Silica gel

Carbonation Chamber
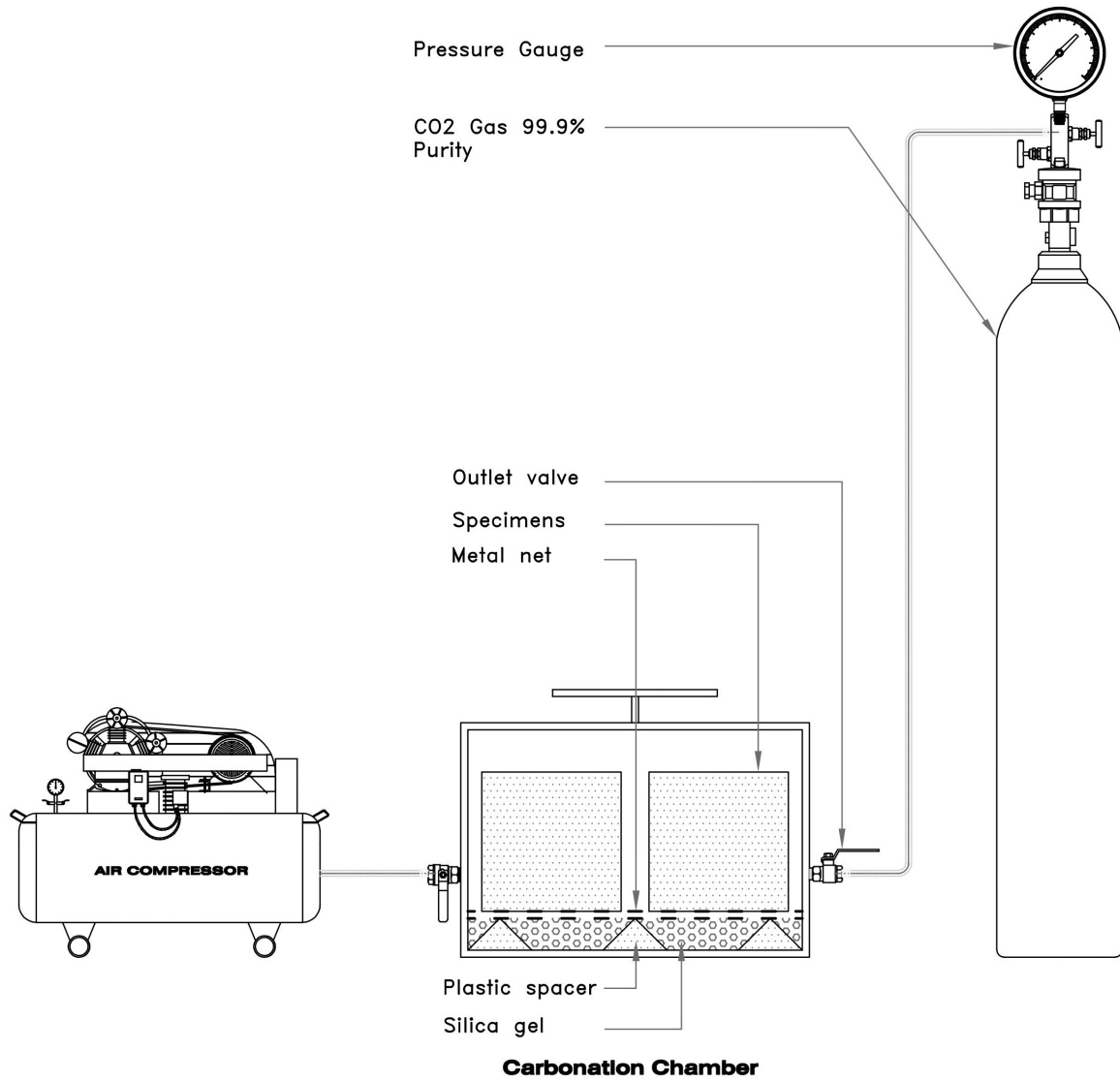
Figure 3.6: AutoCAD schematic drawing of the carbonation curing setup.

3.3.1 Mixtures Coding System

In order to create a clear overview over the 8 mixtures, a coding system has been assigned to these mixtures concerning water-cement ratio, carbonation pressure, carbonation duration and compression test, as shown in Table 3.4. The code starts with WC which is the selected water-cement ratio followed by $P_x T_y$ or Ref. where, P_x is the applied pressure in bar, T_y is the carbonation duration in hours and Ref. is the reference specimen without carbonation. D_z is the performed compression test after 1 or 28 days. As an example, WC0.6-P4T3-D1 can be read as a mixture of water-cement ratio of 0.6 cured at applied gas pressure of 4 bar, for 3 hours and tested at day 1.

Table 3.4: Coding system of mixtures

Mixture No.	M1	M2	M4	M3
Code	WC0.6-P4T3-D1 WC0.6-Ref-D1	WC0.6-P6T4-D1 WC0.6-Ref-D1	WC0.6-P4T3-D28 WC0.6-Ref-D28	WC0.6-P6T4-D28 WC0.6-Ref-D28
Mixture No.	M6	M7	M8	M5
Code	WC04-P4T3-D1 WC0.4-Ref-D1	WC0.4-P6T4-D1 WC0.4-Ref-D1	WC0.4-P4T3-D28 WC0.4-Ref-D28	WC0.4-P6T4-D28 WC0.4-Ref-D28

3.4 Concrete Mixtures

The mix design procedure of the concrete mixtures used in this study is carried out in accordance with Norwegian standard; Methods of testing cement Part 1: Determination of strength (Standard Norge 2016). All the materials such as; cement, aggregates and water have a temperature of 20 ±2 °C and are stored either in sealed bags or airtight containers. Table 3.5 shows the details of the 8 concrete mixtures, where each mixture has a mix design of 30 liters.

Table 3.5: Details of 30 liters concrete mixtures. Mix designs are in appendix B.4 and B.5

Concrete Mixture	M1	M2	M3	M4	M5	M6	M7	M8
[w/c] ratio	0.6	0.6	0.6	0.6	0.4	0.4	0.4	0.4
Cement [Kg]	8.34	8.34	8.34	8.34	12.00	12.00	12.00	12.00
Fine aggregate [Kg]	31.7	31.7	31.7	31.7	30.3	30.3	30.3	30.3
Coarse aggregate [Kg]	27.3	27.3	27.3	27.3	26.1	26.1	26.1	26.1
Water [Kg]	4.0	4.0	4.0	4.0	3.9	3.9	3.9	3.9
Free water in agg. [%]	3	3	3	3	3	3	3	3
SP [Kg]	0.12	0.13	0.11	0.11	0.24	0.37	0.37	0.38
Matrix volume [l/m^3]	310	310	310	310	340	340	340	340
Superplasticizer [g]	110	110	110	110	350	350	350	350

3.5 Moisture Test for Aggregates

Water to cement ratio is one of the most important factors when concrete is being mixed. W/C has the greatest influence on the concrete's final strength, and it's crucial to know how much water is in the aggregates. This is also known as "free water". The amount of free water found in the sand should be subtracted from the amount of water required in the mixture. There are two methods for determining the moisture content of sand, according to Civilseek (2021). The first method is the drying method in an oven, and the second method is the Speedy Moisture test, as follows:

3.5.1 Drying Method in an Oven

This method is based on drying a certain amount of moist sand in an oven. By measuring the difference in weight, the moisture in the sand is then calculated. To get started, weigh a specified amount of moist sand, $W_{wet\,soil}$, and place it in an oven for 24 hours at 110°C. Then the sand is completely dry and all moisture has evaporated. The new weight is recorded as $W_{dry\,soil}$. The sand's water content (M.C) is then defined in the following equation.

$$M.C = \frac{W_{wet\,soil} - W_{dry\,soil}}{W_{dry\,soil}} * 100 \tag{3.1}$$

It's important to note that there are two disadvantages to this approach. The first is that the test takes 24 hours to complete. The second is that an oven is required, which is inconvenient in the case of a quick test.

3.5.2 Speedy Moisture Test

The basis for the Speedy Moisture test is the chemical reaction that occurs when water comes into contact with calcium carbide reagent. It produces Acetylene gas C_2H_2 as shown in the chemical reaction:

$$CaC_2 + 2H_2O \rightarrow Ca(OH)_2 + C_2H_2 \tag{3.2}$$
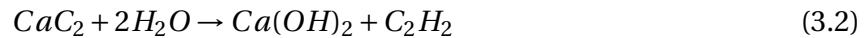
The equipment to perform the test is is shown in Figure 3.7 (left). A pressure gauge is located at the bottom of the Speedy Moisture canister and displays the pressure created by the chemical reaction. The gauge is shown in Figure 3.7 (right).

The Speedy Moisture test is a more effective method than the drying method as it takes less than 5 minutes to perform and is portable. The portability of the test allows it to be used on construction sites to quickly determine the moisture content of fine aggregates. The test kit does not require any calculations as the water percentage content of the sand can simply be read off of the pressure gauge.

The workflow to perform the test is as follows:

- Clean the speedy moisture test container to remove particles from earlier testing using the included brush.

- Weigh the materials using the balance scale in the test box. The correct amount is obtained when the beam is consistently balanced with the red marking on the scale's left side. Put the materials in the Speedy test container.

- Fill the speedy cap with two full measures of reagent; for bulky materials, 3-5 measures are required to ensure adequate coverage.

- To keep the reagent and the sand from coming into contact, seal the speedy test container while holding it horizontally. Bring the stirrup around and tighten the top screw once the
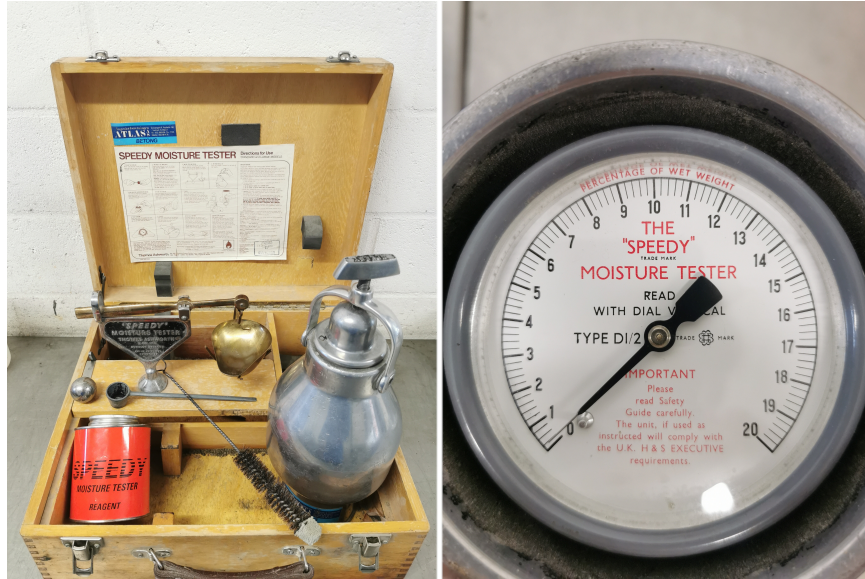
Figure 3.7: Speedy Moisture Test kit is shown in the left photo and the pressure gauge is shown in the right photo. The reagent used in the test is in the red container and the scale is used to weigh the aggregate.

cap is in place.

- After the speedy test container has been sealed, mixing can begin. Shake the container vigorously for five seconds with the pressure gauge facing down, then quickly turn it so the gauge is facing up. Make sure the material falls into the cap by tapping the container. Wait one minute while keeping the container in this position. Repeat the mixing procedure three times at one-minute intervals.

- With the gauge at eye level, hold the speedy container horizontally. Shake it again to make sure the gauge is stable and the chemical reaction is completed. When this is done, take the reading.

- The test is now finished. Since the produced gas (Acetylene) is flammable, the unit should be vented outside, away from any potential sources of ignition. Unscrew the stirrup while keeping the cap pointing away from the operator.

For some materials two steel balls should be placed inside the container to ensure adequate mixing. This is called the steel ball method. The included steel balls are not used in this study, as they are not necessary when mixing sand and aggregates.

3.6   Mixing Procedure

Figure 3.8 shows the mixer used in this study. The following procedure is followed when preparing the concrete mixtures:

- The cement and aggregates are accurately weighed and kept in separate containers.

- Before starting the cement mixer, the inner surface is moistened with water to prevent mixing water loss.

- Dry materials such as aggregates and cement are added to the mixer, and then dry mixing is conducted for about one minute.

- Half of the water is added during the mixing process until the cement is mixed with sand and aggregates. This process takes about one to two minutes.

- The second half of the water and the superplasticizer are gradually added to the mixture, which is then rotated for three minutes until a homogeneous mixture is obtained.

- Before casting in molds, concrete slump and air content tests are performed immediately after mixing.

Figure 3.8: Concrete mixer on the left, and the mixing chamber is shown on the right.

3.7 Slump Test

Concrete workability and consistency can be determined by several methods: Slump test, Flow table, Compaction Factor test, Flow test, Vee Bee Consistometer test and Kelly Ball test (Ball Penetration test) (Patel 2019). Slump test is used in this study. This test can be performed either at the laboratory as shown in Figure 3.9 or at the construction site. Concrete slump tests are performed from batch to batch immediately after mixing. The workability, which indicates a water cement ratio, is generally determined by using concrete slump value. However, different factors, including properties of the materials, mixing methods, dosages, admixtures etc. also affect the value of the concrete slump (Theconstructor 2020). The slump test is carried out as per procedure mentioned in Norwegian Standard; Testing fresh concrete Part 2: Slump test (Standard Norge 2019a) as follows,

- Clean and moisten the internal surface of the slump cone and the smooth horizontal steel plate.

- Place the cone on the steel plate. One person should hold the cone's sides to prevent concrete from leaking out from the bottom of the cone.

- Fill the cone with prepared concrete mixture in approximately 3 equal layers.

- Tamp each layer with 25 strokes using the tamping rod over the cone's cross section.

- Level and smooth the top surface of the cone with taming rod and remove any excess concrete from the plate.

- Lift the cone slowly horizontal over a 5 second period, to allow the fresh concrete to flow freely.

- Place the cone next to the concrete mass. Measure the slump, as given by the difference between the height of the cone and the highest point of the concrete mass.

Figure 3.9: Slump test. The slump height is measured after the concrete is allowed to move freely and compared to the height of the cone.

3.8   Measurement of Air Content in Concrete

The pressure air measurement method is used to measure air content of fresh concrete by using an air pressure gauge. This method does not require the concrete mixture weights or specific gravities. In hardened concrete, air bubbles become air voids. The main benefit from adding additional air into concrete is to reduce the possibility of the concrete cracking from water expansion as it freezes. Additional benefits are reduced water demand for mixing and curing, and reduced bleeding and segregation (Globalgilson 2020). Figure 3.10 shows the air entertainment meter that is used to measure air content in accordance with Norwegian Standard (Standard Norge 2019c). The procedure to measure the air content is as follows:

- Ensure that the internal surface of the air meters is humid by wiping the container with a

moist cloth.

- Fill the container with prepared concrete mixture in approximately 3 equal layers.

- Tamp each layer with 25 strokes using the tamping rod over the cross section of the container. The top layer should be smooth and leveled with the top of the container.

- Clean the container's edge with a sponge so that the lid's gasket makes good contact with the top of the test device. The top of the air-content test device should then be secured over the base.

- Open both valves and completely fill the air gap between the top of the concrete and the underside of the top of air meter with water until water comes out from another valve, and then close the ball valves.

- The top of the meter is then pressurized to zero percent with the integrated hand pump. Release the pressure at the top, and check that the gauge is stable before reading the air void contents in percent on the gauge at the top of the meter.

Figure 3.10: Concrete air meter

3.9 Casting Procedure

The casting procedure starts after the testing of fresh concrete is completed and it involves casting the fresh concrete in 100 x 100 x 100mm molds. For each mixture, 8 cubes are cast. The casting procedure is done in accordance with Norwegian Standard (Standard Norge 2019d). On the inner surface of the molds, a thin layer of oil is applied to prevent the concrete from sticking to the moulds. Fresh concrete is filled into the molds in three layers. Each layer is compacted with 25 strokes by hand using compacting rod across the molds' cross section. The excess concrete above the upper edge of each mold is removed with a towel, and the top surface of the molds is carefully leveled using the compacting rod.

3.10 Curing Regimes

After casting, all specimens are cured using 3 different curing regimens. All specimens are kept in a climate chamber for pre-conditioning. After 5-6 hours of initial air curing all the specimens are divided in two groups, reference group and ACC group. Reference specimens are immersed into a water container for 1 and 28 days of water curing. ACC specimens are placed in the carbonation chamber for carbonation curing. After carbonation curing, all the carbonated specimens are kept in a water container at about 20±2°C for further water curing for 1 and 28 days. Curing regimes are carried out as follows:

3.10.1 Air Conditioning

All concrete specimens from both groups are pre-conditioned in a climate chamber at a RH of 65% and at a temperature of 25°C. The pre-conditioning time ranged from 5 to 6 hours of air curing. The reason behind 5-6 hours of initial air curing is the setting time of industrial cement. Therefore, after pre-conditioning, the specimens are hardened enough to be demoulded and transported at young age without any damages for further ACC and water curing. The climate chamber used in this study is of type CTS C-40/600 as shown in Figure 3.11. After the initial air curing, all the specimens are demoulded and then tagged based on the assigned coding system, without damaging the surfaces, as it can be seen to the right in Figure 3.12
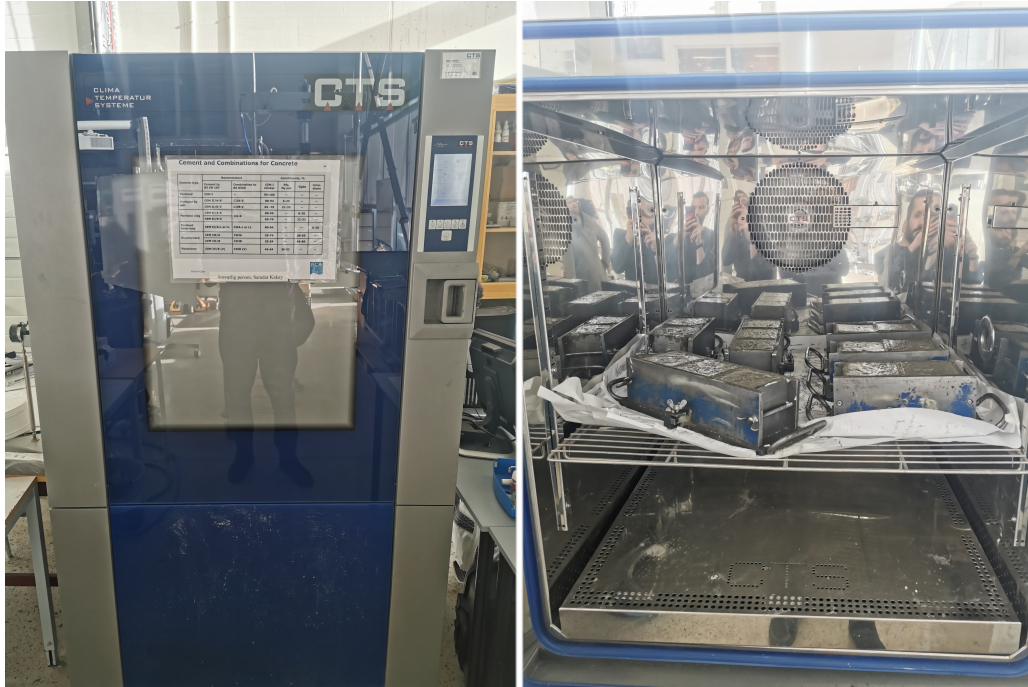
Figure 3.11: Pre-conditioning in Climate Chamber

Figure 3.12: Specimens after demoulding

3.10.2 Water Curing

After air conditioning, all the concrete specimens from the reference group are demoulded and then placed in room temperature water at 20±2 °C for the 1 (initial) and 28 days compressive strength testing. Figure 3.13 shows water curing of reference specimens.
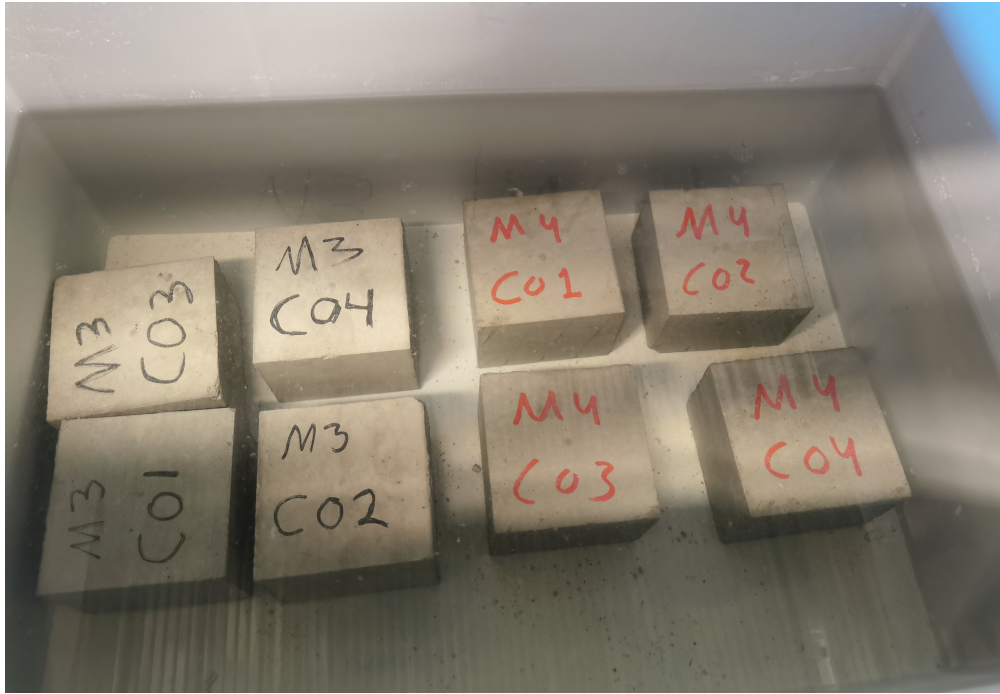
Figure 3.13: Specimens immersed in water

3.10.3 Carbonation Curing

After pre-conditioning, the ACC specimens are demoulded and then placed into the carbonation chamber. The carbonation chamber is in a laboratory environment with a temperature of 20±2 °C. A metal net sheet of 2mm thickness is placed over a plastic spacer inside the chamber. This is to allow the bottom surface of specimens to be exposed to CO_2 gas and so have the same condition for all specimens inside the chamber. Four specimens are placed on the top of the metal net sheet concurrently. The inlet and outlet valves are fixed to the carbonation chamber in order to vacuum the chamber and then fill it with CO_2 gas. The air inside the chamber is removed by using a vacuum pump (an air compressor) before injecting CO_2 gas. The CO_2 inlet valve is closed while the outlet valve is opened during the vacuum process. The CO_2 gas is then

injected inside the chamber until the pressure gauge showed the desired pressure (4 and 6 bar). The airtight chamber is kept pressurized for the whole carbonation time (3 and 4 hours). Table 3.6 shows the applied duration and pressure on each mixture. The specimens and combinations of CO_2 pressures and exposure time to CO_2 are listed below:

- A total eight mixtures, M1 to M8 of industrial concrete specimens are casted with 2 different water to cement ratios, 0.4 and 0.6.

- Two different pressure combinations of 4 and 6 bar and 2 exposure durations of 3 and 4 hours, respectively are chosen to carry out the accelerated carbonation curing.

- Four cubes of 100mm size from each concrete mixture are cured at the same time.

- To calculate the weight gain, the weight of each specimen is recorded before and after carbonation using a high-sensitivity electronic scale.

Table 3.6: Applied duration and pressure on mixtures

CO_2 curing	M1	M2	M3	M4	M5	M6	M7	M8
[W/C] ratio	0.6	0.6	0.6	0.6	0.4	0.4	0.4	0.4
Duration [Hour]	3	4	4	3	4	3	4	3
Pressure [Bar]	4	6	6	4	6	4	6	4

The procedure of carbonation curing is as follows:

- Silica gel is weighed and placed at the bottom surface of the chamber before carbonation. After carbonation the silica gel is weighed again in order to calculate the released water during ACC. Silica gel is chosen because of its ability to absorb emitted water due to the chemical reaction between CO_2 gas and cementitious material and hydration process.

- ACC specimens are placed inside the chamber and the chamber is closed and sealed.

- The air compressor is then turned on for 3–5 minutes until the curing chamber is completely devoid of air.

- The CO_2 inlet valve and gas supply are opened when the chamber outlet valve is closed.

- The pressure gauges mounted on the CO_2 gas cylinder are used to regulate and stabilize the gas flow rate for about 2-3 minutes. This step is done to maintain a constant pressure inside the curing chamber.

Figure 3.14 shows specimens placed inside the carbonation chamber just before the carbonation process begins, as well as the pressure gauge during carbonation process.

Figure 3.14: Specimens placed inside the airtight chamber to the left and pressure gauges to the right

3.10.4 After Carbonation Curing

After carbonation curing, further water curing is conducted. All ACC specimens are immersed in water at a temperature of 20±2°C for the rest of the curing (1 and 28 days).

3.11 Density

The density of concrete has a significant impact on its mechanical properties. Denser concrete has more strength, less voids and porosity than less dense concrete. Concrete with fewer voids is less permeable to water and soluble elements. As a result, water absorption will be reduced, and this type of concrete should last longer (Iffat 2015). It is possible to measure the density of concrete in both fresh and hardened conditions in accordance with Norwegian Standards; Testing fresh concrete - Part 6: Density (Standard Norge 2019b) and Testing hardened concrete part 7: Density of hardened concrete (Standard Norge 2019f). In this study, the density measurement of fresh and hardened concrete are performed.

3.11.1 Density of fresh concrete

The following procedure is used to determine the density of fresh concrete:

- Before performing the test, the density container is cleaned and dampened with a damp cloth.

- The density container is weighed to determine its mass (m_1) to the nearest 0.01 kg.

- Fresh concrete is filled into the container in three layers. Each layer is compacted with 25 strokes by hand using compacting rod across the container's cross section.

- The top surface of the container is smoothed and leveled with compacting rod and the excess concrete above the upper edge of the container is removed with a trowel.

- The density container is weighed with its contents to determine its mass (m_2) to the nearest 0.01 kg.

- The density of fresh concrete is then calculated by the following formula:

$$D = \frac{m_1 - m_2}{V},\tag{3.3}$$

where D is the density of fresh concrete in kg/m^3, m_1 is the mass of the empty density container in kg, m_2 is the mass of the density container completely filled with compacted concrete in kg and V is the volume of the density container in m^3. The density of fresh concrete is set to the

nearest 10 kg/m^3 according to Standard Norge (2019b). The density container has a volume of 8L as shown in Figure 3.15.

Figure 3.15: Density container filled with fresh concrete

3.11.2   Density of hardened concrete

For measuring the volume of the concrete specimens by water displacement, a typical stirrup arrangement as shown in Figure 3.16 is used. To determine the density of hardened concrete, the mass (m) of a specimen is measured in air. A water container is then placed on a scale, and the scale is zeroed. The specimen is submerged in water while hanging in an apparatus (illustrated in Figure 3.16) to prevent it from touching the container's walls. The weight displayed on the scale represents the volume V of the specimen as water has a density of 1000 kg/m^3. The density

of the concrete is determined by the following formula:

$$D = \frac{m}{V} \tag{3.4}$$

where D is the density of hardened concrete in kg/m^3, m is the mass of the concrete specimen in kg and V is the volume of the concrete specimen in m^3 as shown in equation 3.5 and illustrated in Figure 3.16

$$V = \frac{\text{Displaced water weight}}{\rho_w} \tag{3.5}$$

Figure 3.16: Typical stirrup arrangement

3.12 Porosity Measurement of hardened concrete (PF-Method)

The number of pores or cavities in a material, such as pores in concrete, is known as porosity. Porosity is usually given as a percentage of the total volume. In general, porosity can be defined as the internal volume that can be filled with water. The porosity of concrete affects its properties in a variety of ways such as the composition of concrete, casting in practice, maturing and hardening, cement reactions, and freezing risks. It is critical to have the ability to influence the type of porosity (Tepfers 2012). It should be noted that not just the pores but also their shapes and dimensions influence the concrete properties. Figure 3.17 shows the distribution between solids and different pores in hardened cement with varying w/c ratio. It can be seen that capillary pores occur at w/c = 0.4, and the amount increases sharply with an increasing w/c ratio. Increasing the w/c ratio therefore gives an increasing proportion of pores, while the solid proportion decreases. This is the reason why the strength and the density decreases rapidly with an increasing w/c ratio (Gjerp et al. 2004). For example, we can read from Figure 3.17 that at w/c = 0.4, will approx. 70% be solids and approx. 30% pores. If the w/c ratio is increased to 0.6, the solids content will decrease to 50%, and the pore volume increases correspondingly to close to 50%.
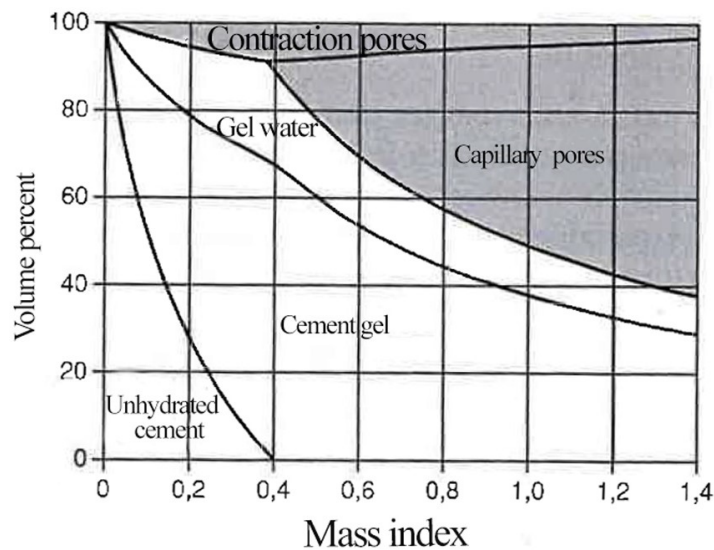
Figure 3.17: The distribution between solids and different pores in hardened concrete with varying w/c ratio. Figure from (Gjerp et al. 2004)

3.12.1 The PF-Method

The PF-method is used to calculate different porosities in hardened concrete. The workflow of this procedure is given in the following steps, as given in the Norwegian Public Roads Administration handbook R210 Laboratory investigations (Statens Vegvesen 2015, p.327-330), see attachment C.1 for full procedure (limited procedure 4.2 The PF-method is conducted in this study).

When performing this test, the total sample volume should be greater than 200 cm^3. Each of the samples should also have a volume equal to, or greater than 50 cm^3. And last, the smallest dimension of the specimen should be between 10 mm and 50 mm (i.e the diameter or thickness of a cylinder, or the smallest thickness of a cube).

- The test samples should be air dried in an oven, at 105°C for 7 days (or, until the total weight loss is less than 0.01% per hour). The specimens should then be covered with plastic and left in room temperature for a minimum of 2 hours to cool down. The weight g_1 is then measured with a digital scale.

- The specimens are then submerged in a container filled with water and left for 7 days. The specimens are then taken out and wiped with a damp cloth to remove any excess moisture. Immediately after this, the weight g_2 should be recorded to prevent loss of absorbed water.

- The next step will be to immerse the samples in a pressurized tank filled with distilled water at a pressure of 50 atm. Leave the samples in the tank for 48 hours before extracting them. Wipe the specimens with a cloth and record the weight g_4 immediately after the extraction. This is in order to prevent the water from being squeezed out of the specimens.

The machines and equipment that are used to perform the PF-method is shown in Figure 3.18.

Figure 3.18: Equipment used to carry out the PF-method. The cutting machine is shown on the left and the pressurized tank setup is shown on the right.

The following four formulas 3.6, 3.7, 3.8 and 3.9 are used to calculate the different porosities of hardened concrete:

$$P_s = \frac{g_2 - g_1}{V \cdot \rho_w} \tag{3.6}$$

P$_s$ is the unitless suction porosity, g$_1$ and g$_2$ are the weights in kg and V is the volume of the test samples are calculated using the typical stirrup arrangement as described in subsection 3.11.2 and also shown in Figure 3.19. The water density ρ_w, is set equal to 1000 kg/m^3. According to Statens Vegvesen (2015), suction porosity (capillary porosity) refers to the proportion of pores in hardened concrete that is relative to the volume of the tested specimen and is large enough to absorb water by capillary action.

$$P_m = \frac{g_4 - g_2}{V \cdot \rho_w} \tag{3.7}$$

P$_m$ is the unitless macro porosity, g$_2$ and g$_4$ are the weights in kg and V is the volume in m^3 of the test samples as it also is in the formula above. The macro porosity is the proportion of pores that are first filled with water when the specimens are exposed to water while under pressure.

This is also relative to the volume of the tested specimen.

$$P_t = P_s + P_m \tag{3.8}$$

P_t is the unitless total porosity. The total porosity is the sum of suction porosity (P_s) and macro porosity (P_m). Figure 3.18 illustrates the pressure tank and cutting machine used in this procedure and Figure 3.19 shows the equipment used for determining the volume of the specimens. The weight of the displaced water divided by ρ_w is the volume (V) of the specimen placed in water shown in equation 3.5. This is the same method as used in section 3.11.2.

$$PF = \frac{P_m}{P_t} \tag{3.9}$$

The PF-value gives an indication on how durable the concrete is regarding frost resistance according to Stefan Jacobsen (1999) and shown in equation 3.9. A study performed by Shao (2014) shows that concrete subjected to ACC is more durable against freeze-thaw exposure when comparing to steam and sealed-hydrated cured as illustrated in Figure 2.3. This is because dilation decreases when the PF value increases as illustrated in 3.20. Since PF = P_m/P_t (3.9) and $P_t = P_s + P_m$ (3.8), by substituting equation 3.8 into 3.9 the following equation 3.10 is given.

$$PF = \frac{1}{\frac{P_s}{P_m} + 1} \tag{3.10}$$

To obtain a higher PF value suction porosity (P_s) should decrease and macro porosity (P_m) should increase as shown in equation 3.10.

Figure 3.19: Specimen samples placed in water to the left, and typical stirrup arrangement to the right
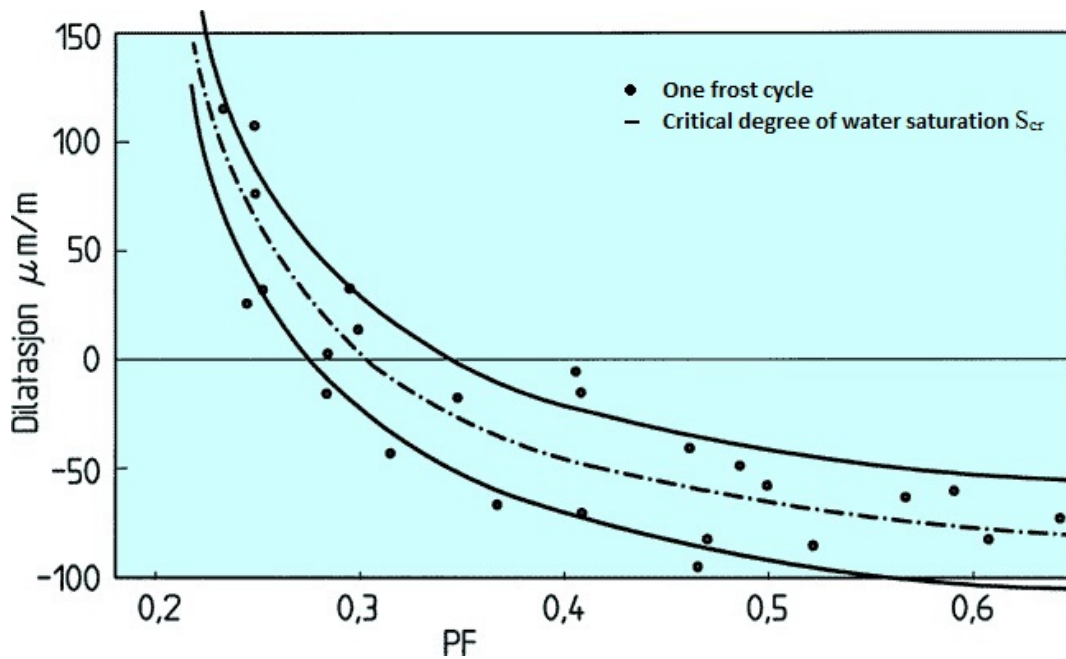
Figure 3.20: When PF-value increases the dilation decreases hence better frost resistance according to Stefan Jacobsen (1999)

3.13   pH Measurement of Hardened Concrete

Determination of the pH value in the hardened concrete is performed according to the procedure prepared by Grubb et al. (2007) and is described in Testing pH of concrete - Need for a standard procedure (se attachment C.5). An aqueous solution of the powdered material must be made to measure the pH of solid materials such as concrete. This dilutes the solid material's concentration. A review of various standards and commentaries indicates that dilution ratios vary between 1:9 and 1:20.

This method is based on mixing pulverized powder samples with solvent and measuring the pH of each concrete mixture after 1 and 28 days of curing. The pH measurement of solution is performed using VWR pH 110M meter (range = -2.00 to 16.00 pH, accuracy = ±0.01% of full scale) at a room temperature of 23±2°C with a combination of a pH electrode and an Automatic Temperature Compensation (ATC) probe. The procedure begins with calibration of the electronic pH meter by using two buffer solutions with pH values of 4.01 and 7.00 before each use. The pH value is recorded when the rate of change is less than 0.01 pH per minute. To verify the sensitivity of the pH measurement system, pure distilled water with a pH of 7.00 is tested as a reference prior to any pH measurement on cement-based products. Figure 3.21 shows the pH Instrument (right picture) and equipment (left picture) used to measure pH value. The workflow for performing this test is described in the following steps:

- All pH measurements are performed using distilled water as a solvent at room temperature.

- A thin layer of the specimens' outer surface is crushed and grinded by hand using a mortar. After grinding, the powder samples are sieved passing 45 μ particle size fraction.

- A total of 5 grams of fine grinded concrete powder is then mixed with 10ml of distilled water in a small plastic container.

- The solutions are vigorously mixed for 5 minutes and settled for 1-2 minutes after mixing.

- Filtration is not required for the solutions because it has little effect on pH measurement.

Figure 3.22 illustrate the tools used in sieving.

Figure 3.21: Equipment used in pH test to the left and pH Instrument to the right.

Figure 3.22: Illustration of the mortar on the left, fine cement powder in the middle and scale used for testing on the right.

3.14 Compressive Strength

Concrete's compressive strength is the largest force that is calculated by dividing the failure load by the cross sectional area resisting the load and reported in MPa = N/mm^2. The compression test is conducted on the concrete specimens in accordance with Norwegian Standard, Testing hardened concrete Part 3: Compressive strength of test specimens (Standard Norge 2019e). The compressive strength F_c is given by

$$F_c = \frac{F}{A_c} \tag{3.11}$$

where F is the failure load in newton and A_c is the cross-sectional area of the specimen in mm². The compressive strength of all mixtures are determined using the 100mm cubical concrete specimens. Compressive strength is measured after 1 and 28 days for both carbonated and water cured specimens. An hydraulic, automatic compressive testing machine (Toni Technik 1142, shown in Figure 3.23) is used to crush the specimens with an applied loading rate of 0.6 MPa/s until failure.
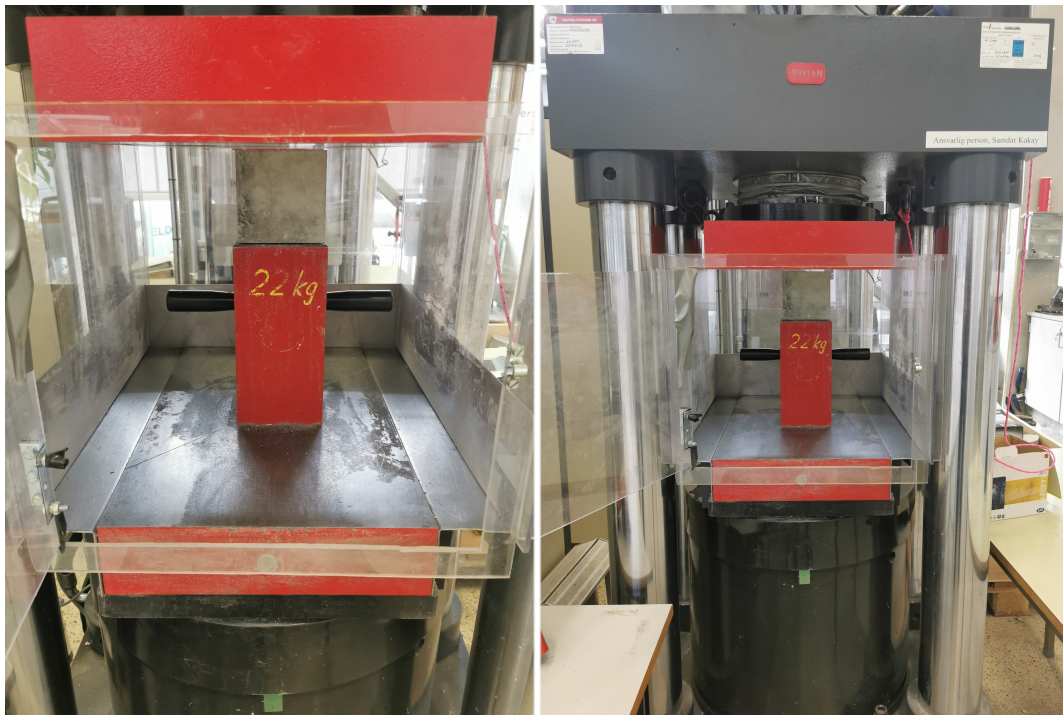
Figure 3.23: Compressive strength testing machine

3.15   Water Loss and Weight Gain

The amount of CO_2 successfully sequestered in concrete can be used to directly evaluate ACC's effectiveness. The effectiveness of ACC is expressed in terms of the net CO_2 uptake as a percentage of dry binder during carbonation curing. The general expression for CO_2 uptake can be expressed as:

$$CO_2\,uptake\% = \frac{Mass_{aft.CO_2} + Water_{lost} - Mass_{bef.CO_2}}{Mass_{binder}}, \tag{3.12}$$

where $Mass_{aft.CO_2}$ is the mass after carbonation curing and $Mass_{bef.CO_2}$ is the mass before carbonation curing. For all concrete specimens the weight is noted before and after carbonation as shown in Figure 3.24. A water loss occurs as a result of moisture evaporation, which condenses on the curing chamber's wall as it can be seen in Figure 3.25 (right picture). The evaporation occurs as a result of the heat generated by the carbonation reaction. The weight of emitted water is measured by weighing the placed Silica Gel inside the chamber before and after carbonation process. Tissue papers are used to wipe the condensed water off the chamber's wall, and weighted before and after wiping. All readings are recorded by a digital balance with an accuracy of 0.1g.

Figure 3.24: Weight gain test "specimen". Measurement before (left) and after (right) carbonation.

Figure 3.25: Silica gel to the left and water loss to the right. Note the water moisture on the sides of the chamber and on the top of the concrete.

Figure 3.26: Weight gain test "tissue paper". The dry paper (left) is used on the inside of the chamber after carbonation curing and then weighed again (right).

Chapter 4

Results and Discussion

In this chapter, results from the lab will be presented followed by our interpretation of the results. The main properties of the concrete is shown sequentially. First slump and air content followed by density, porosity, pH, weight gain due to carbonation and differences in compressive strength. The resulting concrete properties of ACC is compared with the reference samples that has been water-cured.

4.1   Slump and Air Content

The slump test and air content measurements for the eight mixtures are presented in Table 4.1 The data shows that there are small differences between mixtures of 0.4 and 0.6 w/c ratio. All mixtures except M5 had a total slump collapse, this is most likely due to high amount of water and superplasticizer in the concrete mixtures. When additional water is added to the concrete and when the composition of the cement and the aggregates is unchanged, the distance between the solid particles will be greater. This causes the particles to flow more easily around each other and therefore the slump becomes larger (Gjerp et al. 2004). M5 with a 0.4 w/c ratio had the lowest amount of added superplasticizer. This is likely the reason for the lower slump observed.

The amount of air content in the concrete for all mixtures varies between 0.7 to 2.0 % which is expected in concrete mixtures without adding air-entraining agents. Concrete without added air-entraining agents will contain approx. 2% air (Gjerp et al. 2004)

Table 4.1: Slump and Air content results. The table is sorted based on the case column, therefore the mixture numbers are not in order.

Mixture No.	Case	Air content [%]	Slump [cm]
M1	WC0.6-P4T3-D1 WC0.6-Ref-D1	1.2	21
M2	WC0.6-P6T4-D1 WC0.6-Ref-D1	1.1	20
M4	WC0.6-P4T3-D28 WC0.6-Ref-D28	0.7	24
M3	WC0.6-P6T4-D28 WC0.6-Ref-D28	0.7	24
M6	WC0.4-P4T3-D1 WC0.4-Ref-D1	1.2	23
M7	WC0.4-P6T4-D1 WC0.4-Ref-D1	1.0	23
M8	WC0.4-P4T3-D28 WC0.4-Ref-D28	1.0	24
M5	WC0.4-P6T4-D28 WC0.4-Ref-D28	2.0	16

4.2 Density

The density measurements of fresh and hardened concrete is presented in table 4.2. Fresh density is measured before casting in molds. The hardened density is measured after 1 and 28 days of further water curing. For hardened density, each value in the table represents an average of 2 specimens. The higher the w/c ratio is, the lower the concrete density is, which is in agreement with the fresh density where mixtures with w/c ratio of 0.6 have lower fresh density than mixtures with w/c ratio of 0.4. Previous studies have shown an increase in density of concrete subjected to short-term carbonation ((Jerga 2004),(Monkman and Shao 2010). Hardened density differences between ACC specimens and reference specimens are observed. It is not possible to deduce a pattern from the results as these differences vary from specimen to specimen. This is likely due to inaccurate measurement equipment as the differences are relatively small.

Table 4.2: Density of fresh and hardened concrete

Mixture No.	Case	Hardened Density [Kg/m^3]	Fresh Density [Kg/m^3]
M1	WC0.6-P4T3-D1	2400	2420
	WC0.6-Ref-D1	2390	
M2	WC0.6-P6T4-D1	2390	2440
	WC0.6-Ref-D1	2430	
M4	WC0.6-P4T3-D28	2410	2420
	WC0.6-Ref-D28	2450	
M3	WC0.6-P6T4-D28	2400	2400
	WC0.6-Ref-D28	2380	
M6	WC0.4-P4T3-D1	2410	2450
	WC0.4-Ref-D1	2400	
M7	WC0.4-P6T4-D1	2440	2450
	WC0.4-Ref-D1	2400	
M8	WC0.4-P4T3-D28	2460	2460
	WC0.4-Ref-D28	2430	
M5	WC0.4-P6T4-D28	2450	2440
	WC0.4-Ref-D28	2470	

4.3 Porosity

The porosity results are shown in Table 4.3. It includes suction porosity, macro porosity, total porosity, and PF-value. All tests are carried out in accordance with the PF-method, which is a limited procedure of the "426 Capillary suction rate and porosity" (Statens Vegvesen 2015, p.327, own translation) given by the Norwegian Public Roads Administration handbook R210.

Compressive strength - is expected to increase when the porosity decreases according to Lian et al. (2011). The results show no indication that compressive strength is increased when porosity decreases. Since porosity measurements take approximately 14 days to finish and are started at the same time as the compression test. The porosity might experience small changes due to a continuous hardening for 14 days since the test samples are 14 days old when the test is finished. This could also be a possible source of error in the testing. Porosity is measured by absorbed water weight inside the pores. If the measurement is not performed at exactly the same time the specimen samples are removed from the water, then the absorbed water that is going to measure the volume of the pores can flow out of the samples before it is measured. The relationship between porosity and compressive strength is shown in Figure 4.1 for all mixtures.

Table 4.3: Porosity results

Mixture No.	Case	Suction porosity	Macro porosity	Total porosity	PF- value
M1	WC0.6-P4T3-D1	0.141	0.008	0.133	0.064
	WC0.6-Ref-D1	0.145	0.007	0.138	0.052
M2	WC0.6-P6T4-D1	0.149	0.010	0.139	0.072
	WC0.6-Ref-D1	0.153	0.010	0.143	0.070
M4	WC0.6-P4T3-D28	0.133	0.008	0.126	0.062
	WC0.6-Ref-D28	0.128	0.007	0.121	0.058
M3	WC0.6-P6T4-D28	0.141	0.007	0.133	0.056
	WC0.6-Ref-D28	0.155	0.005	0.150	0.031
M6	WC0.4-P4T3-D1	0.128	0.008	0.120	0.062
	WC0.4-Ref-D1	0.143	0.003	0.139	0.024
M7	WC0.4-P6T4-D1	0.130	0.003	0.127	0.022
	WC0.4-Ref-D1	0.137	0.002	0.134	0.017
M8	WC0.4-P4T3-D28	0.113	0.009	0.103	0.091
	WC0.4-Ref-D28	0.117	0.006	0.111	0.055
M5	WC0.4-P6T4-D28	0.107	0.011	0.096	0.119
	WC0.4-Ref-D28	0.118	0.012	0.106	0.116

Figures 4.2 and 4.3 show the specimens with a w/c ratio of 0.4 and 0.6 respectively. The results indicate that total porosity in concrete is reduced as a result of carbonation curing. Only one of the specimens shown in Figure 4.3 deviates from this pattern. The reason for this outlier may be due to an error during testing of that specimen. Porosity measurements are highly reliant on executing the same weighing procedure each time. When the specimens are finished in the pressure tank the measurement needs to be performed quickly before water in the specimen flows back out. If this was not done for that particular sample it could be the reason for the one reference sample in the top left corner of Figure 4.3 showing a lower total porosity than the CO_2 cured one.
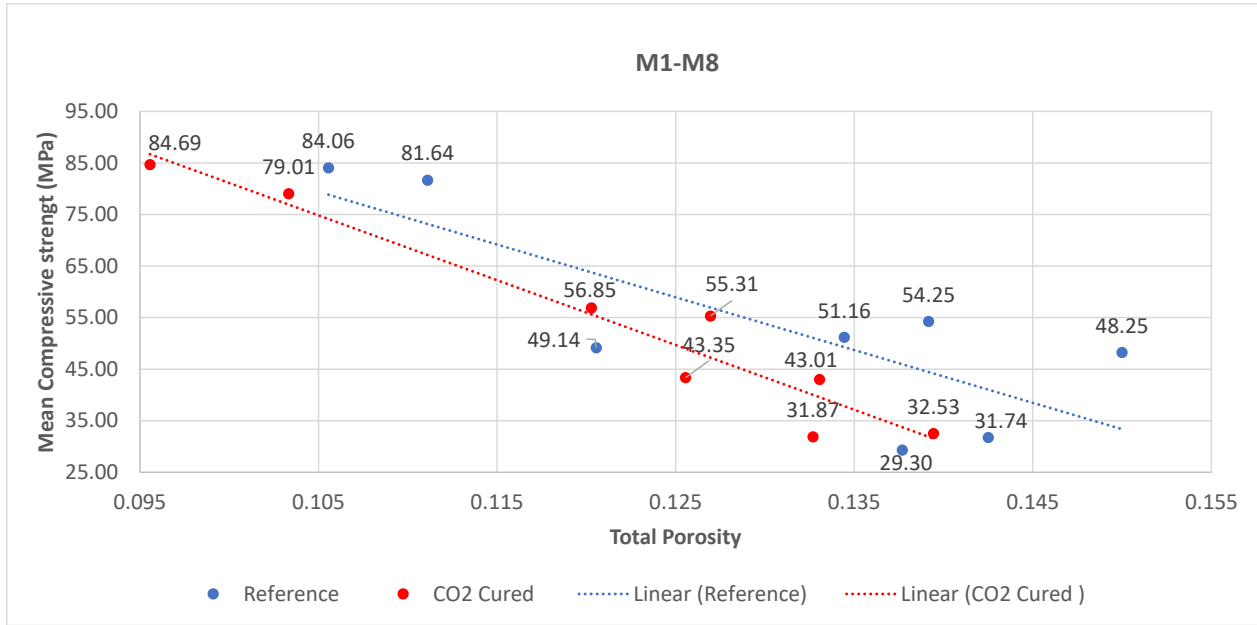
Figure 4.1: Total porosity, compressive strength and trend lines for all mixtures when ACC is performed.
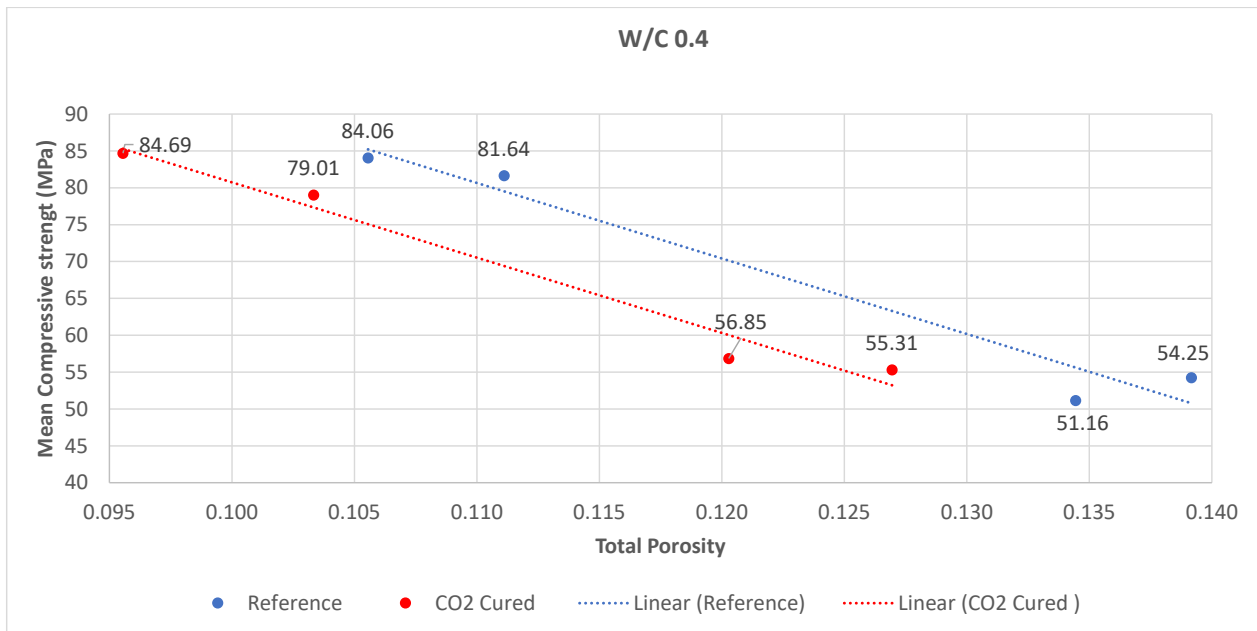
Figure 4.2: Total porosity, compressive strength and trend lines for specimens with w/c ratio of 0.4
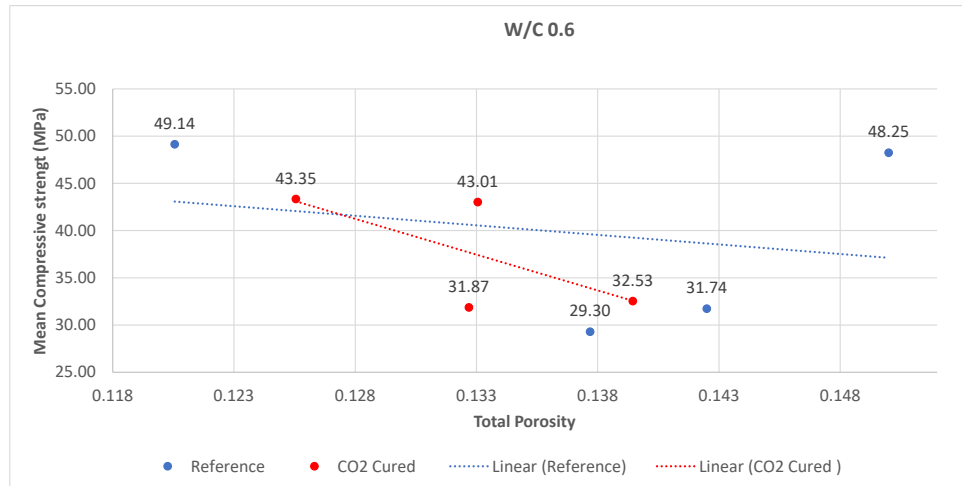
Figure 4.3: Total Porosity, compressive strength and trend lines for specimens with w/c ratio of 0.6. The reference on the top left, is the only reference to show lower total porosity value than the CO_2 cured specimens.

Frost resistance - Cement with higher PF-Value is more durable against freezing and thawing as illustrated in Figure 2.3 due to lower dilation (illustrated in Figure 3.20). When comparing the results of the CO_2 cured specimens and the reference, a clear indication can be seen that CO_2 curing has positive effects for frost resistance. In order to obtain a higher PF Value (shown with equation 3.10) macro porosity should increase, and suction porosity should decrease. The results illustrated in Figures (4.5) and (4.6) show exactly this, macro porosity is higher for all specimens subjected to ACC except for mixture (M6) and suction porosity is reduced for all mixtures except for (M4). All mixtures exposed to ACC show greater PF-Value (shown in Figure 4.4) hence is expected to have better frost resistance properties.

Figure 4.4: PF-Value

W/C Ratio 0.6

	M1		M2		M3		M4	
	CO2	Ref.	CO2	Ref.	CO2	Ref.	CO2	Ref.
Macro Porosity	0.008	0.007	0.010	0.010	0.007	0.005	0.008	0.007
Suction Porosity	0.141	0.145	0.149	0.153	0.141	0.155	0.133	0.128
Total Porosity	0.133	0.138	0.139	0.143	0.133	0.150	0.126	0.121
PF Value	0.064	0.052	0.072	0.070	0.056	0.031	0.062	0.058
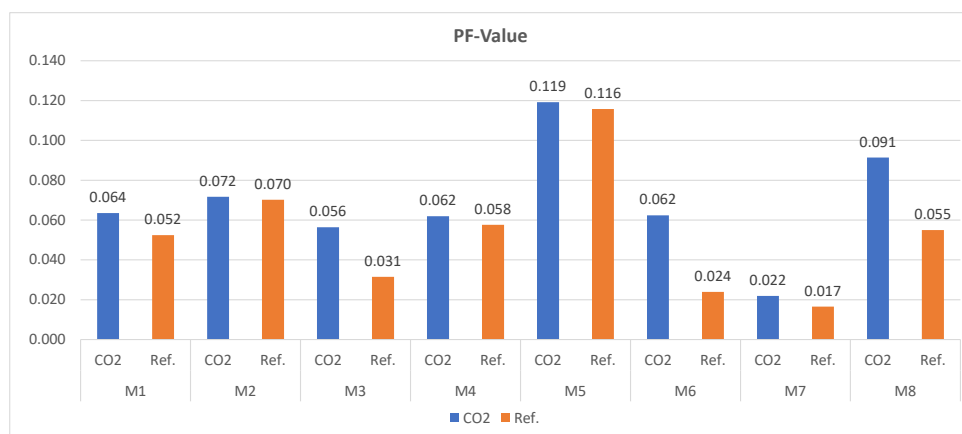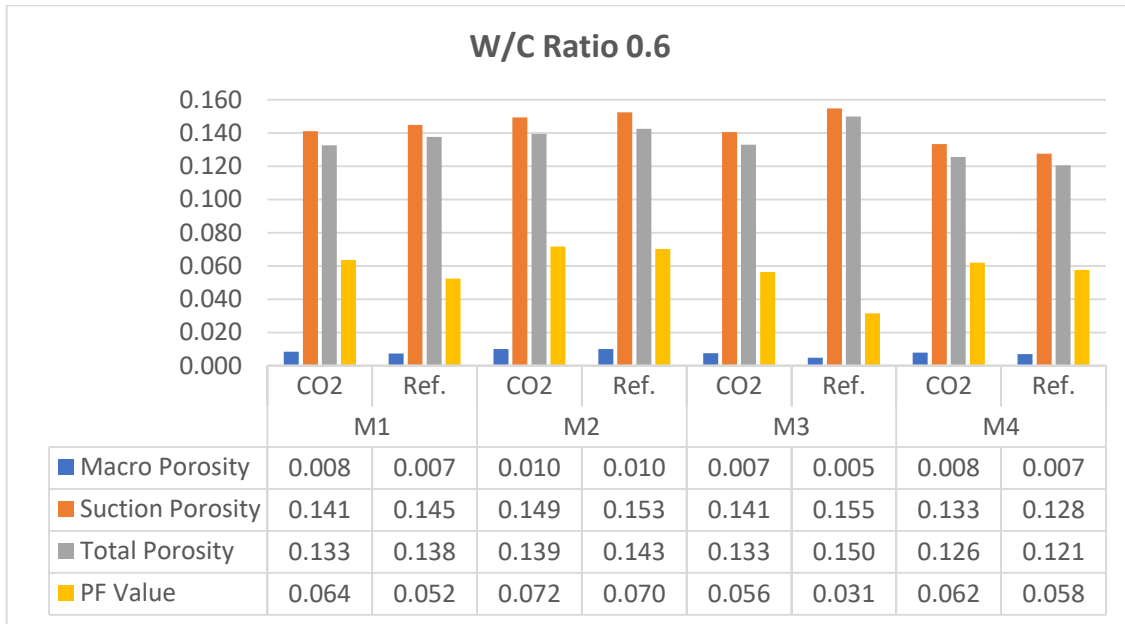
Figure 4.5: Porosity results for specimens with water to cement ratio of 0.6

W/C Ratio 0.4

	M5		M6		M7		M8	
	CO2	Ref.	CO2	Ref.	CO2	Ref.	CO2	Ref.
Macro Porosity	0.011	0.012	0.008	0.003	0.003	0.002	0.009	0.006
Suction Porosity	0.107	0.118	0.128	0.143	0.130	0.137	0.113	0.117
Total Porosity	0.096	0.106	0.120	0.139	0.127	0.134	0.103	0.111
PF Value	0.119	0.116	0.062	0.024	0.022	0.017	0.091	0.055
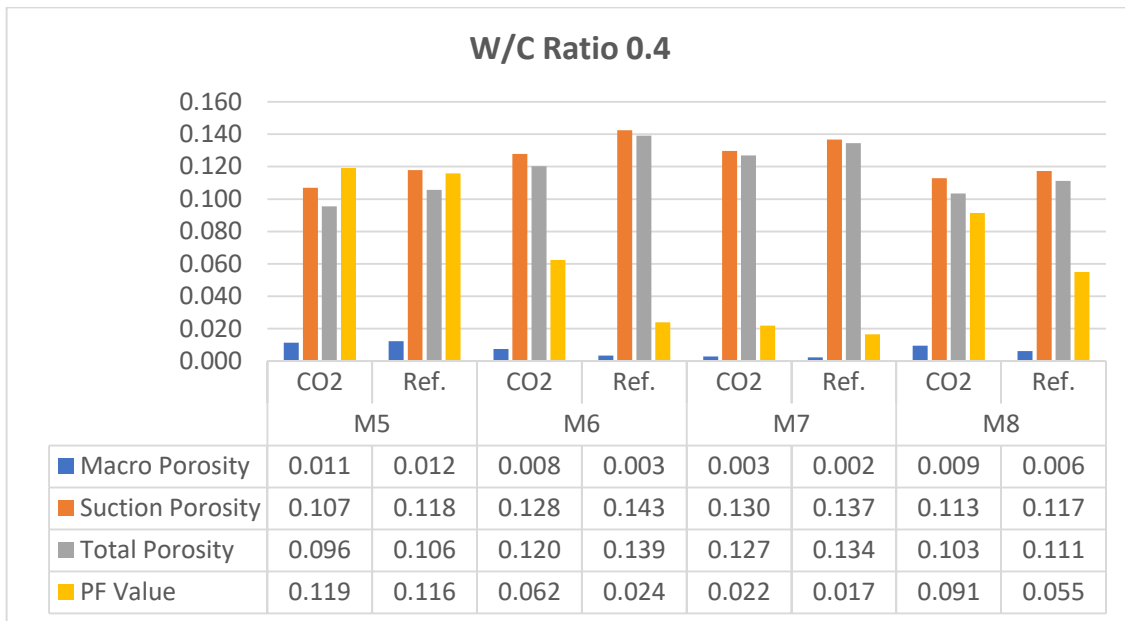
Figure 4.6: Porosity results for specimens with water to cement ratio of 0.4

4.4 pH Measurement

The results from the test of the pH value in the hardened concrete are presented in Figures 4.7 and 4.8. The y-axis shows the pH value. Concrete powder is ground from one cube of each mixture after 1 day and 28 days of curing. The concrete powder is collected after the compression test is performed. All results are presented in Table 4.4
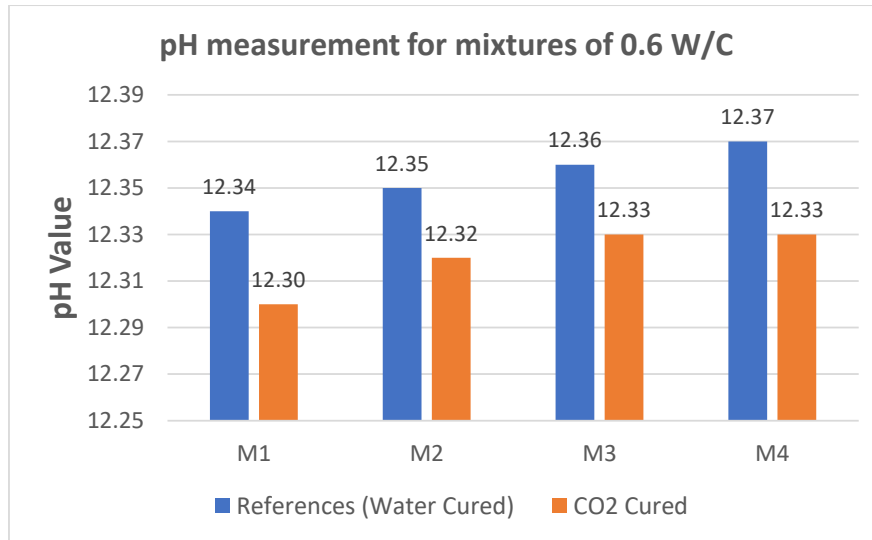
Figure 4.7: pH values for mixtures of 0.6 w/c cured at 1 and 28 days
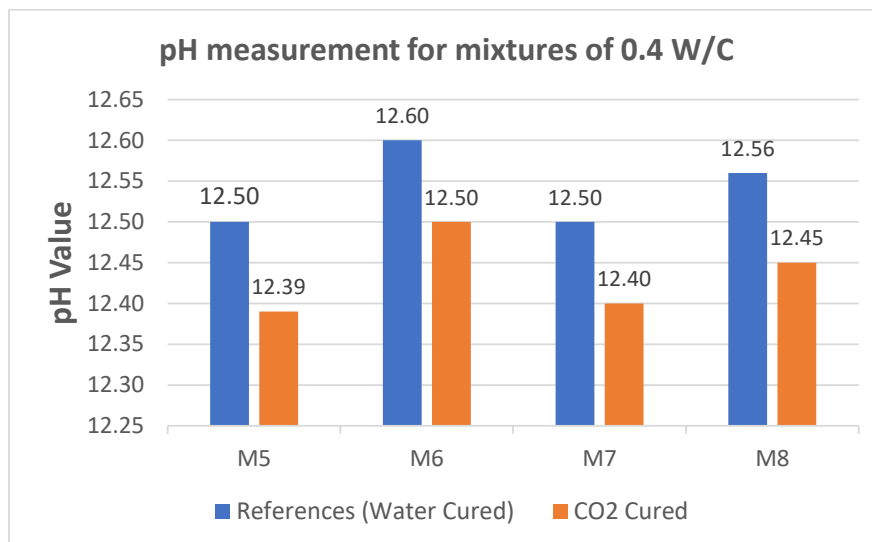
Figure 4.8: pH values for mixtures of 0.4 w/c cured at 1 and 28 days

Table 4.4: pH values of hardened concrete

Mixture No.	Case	pH
M1	WC0.6-P4T3-D1	12.30
	WC0.6-Ref-D1	12.34
M2	WC0.6-P6T4-D1	12.32
	WC0.6-Ref-D1	12.35
M4	WC0.6-P4T3-D28	12.33
	WC0.6-Ref-D28	12.37
M3	WC0.6-P6T4-D28	12.33
	WC0.6-Ref-D28	12.36
M6	WC0.4-P4T3-D1	12.50
	WC0.4-Ref-D1	12.60
M7	WC0.4-P6T4-D1	12.40
	WC0.4-Ref-D1	12.50
M8	WC0.4-P4T3-D28	12.45
	WC0.4-Ref-D28	12.56
M5	WC0.4-P6T4-D28	12.39
	WC0.4-Ref-D28	12.50

As can be seen from Figures 4.7 and 4.8, the pH values for carbonated samples of all mixtures were in the range of 12.3 to 12.5 compared to their references (non-carbonated samples) that were in the range of 12.34 to 12.6. Gas pressure effect and carbonation curing duration effect was not noticeable for pH change, because gas pressures of both 4bar and 6bar of 3 hours and 4 hours, respectively resulted in similar pH values after 1 and 28 days of curing.

4.5 Weight Gain due to Carbonation

The amount and differences in weight gain is a result of varying the CO_2 exposure durations, applied pressure and the purity of the gas used. All results from testing are shown in Table 4.5. Each weight gain value in this table represents an average of four carbonated specimens.

Table 4.5: Weight gain as % of cement based on CO_2 exposure duration

Mixture No.	Case	Weight gain as [%]
M1	WC0.6-P4T3-D1	8.46
	WC0.6-Ref-D1	-
M2	WC0.6-P6T4-D1	8.9
	WC0.6-Ref-D1	-
M4	WC0.6-P4T3-D28	9.54
	WC0.6-Ref-D28	-
M3	WC0.6-P6T4-D28	9.34
	WC0.6-Ref-D28	-
M6	WC0.4-P4T3-D1	5.35
	WC0.4-Ref-D1	-
M7	WC0.4-P6T4-D1	6.40
	WC0.4-Ref-D1	-
M8	WC0.4-P4T3-D28	5.08
	WC0.4-Ref-D28	-
M5	WC0.4-P6T4-D28	7.31
	WC0.4-Ref-D28	-

The amount of CO_2 successfully sequestered in concrete is a critical factor in determining the effectiveness of accelerated carbonation curing. The net uptake of CO_2 as a percentage of dry binder expresses the actual sequestrated amount of CO_2 into concrete (Rostami et al. 2012), (Shao et al. 2006) (Rostami et al. 2011). The actual mass of a carbonated concrete element does not include the amount of water lost due to the exothermic reaction that occurs during accelerated carbonation curing (Rostami et al. 2012). As a result, the actual mass of the carbonated concrete element must be increased by the amount of water lost. All ACC specimens showed an increment in weight gain. It seems that concrete with higher water-cement ratio gained more carbonated products as a result of carbonation curing. Considering the mean weight gain for mixtures with 0.4 water-cement ratio at 6 bar pressure and 4 hours of ACC gave about 31% more

weight than the low pressure of 4 bar at 3 hours ACC. It can be noticed that the high pressure of 6 bar at 4 hours ACC for mixtures with 0.6 w/c ratio obtained a slightly mean weight gain of 1 %, compared to the lower pressure of 4 bar at 3 hours ACC for the same mixtures with same w/c ratio. Besides, all ACC specimens of mixtures of 0.6 w/c ratio obtained higher weight gain compared to ACC specimens of mixtures of 0.4 w/c ratio. Therefore, considering the maximum CO_2 sequestration potential, ACC at 6 bar and 4 hours curing exhibited the best performance.

4.6   Compressive Strength

The compressive strength results of all mixtures for both accelerated carbonated specimens subjected to further water curing and water cured specimens (references) are shown and Figures 4.9, 4.10, 4.11 and 4.12 and listed in Appendix B.1. The y-axis shows the compressive strength in megapascal (MPa), each value in figures represents an average of 3 specimens. For ACC curing, the compressive strength test is performed at different stages as follows:

- For the reference samples the measurement is performed after 24 hours of water curing, and for the ACC samples 3 to 4 hours of CO_2 curing followed by continuous water curing for a total of 24 hours

- And second stage is measured after 28 days in water curing for the reference, and for the ACC samples 3 to 4 hours of CO_2 curing followed by continuous water curing for a total of 28 days.

It can be observed from the figures that the compressive strength at 1 day of curing is increased for all ACC specimens compared to their references. M1 and M6 specimens with w/c ratio of 0.6 during 3 hours carbonation curing at 4 bar gas pressure, have shown an 8.8% and 4.8%, respectively increase in compressive strength compared to their references. Moreover, specimens of mixtures M2 and M7 with w/c ratio of 0.6, accelerated carbonation curing of 4 hours at gas pressure of 6 bar have shown about 2.5% and 8.1% increase in strength compared to their references.

For the specimens subjected to water curing for 1 day, the rate of strength gain is slower than that of ACC specimens exposed to water curing for 1 day. On the contrary, the specimens subjected
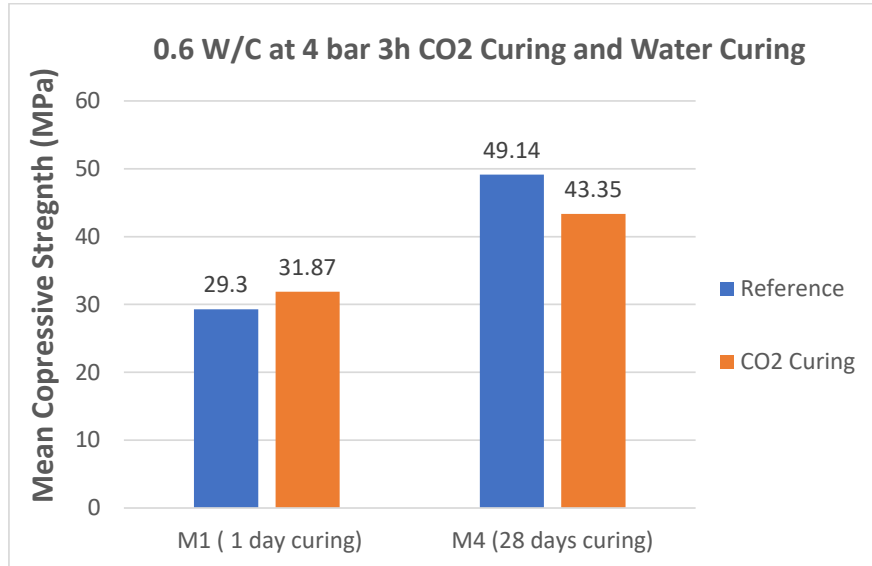
Figure 4.9: Compressive strength for mixtures of 0.6 w/c at 4 bar and 3h ACC curing
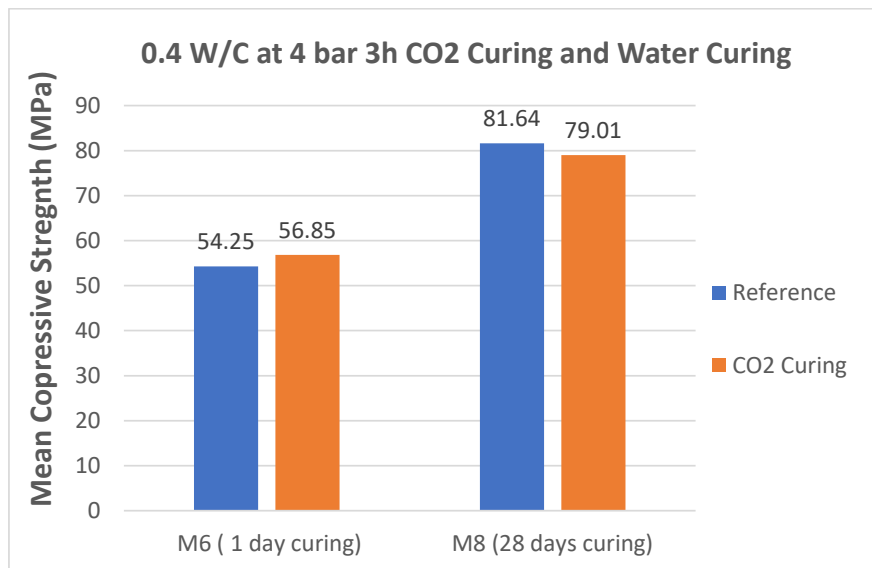
Figure 4.10: Compressive strength for mixtures of 0.4 w/c at 4 bar and 3h ACC curing

to water curing for 28 days showed higher strength gain than ACC's specimens followed with 28 days of water curing. The reduction in strength due to 4 bar pressure and 3 hours of ACC were calculated for M4 and M8 as: 13.4 and 3.3%, respectively. The reduction in strength due to 6 bar pressure and 4 hours of ACC were calculated for M2 to be 12.2%. Whereas M5 showed a slight strength gain with 0.75% compared to its reference. It is worth mentioning that ACC and water cured specimens from mixtures of w/c of 0.4 showed a higher strength gain than specimens of w/c of 0.6 after 1 and 28 days curing. The lower compressive strength of ACC specimens after
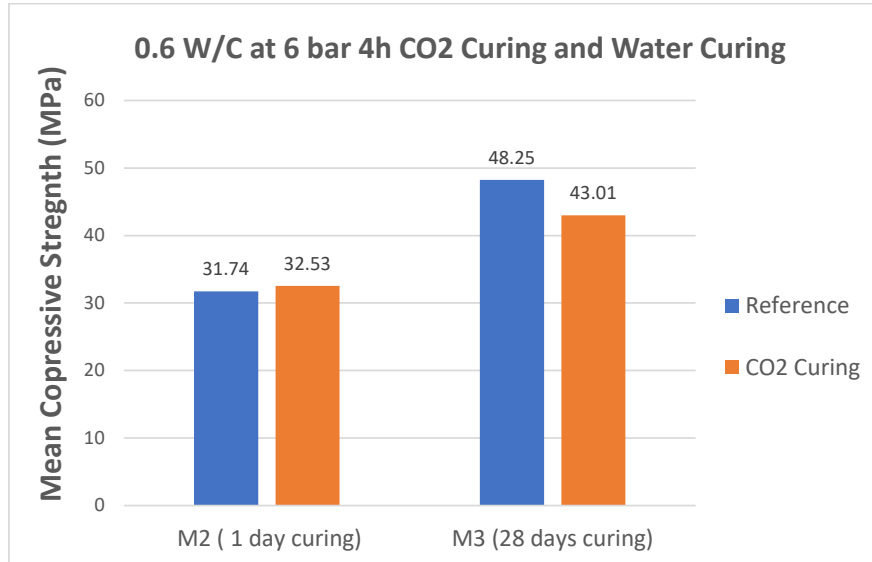
Figure 4.11: Compressive strength for mixtures of 0.6 w/c at 6 bar and 4h ACC curing
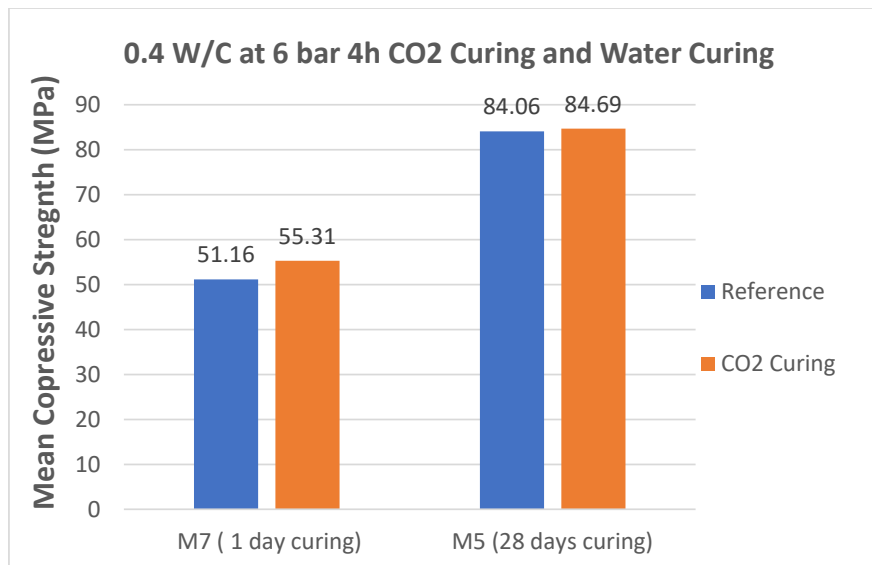
Figure 4.12: Compressive strength for mixtures of 0.4 w/c at 6 bar and 4h ACC curing

28 days of curing can be explained by the fact that larger amounts of nano-calcium carbonate in the cement will no longer be finely divided, but will clump together. As a result, the total specific surface area will be reduced, as will the number of new growth areas for C-S-H formation, as presented in previous chapters. Lower compressive strength can also be caused by the fact that hydration products were decomposed and decreased (Chen et al. 2018).

Chapter 5

Conclusion and Recommendations

5.1 Conclusions

Based on the results of this study the following conclusions can be drawn:

- 5-6 hours of pre-conditioning curing at 60% RH and a temperature of 25°C inside the climate chamber resulted in a max CO_2 uptake of 7.31% and 9.54% by cement mass for the mixtures of w/c ratio of 0.4 and 0.6 respectively.

- Specimens demoulding after initial air pre-conditioning curing for 5-6 hours in a climate chamber is optimal to start ACC since specimens are hard enough to be demoulded without damaging them.

- Concrete specimens with w/c of 0.6 show the highest potential for CO_2 uptake after 3 and 4 hours carbonation curing compared to concrete specimens of w/c of 0.4.

- All carbonated specimens show an increase in compressive strength in the measurements performed after a total of 24 hours starting with a 3-4 hours of carbonation curing and with the remaining hours of water curing compared to their references of 24 hours of water curing exclusively.

- Carbonation cured specimens show a reduction in compressive strength compared to their reference specimens after 28 days of curing. Specimens with w/c of 0.4 obtained a reduction of 3.36% (M8) and a gain of 0.75% (M5) in compressive strength compared to specimens with w/c of 0.6 which had a reduction in compressive strength of 13.35 % (M4) and 12.18 % (M2).

- Specimens with w/c of 0.4 show the highest increase in compressive strength compared to specimens with w/c of 0.6.

- 4 hours of carbonation curing at a pressure of 6 bar show significant increase in compressive strength in comparison with 3 hours of carbonation at 4 bar pressure.

- All ACC specimens show a slight reduction in pH value compared to their reference specimens. This is in line with the expectations as the CO_2 injected into the concrete is acidic.

- Both suction porosity and the total porosity decreased as a consequence of early carbonation curing. The probable reason is that calcium carbonate products filled the free space between solid phases and led to a reduction in porosity.

5.2   Reflections on the research

- **CO_2 uptake** - When using the weight gain method to calculate the CO_2 uptake in the concrete, water loss and mass gained from CO_2 is divided by the mass of cement. This indicates that the CO_2 uptake would be greater if the water to cement ratio is higher. Results from testing show exactly this as the mean value for CO_2 uptake is the highest in specimens containing a higher w/c ratio. The mean value for 0.6 w/c ratio is 9% compared to the 0.4 ratio with only 6%.

- **Change in Density** - How the density is affected as a result of CO_2 curing is challenging to quantify. The scale used to calculate the volume of the specimens gave the exact same volume for all the cubes tested. There may be density differences. However, these differences could be small enough that the measurement equipment was not able to detect it.

- **Porosity** - It is not possible to see any correlation between porosity and compressive strength from the results even though the theory states that less porous materials should withstand higher compression loads. However, differences can be seen for the PF value as it is higher for all the concrete specimens that are CO_2 cured. This is likely because the proportion of macro porosity is increasing and the suction porosity is declining. A higher PF value should lead to increased frost resistance due to less dilation of the concrete.

5.3   Further Work Recommendations

- This study used a single cement (industrial) type for all specimens. Using different types of cement when performing ACC could indicate if a certain cement type is a better choice for ACC.

- Investigate if the use of different mineral admixtures including fly ash (FA), silica fume (SF), ground granulated blast furnace slag (GGBS), metakaolin (MK), and rice husk ash (RHA) could lead to better results.

- Replacing natural aggregates with recycled aggregates, to study the impact it has on ACC, and the differences in physico mechanical properties of the concrete. As an added bonus, recycled aggregates have a lower environmental impact as they usually require less use of concrete.

- Investigate different combinations of CO_2 pressures and exposure durations to determine the optimum conditions of ACC.

- Selection of an optimum duration of air curing as an alternative for further water curing of concrete in post-ACC based on the effective gain of compressive strength.

- Different tests for mechanical properties (Splitting tensile strength and Elastic modulus), durability evaluation (Water permeability and Chloride permeability), drying shrinkage test and Physico-chemical tests (Scanning electron microscopy (SEM) and X-ray diffraction (XRD)) could be investigated.

- More accurate scales should be used to calculate the volume of the different specimens to get a higher degree of accuracy on the test results for density and porosity.

References

Ahmad, S. (2003). Reinforcement corrosion in concrete structures, its monitoring and service life prediction—-a review. *Cement and concrete composites*, 25(4-5):459–471.

Asavapisit, S., G. Fowler, and C. Cheeseman (1997). Solution chemistry during cement hydration in the presence of metal hydroxide wastes. *Cement and Concrete Research*, 27(8):1249–1260.

Atiş, C. D. (2003). Accelerated carbonation and testing of concrete made with fly ash. *Construction and Building Materials*, 17(3):147–152.

Berger, R., J. Young, and K. Leung (1972). Acceleration of hydration of calcium silicates by carbon dioxide treatment. *Nature Physical Science*, 240(97):16–18.

Bertos, M. F., S. Simons, C. Hills, and P. Carey (2004). A review of accelerated carbonation technology in the treatment of cement-based materials and sequestration of co2. *Journal of hazardous materials*, 112(3):193–205.

Chen, Y., P. Liu, and Z. Yu (2018). Effects of environmental factors on concrete carbonation depth and compressive strength. *Materials*, 11(11):2167.

Civilseek (2021). Moisture content determination of soil; oven speedy tester. `https://civilseek.com/moisture-content-determination/`. Accessed: March-2021.

El-Hassan, H., Y. Shao, and Z. Ghouleh (2013). Reaction products in carbonation-cured lightweight concrete. *Journal of materials in civil engineering*, 25(6):799–809.

Fattuhi, N. (1988). Concrete carbonation as influenced by curing regime. *Cement and Concrete Research*, 18(3):426–430.

Gjerp, P., M. Opsahl, and S. Smeplass (2004). Grunnleggende betongteknologi. *Byggenæringens forlag*.

Globalgilson (2020). Concrete air testing: Why, when, how: An in-depth look. `https://www.globalgilson.com/blog/air-content-test`. Accessed: March-2021.

Goto, S., K. Suenaga, T. Kado, and M. Fukuhara (1995). Calcium silicate carbonation products. *Journal of the American Ceramic Society*, 78(11):2867–2872.

Grubb, J. A., H. S. Limaye, and A. M. Kakade (2007). Testing ph of concrete. *Concrete international*, 29(4):78–83.

Guhua, L. (2006). Effect of nano-materials on durability of concrete. *Chen Du: Southwest Jiaotong University*.

Haselbach, L. M. and J. N. Thomle (2014). An alternative mechanism for accelerated carbon sequestration in concrete. *Sustainable Cities and Society*, 12:25–30.

Iffat, S. (2015). Relation between density and compressive strength of hardened concrete. *Concrete Research Letters*, 6(4):182–189.

Jerga, J. (2004). Physico-mechanical properties of carbonated concrete. *Construction and Building Materials*, 18(9):645–652.

Kashef-Haghighi, S. and S. Ghoshal (2010). Co2 sequestration in concrete through accelerated carbonation curing in a flow-through reactor. *Industrial & engineering chemistry research*, 49(3):1143–1149.

Kashef-Haghighi, S. and S. Ghoshal (2013). Physico–chemical processes limiting co2 uptake in concrete during accelerated carbonation curing. *Industrial & Engineering Chemistry Research*, 52(16):5529–5537.

Lee, S., W. Park, and H. Lee (2013). Life cycle co2 assessment method for concrete using co2 balance and suggestion to decrease lcco2 of concrete in south-korean apartment. *Energy and Buildings*, 58:93–102.

Lian, C., Y. Zhuge, and S. Beecham (2011). The relationship between porosity and strength for porous concrete. *Construction and Building Materials*, 25(11):4294–4298.

Liang, C., B. Pan, Z. Ma, Z. He, and Z. Duan (2020). Utilization of co2 curing to enhance the properties of recycled aggregate and prepared concrete: A review. *Cement and Concrete Composites*, 105:103446.

Lindsey, R. (2020). Climate change: Atmospheric carbon dioxide. `https://www.climate.gov/news-features/understanding-climate/` `climate-change-atmospheric-carbon-dioxide`. Accessed: May-2021.

Liu, L., J. Ha, T. Hashida, and S. Teramura (2001). Development of a co2 solidification method for recycling autoclaved lightweight concrete waste. *Journal of materials science letters*, 20(19):1791–1794.

Maries, A. (1992). The activation of portland cement by carbon dioxide. In *Proceedings of Conference in Cement and Concrete Science, Oxford, UK*.

Mo, L. and D. K. Panesar (2012). Effects of accelerated carbonation on the microstructure of portland cement pastes containing reactive mgo. *Cement and Concrete Research*, 42(6):769–777.

Mo, L. and D. K. Panesar (2013). Accelerated carbonation–a potential approach to sequester co2 in cement paste containing slag and reactive mgo. *Cement and Concrete Composites*, 43:69–77.

Monkman, S., P. A. Kenward, G. Dipple, M. MacDonald, and M. Raudsepp (2018). Activation of cement hydration with carbon dioxide. *Journal of Sustainable Cement-Based Materials*, 7(3):160–181.

Monkman, S. and Y. Shao (2006). Assessing the carbonation behavior of cementitious materials. *Journal of Materials in Civil Engineering*, 18(6):768–776.

Monkman, S. and Y. Shao (2010). Carbonation curing of slag-cement concrete for binding co 2 and improving performance. *Journal of Materials in Civil Engineering*, 22(4):296–304.

Moorehead, D. (1986). Cementation by the carbonation of hydrated lime. *Cement and Concrete research*, 16(5):700–708.

Norcem (2016). Produktinformasjon norcem industrisement. `https://www.norcem.no/no/` `Industri`. Accessed: January-2021.

Northern lights (2021). Accessed: May-2021, https://northernlightsccs.com/what-we-do/.

Panesar, D. K. and L. Mo (2013). Properties of binary and ternary reactive mgo mortar blends subjected to co2 curing. *Cement and Concrete Composites*, 38:40–49.

Patel, H. (2019). 5 tests to measure the workability of concrete! Accessed: May-2021, https://gharpedia.com/blog/tests-to-measure-workability-of-concrete.

Pizzol, V., L. Mendes, H. Savastano Jr, M. Frías, F. Davila, M. Cincotto, V. John, and G. Tonoli (2014). Mineralogical and microstructural changes promoted by accelerated carbonation and ageing cycles of hybrid fiber–cement composites. *Construction and Building Materials*, 68:750–756.

Rogelj, J., D. Shindell, K. Jiang, S. Fifita, P. Forster, V. Ginzburg, C. Handa, H. Kheshgi, S. Kobayashi, E. Kriegler, et al. (2018). Mitigation pathways compatible with 1.5 c in the context of sustainable development. In *Global warming of 1.5° C*, Pp. 93–174. Intergovernmental Panel on Climate Change (IPCC).

Rostami, V., Y. Shao, and A. J. Boyd (2011). Durability of concrete pipes subjected to combined steam and carbonation curing. *Construction and Building Materials*, 25(8):3345–3355.

Rostami, V., Y. Shao, A. J. Boyd, and Z. He (2012). Microstructure of cement paste subject to early carbonation curing. *Cement and Concrete Research*, 42(1):186–193.

Sato, T. and F. Diallo (2010). Seeding effect of nano-caco3 on the hydration of tricalcium silicate. *Transportation Research Record*, 2141(1):61–67.

Shao, Y. (2014). Beneficial use of carbon dioxide in precast concrete production. Technical report, McGill Univ., Montreal, QC (Canada).

Shao, Y., V. Rostami, Z. He, and A. J. Boyd (2014). Accelerated carbonation of portland limestone cement. *Journal of Materials in Civil Engineering*, 26(1):117–124.

Shao, Y., X. Zhou, and S. Monkman (2006). A new co2 sequestration process via concrete products production. In *2006 IEEE EIC Climate Change Conference*, Pp. 1–6. IEEE.

Shi, C., F. He, and Y. Wu (2012a). Effect of pre-conditioning on co2 curing of lightweight concrete blocks mixtures. *Construction and Building materials*, 26(1):257–267.

Shi, C., M. Liu, P. He, and Z. Ou (2012b). Factors affecting kinetics of co2 curing of concrete. *Journal of Sustainable Cement-Based Materials*, 1(1-2):24–33.

Shi, C., M. Liu, Q. Zou, and F. He (2011). A study on factors influencing compressive strength of co2-cured concrete. In *International RILEM conference on advances in construction materials through science and engineering*, Pp. 703–711. RILEM Publications SARL.

Silvestre, J., N. Silvestre, and J. De Brito (2016). Review on concrete nanotechnology. *European Journal of Environmental and Civil Engineering*, 20(4):455–485.

Sorochkin, M., A. Shchurov, and I. Safonov (1975). Study of possibility of using carbon-dioxide for accelerating hardening of products made from portland-cement. *Journal of Applied Chemistry of the USSR*, 48(6):1271–1274.

Standard Norge (2016). Methods of testing cement part 1: Determination of strength. *NS-EN 196-1:2016*, 1.

Standard Norge (2019a). Testing fresh concrete. part 2: Slump test. *NS-EN 12350*, 2:2019.

Standard Norge (2019b). Testing fresh concrete. part 6: Density. *NS-EN 12350*, 6:16.

Standard Norge (2019c). Testing fresh concrete. part 7: Air content - pressure methods. *NS-EN 12350*, 7:2019.

Standard Norge (2019d). Testing hardened concrete - part 2: Making and curing specimens for strength tests. *NS-EN 12390-2:2019*.

Standard Norge (2019e). Testing hardened concrete part 3: Compressive strength of test specimens. *NS-EN 12390-3:2019*.

Standard Norge (2019f). Testing hardened concrete part 7: Density of hardened concrete. *NS-EN 12390-7:2019*.

Statens Vegvesen (2015). 426 kapillær sugehastighet og porøsitet pf-metoden. `https://www.vegvesen.no/_attachment/185231/binary/1090658`.

Stefan Jacobsen (1999). 520.067 frostnedbrytning av betong og andre porøse byggemate-rialer. `https://www.byggforsk.no/dokument/2624/frostnedbrytning_av_betong_og_andre_poroese_byggematerialer`. (Accessed on 03/31/2021).

Tam, V. W., A. Butera, and K. N. Le (2016). Carbon-conditioned recycled aggregate in concrete production. *Journal of cleaner Production*, 133:672–680.

Tam, V. W., A. Butera, K. N. Le, and W. Li (2020). Utilising co2 technologies for recycled aggregate concrete: A critical review. *Construction and Building Materials*, 250:118903.

Tepfers, R. (2012). Concrete technology - porosity is decisive. *fastening technology, reinforcement technology and ... II. ibidem-Verlag*.

Theconstructor (2020). Concrete slump test for workability – procedure and results. `https://theconstructor.org/concrete/concrete-slump-test/1558/`. Accessed: March-2021.

Walton, J. C., S. Bin-Shafique, R. W. Smith, N. Gutierrez, and A. Tarquin (1997). Role of carbonation in transient leaching of cementitious wasteforms. *Environmental science & technology*, 31(8):2345–2349.

Watts, J. (2019). Concrete: the most destructive material on earth. `https://www.theguardian.com/cities/2019/feb/25/concrete-the-most-destructive-material-on-earth`. Accessed: 14-03-2018.

Zhan, B., C. Poon, and C. Shi (2013). Co2 curing for improving the properties of concrete blocks containing recycled aggregates. *Cement and Concrete Composites*, 42:1–8.

ZOU, Q.-y., C.-j. SHI, K.-r. ZHENG, and F.-q. HE (2008). Effect of pre-conditioning on co2 curing of block concretes. *Journal of Building Materials*, 1:024.

Appendix A

Data Sheets

This page is kept empty with purpose.

PRODUKTDATABLAD

INDUSTRISEMENT
CEM I 52,5 R
SIST REVIDERT JULI 2016

Sementen tilfredsstiller kravene i NS-EN 197-1:2011 til Portlandsement CEM I 52,5 R.

Egenskap		Deklarerte data	Krav ifølge NS-EN 197-1:2011
Finhet (Blaine m²/kg)		550	
Spesifikk vekt (kg/dm³)		3,13	
Volumbestandighet (mm)		1	≤ 10
Begynnende størkning (min)		110	≥ 45
Trykkfasthet (MPa)	1 døgn	33	
	2 døgn	41	≥ 30
	7 døgn	50	
	28 døgn	59	≥ 52,5
Sulfat (% SO$_3$)		≤ 4,0	≤ 4,0
Klorid (% Cl⁻)		≤ 0,085	≤ 0,10
Vannløselig krom (ppm Cr^6+)		≤ 2	≤ 2 [1]
Alkalier (% Na$_2$O$_{ekv}$)		1,3	
Klinker (%)		96	95-100
Sekundære bestanddeler (%)		4	0-5

1. I henhold til EU forordning REACH Vedlegg XVII punkt 47 krom VI forbindelser.

NORCEM
HEIDELBERGCEMENT Group

Norcem AS, Postboks 142, Lilleaker, 0216 Oslo
Tlf. 22 87 84 00 firmapost@norcem.no www.norcem.no

Figure A.1: Industrial Cement

Legg inn fraksjon:		*0/8mm. Industri - S*	
Dato	20.09.2017		
Innlagt av	Kamil		

Våtsikte

Vekt våt	**1132,8** g	**Vekt tørr**	**1109,6** g
innveid masse	**1109,6** g		

Åpning (mm)	Sikterest (g)	Sikterest (%)	Gjennom- gang (%)
32	0	0,0 %	**100 %**
22,4		0,0 %	**100 %**
16	0	0,0 %	**100 %**
11,2	0	0,0 %	**100 %**
8	13,2	1,2 %	**98,8 %**
5,6	122	11,0 %	**89,0 %**
4	225,2	20,3 %	**79,7 %**
2	350,4	31,6 %	**68,4 %**
1	558,3	50,3 %	**49,7 %**
0,5	746,7	67,3 %	**32,7 %**
0,25	891,8	80,4 %	**19,6 %**
0,125	979,8	88,3 %	**11,7 %**
0,063	1028,7	92,7 %	**7,3 %**
Bunn	1110		

Siktetap	0,0 %	Overstørrelse	1 %
Fukt%	2,05 %	Understørrelse	F(MicrInc)=2,07%

Figure A.2: Sieve curve Årdal 0-8mm

Legg inn fraksjon:			*8/16 Industri*

| Dato | 20.09.2017 | | |
| Innlagt av | Kamil | | |

VELDE

Våtsikte

Vekt våt	3883,8 g		Vekt törr	3845,9 g
innveid masse	3845,9 g			

Åpning (mm)	Sikterest (g)	Sikterest (%)	Gjennom- gang (%)
32	0	0,0 %	100,0 %
22,4	0	0,0 %	100,0 %
16	313,6	8,2 %	91,8 %
11,2	2131,9	55,4 %	44,6 %
8	3443,3	89,5 %	10,5 %
5,6	3769,4	98,0 %	2,0 %
4	3784,5	98,4 %	1,6 %
2	3790,5	98,6 %	1,4 %
1	3794,5	98,7 %	1,3 %
0,5	3798,1	98,8 %	1,2 %
0,25	3802,4	98,9 %	1,1 %
0,125	3807,3	99,0 %	1,0 %
0,063	3814,2	99,2 %	0,8 %
Bunn	3846		

Siktetap	0,0 %	Overstörrelse	8 %
Fukthalt	0,98 %	Understörrelse	10 %

Figure A.3: Sieve curve Årdal 8-16mm

05

CE **1111**

VELDE

YTELSESERKLÆRING
NR. 118B
CPR 2020.03.12

1.	Varetypens unike identifikasjonskode:	**Naturlig gradert, knust tilslag til bruk i betong**
2.	Tilsiktet bruksområde:	**Naturlig gradert tilslag 0/8 mm.**
3.	Produsent:	**Velde Pukk AS, Noredalsveien 294, 4308 Sandnes**
4.	Autorisert representant:	**Ikke relevant**
5.	System eller systemer for vurdering og verifikasjon av byggevarers ytelser:	**System +2.**
6.	Harmonisert produktstandard:	**NS-EN 12620:2002 + A1:2008+NA:2016**
	Teknisk(e) kontrollorgan:	**Kontrollrådet (1111).**

7. Angitte ytelser:

Vesentlige egenskaper	Ytelser
Tilslagsstørrelse	0/8 mm.
Gradering	Gf85
Korndensitet vannmettet og overflatetørr Korndensitet ovntørr	2,64 +/- 0,01 Mg/m3 2,63 +/- 0,01 Mg/m3
Vannabsorpsjon	1,0%
Finstoffinnhold	*Kategori f$_{10}$*
Kvalitet på finstoff	Ikke skadelig.
Motstand mot knusing for grov tilslag	LA25
Kornform for grovt tilslag	Fl15
Alkali – silika-reaktivitet	0,45% - Ikkje alkalireaktiv
Klorider	Ingen
Syreløselig sulfat	AS$_{0,2}$
Totalt innhold av svovel	0,01% (Krav<0,1%)
Indikasjon på magnetkis: Ja/Nei	Nei (Totalt innhold av svovel $\leq 0,1\%$)
% Glimmerinnhold	< 1% (Krav < 20%)
Innhold av kalkstein i grovt tilslag	< 1% (Krav <15%)
Bestanddeler som påvirker størknings – og herdetiden for betong	Ingen
Farlige stoffer	Ikke påvist
Forenklet petrografisk sammedrag	Knust fjell forekomst av granitt hovedsakelig sammensatt av kubisk skarpkantede korn. Ingen belegg på kornoverflater, ingen forvitrede korn og ingen meget svake korn.
Volumstabilitet	Ikke bestemt
Sammensetning/innhold: • Bestanddeler i grovt resirkulert tilslag • Innhold av vannløselig sulfat i resirkulert tilslag • Innflytelse på begynnende størkning av sement (resirkulert tilslag) • Karbonatinnhold i fint tilslag for overflatelag av betong	Ikke bestemt

Kornkurve (Gjennomgag i masseprosent) ISO-Sikt	Grenser i masseprosent	Gjennomgag i masseprosent
11,2 mm.	100 %	100 %
8,0 mm.	90 – 100 %	96,0 %
5,6 mm.	83 – 93 %	88,0 %
4,0 mm.	75 – 85 %	80,0 %
2,0 mm.	62 – 75 %	68,0 %
1,0 mm.	43 – 58 %	50,0 %
0,5 mm.	23 – 37 %	30,0 %
0,25 mm.	10 – 22 %	16,0 %
0,125 mm.	4 – 12 %	8,0 %
0,063 mm.	2 – 8 %	5,0 %

8.   Bruk av hensiktsmessig teknisk dokumentasjon og/eller spesifikk teknisk dokumentasjon:

Ytelser for denne byggevaren, som er anført ovenfor, er i overensstemmelse med de angitte ytelsene. Denne ytelseserklæringen er utarbeidet i overensstemmelse med forordning (EU) nr. 305/2011 under eneansvar til produsenten, som er anført ovenfor.

Underskrevet for produsenten og på dennes vegne av:

Sandnes, 12 mars 2020   Hernan Mujica, Produktsjef
Id: 18208

Figure A.4: Fine Aggregates Årdal 0-8mm

05

CE

1111

VELDE

YTELSESERKLÆRING
NR. 117B
CPR 2020.03.12

1.	Varetypens unike identifikasjonskode:	**Grovt, knust tilslag til bruk i betong.**
2.	Tilsiktet bruksområde:	**Grovt tilslag 8/16 mm.**
3.	Produsent:	**Velde Pukk AS, Noredalsveien 294, 4308 Sandnes**
4.	Autorisert representant:	**Ikke relevant**
5.	System eller systemer for vurdering og verifikasjon av byggevarers ytelser:	**System +2.**
6.	Harmoniseret produktstandard:	**NS-EN 12620:2002 + A1:2008+NA:2016**
	Teknisk(e) kontrollorgan:	**Kontrollrådet (1111).**

7. Angitte ytelser:

Vesentlige egenskaper	Ytelser
Tilslagsstørrelse	8/16 mm.
Gradering	Gc80/20 G$_T$15
Korndensitet vannmettet og overflatetørr	2,64 +/- 0,01 Mg/m3
Korndensitet ovntørr	2,63 +/- 0,01 Mg/m3
Vannabsorpsjon	0,4 %
Finstoffinnhold	f1,5
Kvalitet på finstoff	Ikke skadelig.
Kornform for grovt tilslag	Fl15
Skjellinnhold i grovt tilslag	SC10
Motstand mot knusing for grov tilslag	LA25
Motstand mot frysing og tining for grovt tilslag	Frostsikkert (Vannabsopsjon $\leq$ 1%)
Alkali – silika-reaktivitet	0,45% - Ikke alkalireaktivt
Klorider	Ingen
Syreløselig sulfat	AS0,2
Totalt innhold av svovel	0,01% (Krav<0,1%)
Indikasjon på magnetkis: Ja/Nei	Nei (Totalt innhold av svovel $\leq$ 0,1%)
% Glimmerinnhold	$\leq$ 1% (Krav < 20%)
Innhold av kalkstein i grovt tilslag	$\leq$ 1% (Krav <15%)
Bestanddeler som påvirker størknings – og herdetiden for betong	Ingen
Farlige stoffer	Ikke påvist
Forenklet petrografisk sammedrag	Knust fjell forekomst av granitt hovedsakelig sammensatt av kubisk skarpkantede korn. Ingen belegg på kornoverflater, ingen forvitrede korn og ingen meget svake korn.
Volumstabilitet	Ikke bestemt
Sammensetning/innhold: • Bestanddeler i grovt resirkulert tilslag • Innhold av vannløselig sulfat i resirkulert tilslag • Innflytelse på begynnende størkning av sement (resirkulert tilslag) • Karbonatinnhold i fint tilslag for overflatelag av betong	Ikke bestemt

Kornkurve (Gjennomgag i masseprosent)	Grenser i masseprosent	Gjennomgag i masseprosent
ISO-Sikt		
22,4 mm.	98,0 – 100,0 %	100 %
16 mm..	80,0 – 99,0 %	95,0 %
11,2 mm.	23,0 – 53 %	38,0 %
8 mm.	0 – 20,0 %	5,0 %
5,6 mm.	0 – 12,0 %	1,6 %
4,0 mm.	0 – 5,0 %	1,4 %
2,0 mm.	0 – 4,0 %	1,2 %
1,0 mm.	0 – 3,0 %	1,1 %
0,063 mm.	0 – 1,5 %	0,8 %

8. Bruk av hensiktsmessig teknisk dokumentasjon og/eller spesifikk teknisk dokumentasjon:

Ytelser for denne byggevaren, som er anført ovenfor, er i overensstemmelse med de angitte ytelsene. Denne ytelseserklæringen er utarbeidet i overensstemmelse med forordning (EU) nr. 305/2011 under eneansvar til produsenten, som er anført ovenfor.

Underskrevet for produsenten og på dennes vegne av:

Sandnes 12. mars. 2020   Hernan Mujica, Produktsjef

Figure A.5: Coarse Aggregates Årdal 8-16mm

NIPPON GASES
The Gas Professionals

Karbondioksid (CO2) Standard Kvalitet

Spesifikasjon

Spesifikasjon i henhold til NS-EN ISO 14175:2008 (C1)

Komponenter	Formel	Konsentrasjon	Enhet
Fuktighet	H_2O	< 40	Vol-ppm
Renhet	CO_2	> 99,7	Vol. %

Leveringsformer

- Produktet leveres i gassflasker med Mørke grå skulder (RAL 7037) og Mørke grå flaskekropp (RAL 7010).
- Flasketrykk ved 15°C: 50 bar
- Ventiltilslutning: W21,80x 1/14" høyre, utvendig (DIN 477 nr.6)
- Leveres med interne krav utover NS-EN ISO 14175:2008 (C1)

Varenr.	Varenavn	Flaske-størrelse L	Innhold kg	Eieforhold
500217	Karbondioksid	2 - 8	1,5 - 6	Eieflaske
500207	Karbondioksid m/stigerør	8	6	Leieflaske
500229	Karbondioksid	10	8	Eieflaske
500208	Karbondioksid m/stigerør	14	10	Leieflaske
500231	Karbondioksid	27	20	Eieflaske
500202	Karbondioksid	27	20	Leieflaske
500209	Karbondioksid m/stigerør	27	20	Leieflaske
500233	Karbondioksid	40	30	Eieflaske
500204	Karbondioksid	40	30	Leieflaske
500210	Karbondioksid m/stigerør	40 m/stigerør	30	Leieflaske

Figure A.6: Nippon CO2 Gas

Dynamon SX-N

TECHNICAL DATA (typical values)	
PRODUCT IDENTITY	
Appearance:	liquid
Colour:	yellowish brown
Viscosity:	easy flowing; < 30 mPa·s
Solids content (%:)	18.5 ± 1.0
Density (g/cm³):	1.06 ± 0.02
pH:	6.5 ± 1
Chloride content (%):	< 0.05
Alkali content (Na₂O-equivalents) (%):	< 2.0

6392-07-2017(GB)

MAPEI®

BUILDING THE FUTURE

Figure A.7: Dynamon SX-N Superplasticizer

VWR
BDH CHEMICALS

Product Specification

Material	87185.2500
Material description	Silica gel C 2-6 mm
Grade	Chameleon® granules in sachet with moisture indicator
CAS Number	7631-86-9
Molecular formula	O2Si.xH2O

Characteristics	Specifications
Colour change	Passes test
Particle size	2.0 - 6.0 mm
pH (20°C; 5 %)	2.0 - 5.0
Loss on drying (140°C)	≤ 2.0 %
Water-adsorption capacity (23°C;50 % RH)	≥ 23.0 %

Signature

We certify that this batch conforms to the specifications listed above.

This document has been produced electronically and is valid without a signature.

Anja Vanhalle, Head of Laboratory - Haasrode
VWR International bvba; Geldenaaksebaan 464; BE-3001 Leuven; Belgium

Figure A.8: VWR Silica Gel

Appendix B

Tables of Calculations

This page is kept empty with purpose.

1-day compressive strength test			

At 4 bar pressure & 3h CO2 Curing

	Sample 1	Sample 2	Sample 3	Mean
W/C = 0.6				
M1 (WC0.6-P4T3-D1)	31.72	31.67	32.22	31.87
Reference (WC0.6-Ref-D1)	28.13	30.64	29.14	29.30
W/C = 0.4				
M6 (WC0.4-P4T3-D1)	56.25	56.04	58.25	56.85
Reference (WC0.4-Ref-D1)	54.92	53.01	54.81	54.25

At 6 bar pressure & 4h CO2 Curing

	Sample 1	Sample 2	Sample 3	Mean
W/C = 0.6				
M2 (WC0.6-P6T4-D1)	31.95	32.63	33	32.53
Reference (WC0.6-Ref-D1)	31.54	31.43	32.24	31.74
W/C = 0.4				
M7 (WC0.4-P6T4-D1)	56.25	55.26	54.42	55.31
Reference (WC0.4-Ref-D1)	50.85	51.07	51.57	51.16

28-days compressive strength test			

At 4 bar pressure & 3h CO2 Curing

	Sample 1	Sample 2	Sample 3	Mean
W/C = 0.6				
M4 (WC0.6-P4T3-D28)	44.53	42.96	42.57	43.35
Reference (WC0.6-Ref-D28)	49.8	48.58	49.05	49.14
W/C = 0.4				
M8 (WC0.4-P4T3-D28)	75.17	79.86	81.99	79.01
Reference (WC0.4-Ref-D28)	78.32	81.81	84.78	81.64

At 6 bar pressure & 4h CO2 Curing

	Sample 1	Sample 2	Sample 3	Mean
W/C = 0.6				
M3 (WC0.6-P6T4-D28)	43.07	42.74	43.22	43.01
Reference (WC0.6-Ref-D28)	48.38	47.42	48.95	48.25
W/C = 0.4				
M5 (WC0.4-P6T4-D28)	85.08	85.8	83.2	84.69
Reference (WC0.4-Ref-D28)	84.1	86.21	81.88	84.06

Figure B.1: Compressive strength test

Porosity Calculations (PF - Method)

Mixture No.	Case	Volume M³	Sample #	g1 (Kg)	g2 (Kg)	g4 (Kg)	Mean Suction porosity	Mean Macro porosity	Mean Total porosity	Mean PF-value
M1	WC0.6-P4T3-D1	0.00018	1	0.432	0.460	0.461	0.141	0.008	0.133	0.060
		0.00018	2	0.426	0.454	0.455				
	WC0.6-Ref-D1	0.00018	1	0.431	0.457	0.146	0.145	0.007	0.138	0.051
		0.00018	2	0.433	0.459	0.144				
M2	WC0.6-P6T4-D1	0.00018	1	0.426	0.453	0.455	0.149	0.01	0.139	0.072
		0.00018	2	0.435	0.462	0.464				
	WC0.6-Ref-D1	0.00018	1	0.439	0.466	0.468	0.153	0.01	0.143	0.07
		0.00018	2	0.435	0.462	0.464				
M4	WC0.6-P4T3-D28	0.00018	1	0.435	0.459	0.460	0.133	0.008	0.126	0.063
		0.00018	2	0.432	0.456	0.458				
	WC0.6-Ref-D28	0.00018	1	0.448	0.470	0.471	0.128	0.007	0.121	0.058
		0.00018	2	0.435	0.459	0.460				
M3	WC0.6-P6T4-D28	0.00018	1	0.432	0.460	0.461	0.141	0.007	0.133	0.053
		0.00018	2	0.426	0.454	0.455				
	WC0.6-Ref-D28	0.00018	1	0.430	0.455	0.457	0.155	0.005	0.150	0.033
		0.00018	2	0.434	0.460	0.461				
M6	WC0.4-P4T3-D1	0.00018	1	0.434	0.457	0.459	0.128	0.008	0.120	0.067
		0.00018	2	0.434	0.458	0.459				
	WC0.4-Ref-D1	0.00018	1	0.430	0.456	0.456	0.143	0.003	0.139	0.022
		0.00018	2	0.435	0.460	0.461				
M7	WC0.4-P6T4-D1	0.00018	1	0.435	0.459	0.460	0.13	0.003	0.127	0.024
		0.00018	2	0.442	0.465	0.465				
	WC0.4-Ref-D1	0.00018	1	0.432	0.457	0.457	0.137	0.002	0.134	0.015
		0.00018	2	0.431	0.455	0.456				
M8	WC0.4-P4T3-D28	0.00018	1	0.440	0.461	0.462	0.113	0.009	0.103	0.087
		0.00018	2	0.446	0.466	0.467				
	WC0.4-Ref-D28	0.00018	1	0.434	0.456	0.457	0.117	0.006	0.111	0.054
		0.00018	2	0.442	0.463	0.464				
M5	WC0.4-P6T4-D28	0.00018	1	0.442	0.461	0.463	0.107	0.011	0.096	0.115
		0.00018	2	0.440	0.460	0.462				
	WC0.4-Ref-D28	0.00018	1	0.446	0.467	0.470	0.118	0.012	0.106	0.113
		0.00018	2	0.442	0.463	0.465				

Figure B.2: Porosity calculations (PF-metoden)

Weight gain due to carbonation

Mixture	Silica Gel (g)		Tissue Paper (g)		Water Loss (Kg)	Specimens # (g)								Mass Binder (Kg)	Mass Gained (Kg)	CO_2 Uptake %
						1		2		3		4				
	Before	After	Before	After		Before	After	Before	After	Before	After	Before	After			
M1	262.2	290.6	6	22.8	0.0454	2463	2476	2447	2459	2457	2469	2450	2462	1.11	0.0939	8.46
M2	269.7	294.1	5	19.2	0.0386	2431	2437	2418	2424	2444	2450	2440	2446	1.11	0.0890	8.90
M3	261	290	6	24.3	0.0473	2474	2493	2480	2493	2438	2450	2444	2456	1.11	0.0565	9.34
M4	258.5	288	6	24.5	0.0480	2438	2452	2416	2430	2444	2459	2420	2435	1.11	0.0580	9.54
M5	260.5	300.5	6	23	0.0570	2494	2509	2469	2483	2486	2501	2482	2498	1.60	0.0600	7.31
M6	260.5	284.5	6	25.5	0.0435	2469	2479	2467	2476	2486	2496	2483	2496	1.60	0.0420	5.35
M7	260.7	293	6	20	0.0463	2478	2493	2445	2460	2456	2470	2432	2445	1.60	0.0560	6.40
M8	264.2	284	6	23	0.0368	2456	2467	2438	2450	2446	2457	2449	2459	1.60	0.0445	5.08

Figure B.3: Weight gain

Prosj./id.:	Navn på serie / blandingsnummer				

Blandevolum:	30 liter				
Dato:					
Tidspunkt for vanntilsetning					
Ansvarlig:					
Utført av:					

Materialer	Resept kg/m³	Sats kg	Fukt* %	Korr. kg	Oppveid** kg	
Norcem inds	399.9	11.997			11.997	
Elkem Microsilica	0.0	0.000	50	0.000	0.000	
	0.0	0.000	0	0.000	0.000	
Fritt vann	160.0	4.799		-0.931	3.868	3.868
Absorbert vann	0.0	0.000			0.000	
Årdal 0/8 mm nat. vask.	979.9	29.397	3.0	0.882	30.279	
Årdal 0/2 mm nat. vask	0.0	0.000	0.0	0.000	0.000	
Årdal 8/16mm	869.0	26.069	0.0	0.000	26.069	
Årdal 16/22 mm	0.0	0.000	0.0	0.000	0.000	
	0.0	0.000	0.0	0.000	0.000	
	0.0	0.000	0.0	0.000	0.000	
	0.0	0.000	0.0	0.000	0.000	
	0.0	0.000	0.0	0.000	0.000	
	0.0	0.000	0.0	0.000	0.000	
	0.0	0.000	0.0	0.000	0.000	
Sika Viscocrete FB-2	2.0	0.060	82	0.049	0.060	
	0.0	0.000	100	0.000	0.000	
	0.0	0.000	100	0.000	0.000	
	0.0	0.000	100	0.000	0.000	
Stålfiber	0.0	0.000			0.000	
PP-fiber	0.0	0.000			0.000	

*Se fotnote på delark "Proporsjonering"   ** NB! Våte mengder, også for pozzolaner og fillere

Fersk betong					
Tid etter vanntilsetning					
Synkmål					
Utbredelsesmål					
Luft					
Densitet					

Prøvestykker (antall)					
Utstøpningstidspunkt					
Terninger					
150x300 sylindre					
100x200 sylindre					

Delark "Blandeskjema"

Figure B.4: Concrete mix design of w/c = ratio 0.4

Prosj./id.:	Navn på serie / blandingsnummer

Blandevolum:	30 liter
Dato:	
Tidspunkt for vanntilsetning	
Ansvarlig:	
Utført av:	

Materialer	Resept kg/m³	Sats kg	Fukt* %	Korr. kg	Oppveid** kg	
Norcem inds	277.9	8.336			8.336	
Elkem Microsilica	0.0	0.000	50	0.000	0.000	
	0.0	0.000	0	0.000	0.000	
Fritt vann	166.7	5.002		-0.957	4.044	4.044
Absorbert vann	0.0	0.000			0.000	
Årdal 0/8 mm nat. vask.	1025.8	30.775	3.0	0.923	31.698	
Årdal 0/2 mm nat. vask	0.0	0.000	0.0	0.000	0.000	
Årdal 8/16mm	909.7	27.291	0.0	0.000	27.291	
Årdal 16/22 mm	0.0	0.000	0.0	0.000	0.000	
	0.0	0.000	0.0	0.000	0.000	
	0.0	0.000	0.0	0.000	0.000	
	0.0	0.000	0.0	0.000	0.000	
	0.0	0.000	0.0	0.000	0.000	
	0.0	0.000	0.0	0.000	0.000	
	0.0	0.000	0.0	0.000	0.000	
Sika Viscocrete FB-2	1.4	0.042	82	0.034	0.042	
	0.0	0.000	100	0.000	0.000	
	0.0	0.000	100	0.000	0.000	
	0.0	0.000	100	0.000	0.000	
Stålfiber	0.0	0.000			0.000	
PP-fiber	0.0	0.000			0.000	

*Se fotnote på delark "Proporsjonering"   ** NB! Våte mengder, også for pozzolaner og fillere

Fersk betong					
Tid etter vanntilsetning					
Synkmål					
Utbredelsesmål					
Luft					
Densitet					

Prøvestykker (antall)					
Utstøpningstidspunkt					
Terninger					
150x300 sylindre					
100x200 sylindre					

Delark "Blandeskjema"

Figure B.5: Concrete mix design of w/c ratio = 0.6

Appendix C

Methods

This page is kept empty with purpose.

Statens vegvesen

R210 Laboratorieundersøkelser

4 Betong

42 Undersøkelse av herdnet betong

426 Kapillær sugehastighet og porøsitet, PF–metoden

Juli 2015 (erstatter metode 14.637, november 1996)

1. Hensikt

Metodebeskrivelsen omfatter bestemmelse av kapillær sugehastighet og porøsitet for herdet betong med naturlig tilslag.

Ved full prosedyre bestemmes både tetthetsparametrene motstandstall og kapillaritetstall (basert på kapillær sugehastighet) og porøsitets– og densitetsverdier for betongen. Full prosedyre krever regulære skiveformede prøvestykker.

Begrenset prosedyre omfatter kun bestemmelse av porøsitets– og densitetsverdier. Begrenset prosedyre kalles også PF–metoden og kan benyttes på irregulære prøvestykker. Begrenset prosedyre kan utvides til også å bestemme in–situ vanninnhold.

Begge prosedyrer muliggjør et estimat av betongens masseforhold.

Saksbehandler beskriver i hvert enkelt tilfelle om det skal benyttes full eller begrenset prosedyre, med eller uten bestemmelse av vannmetningsgrad.

2. Definisjoner

Sugporøsitet (kapillærporøsitet): Andel porer i betongen som suger vann kapillært, uttrykt i forhold til betongvolum.

Makroporøsitet (luftinnhold): Andel porer i betongen som først fylles med vann ved neddykking under trykk, uttrykt i forhold til betongvolum.

Totalporøsitet: Summen av sugporøsitet og makroporøsitet

PF (PorskyddsFaktor på svensk): Forholdet mellom makroporøsitet og totalporøsitet. Betongens PF–verdi gir uttrykk for betongens frostbestandighet.

Kapillær vannmetningsgrad (DCS = Degree of Capillary Saturation): Uttrykker hvor stor andel av betongens kapillærporevolum som er fylt med vann.

Total vannmetningsgrad (DS = Degree of Saturation): Uttrykker hvor stor andel av betongens totale porevolum som er fylt med vann.

3. Utstyr

- liten steinsag
- splittemaskin
- plastkasser med rist i bunnen og lokk med dampabsorberende foring
- vekt med nøyaktighet 0,01 g
- stoppeklokke
- ren, fuktig klut
- trykktank til vannmetting (50 atm)
- ventilert tørkeskap (105 °C)
- stålbørste (ved bestemmelse av vanninnhold)

4. Fremgangsmåte

4.1 Full prosedyre

4.1.1 Tildanning av prøvestykker

Prøvestykker tildannes fra utstøpte sylindre eller utborede kjerner. Det skal tilstrebes en diameter på 100 mm, minimum 90 mm. I unntakstilfeller kan det tillates borkjerner med diameter mindre enn 90 mm, men dette krever spesiell forbehandling av prøvestykkene ved maling av sidekanter, se nedenfor.

Prøvestykker tildannes ved saging av skiver med tykkelse (20 ± 1) mm. Skivene skal være planparallelle.

Ett prøvesett består normalt av 4 stk. ø100 mm skiver. Ved bruk av skiver med diameter mindre enn 100 mm skal antall skiver tilpasses slik at samlet areal er minst:

– 20 000 mm² for betong med $d_{maks} \leq 16$ mm

Figure C.1: PF-Method

– 25 000 mm² for betong med d_{maks} > 16 mm

Eksponert flate skal normalt være en sagflate. Det kan unntaksvis utføres prøving av støpehud. Dette skal i så fall være beskrevet av saksbehandler og gå klart fram av rapporten.

4.1.2 Prøving

Prøving gjennomføres som følger:

– måling av skivetykkelser ved bruk av skyvelære
– eventuell maling av sideflatene med epoksy- eller lateksmaling (kun ved diameter < 90 mm)
– tørking i ventilert tørkeskap ved 105 ℃ inntil vekttapet er mindre enn 0,01 % pr. time (eventuelt i 7 døgn dersom konstant tørketid er mer hensiktsmessig), og deretter minimum 2 timer avkjøling i luft ved romtemperatur, tildekket med plastfolie, veiing (vekt g_1)
– 4 døgns suging fra vannspeil (hele sugeflaten skal være i kontakt med vann uten at vannspeilet står mer enn 1–2 mm opp på sideflaten, kassen skal være tildekket med foret lokk som hindrer drypp av kondensert vann). Veiing etter:

  – 10 og 30 minutter
  – 1, 2, 3, 4 og 6 timer
  – 1, 2, 3 og 4 døgn (vekt etter 4 døgn, g_5)

  Ved veiing skal følgende prosedyre følges for hver skive:

  – skiven tas opp fra risten (pass på at det ikke drypper på andre skiver)
  – skiven tørkes av med fuktig klut og veies
  – skiven legges tilbake på risten

– 3 døgns neddykking i vann, avtørking med fuktig klut og veiing i luft (vekt g_2), og under vann (vekt g_3). Dette forutsetter at prøven er opphengt i vekta
– minimum 1 døgns neddykking i vann i trykktank ved 50 atm trykk, <u>umiddelbar</u> avtørking med fuktig klut og veiing i luft (vekt g_4). Avtørking og veiing må skje umiddelbart etter uttak av trykktank for å unngå at vannet presses ut av prøvestykket

Vektene føres inn i eget skjema, som vist i punkt 8 Tillegg.

Kommentar: Når flere prøvesett prøves samtidig må det totale antall prøvestykker normalt ikke være større enn 20 dersom det skal være mulig å gjennomføre prøvingsprosedyren for hvert enkelt prøvestykke uten avvik fra de oppgitte prøvingstidspunktene.

4.2 Begrenset prosedyre (PF-metoden)

Ved prøving i henhold til begrenset prosedyre er prøvestykkenes form av mindre betydning. Én prøve kan bestå av flere prøvestykker hvor følgende retningslinjer gjelder:

– det totale prøvevolumet bør være større enn 200 cm³
– hvert prøvestykke bør ha et minste tverrmål mellom 10 og 50 mm
– hvert prøvestykke bør ha et volum på minimum 50 cm³

Følgende prosedyre benyttes:

– tørking i ventilert tørkeskap ved 105 ℃ i 7 døgn, og deretter minimum 2 timer avkjøling i luft ved romtemperatur, tildekket med plastfolie, veiing (vekt g_1)
– neddykking i vann i 7 døgn, avtørking med fuktig klut og veiing i luft (vekt g_2), og under vann (vekt g_3)
– 2 døgn neddykking i vann i trykktank ved 50 atm, <u>umiddelbar</u> avtørking med klut og veiing i luft (vekt g_4). Avtørking og veiing må skje umiddelbart etter uttak av trykktank for å unngå at vannet presses ut av prøvestykket.

Vektene føres inn på skjema som vist i punkt 8 Tillegg.

4.3 Utvidet PF-metode – bestemmelse av vanninnhold

4.3.1 Uttak av prøvemateriale

Ved uttak av prøvemateriale for bestemmele av vanninnhold, må dette skje ved minst mulig forstyrrelse av in situ vanninnhold. Uttak av prøvemateriale skjer enten ved boring av kjerner eller saging og utknekking av prismer i betong-overflata. Boring av kjerner med vannkjøling må skje med jevn hastighet og vanntilførsel, uten unødig stans, fortrinnsvis med diameter > 90 mm. Umiddelbart etter utboring, tørkes kjernen av med tørkepapir slik at det ikke er fritt vann på over-flatene. Umiddelbart deretter pakkes kjernen inn i flere lag tynnfilmplast, deretter i tykkere plastpose. Det pakkes slik at det blir minimalt med luft mellom plast og betongprøve og det benyttes tape til forsegling. Utborede kjerner sendes raskt til laboratorium for snarlig iverksettelse av prøving. Eventuell mellomlagring skjer i kjølerom, ved ca. + 5 ℃.

4.3.2 Prøving

En utboret kjerne kan splittes i flere sjikt for å bestemme vanninnholdet i ulike avstander fra betongoverflata. Sjiktene bør ha tykkelse 4–5 cm, og kan eventuelt deles i to deler for å tilfredsstille krav til prøvestørrelse (se punkt 3.2).

Figure C.2: PF-Method page 2

Prøvestykkene børstes hardt og grundig med stålbørste, for fjerning av støv og løse biter, før veiing. Utpakking, splitting, børsting og veiing må skje raskt for å unngå unødig vanntap. Kjernen repakkes i plast mellom hver splitte-/børste-/veierunde.

Dersom man har prøvemateriale som er egnet for bestemmelse av vanninnhold (kapillær og total vannmetningsgrad), kan begrenset prosedyre utvides med:

– veiing umiddelbart etter utpakking, eventuell splitting og børsting med stålbørste (vekt g_0)
– neddykking i vann i 7 døgn, avtørking med fuktig klut og veiing (vekt g_6)

Deretter følges prosedyren for begrenset prosedyre, med veiing etter tørking i 7 døgn (vekt g_1), neddykking i 7 døgn (vekt i luft, g_2 og vekt i vann, g_3) og trykkmetning i 2 døgn (vekt g_4).

Til slutt utføres, for kontroll av prøvestykkenes volumstabilitet gjennom prosessen:

– tørking i ventilert tørkeskap ved 105 °C i 7 døgn og deretter minimum 2 timer avkjøling i luft ved romtemperatur, tildekket med plastfolie, veiing (vekt g_7).

Vektene føres inn på skjema som vist i punkt 8 Tillegg.

5. Resultater

5.1 Beregninger

Følgende størrelser beregnes:

Prøvestykkets volum: $V = \frac{g_2 - g_3}{\rho_w}$ (m^3)

Tørrdensitet: $\rho_t = \frac{g_1}{V}$ (kg/m^3)

Faststoffdensitet: $\rho_{fs} = \frac{g_1}{V - (g_4 - g_1)/\rho_w}$ (kg/m^3)

Sugmettet densitet: $\rho_s = \frac{g_2}{V}$ (kg/m^3)

Sugporøsitet: $p_s = \frac{g_2 - g_1}{V \cdot \rho_w}$

Makroporøsitet: $p_m = \frac{g_4 - g_2}{V \cdot \rho_w}$

Totalporøsitet: $p_t = p_s + p_m$

PF-verdi: $PF = p_m / p_t$

hvor:

ρ_w = vannets densitet (settes lik 1000 kg/m^3)

Ved prøving iht. full prosedyre skal i tillegg følgende verdi beregnes:

Åpen makroporøsitet: $p_{åm} = \frac{g_2 - g_5}{V \cdot \rho_w}$

Åpen makroporøsitet uttrykker omfanget av kontinuerlige makroporer som ikke fylles ved kapillærsug, men først ved neddykking i vann.

Dersom prosedyren for utvidet PF-metode er benyttet bestemmes følgende tilleggsverdier:

Kapillær vannmetningsgrad: $DCS = \frac{g_0 - g_1}{g_6 - g_1}$

Total vannmetningsgrad: $DS = \frac{g_0 - g_1}{g_4 - g_1}$

Ved prøving i henhold til full prosedyre brukes de målte absorpsjonsverdiene (uttrykt som mengde absorbert vann pr. arealenhet i kg/m^2) ved angitte tidspunkter til å bestemme et tidspunkt (t_{kap}) og en tilhørende absorpsjonsverdi (Q_{kap}) som tilsvarer at vannfronten akkurat har nådd toppflaten på prøvestykket, dvs. en stigehøyde (h). Dermed kan motstandstallet (m) og kapillaritetstallet (k) bestemmes:

$k = \frac{Q_{kap}}{\sqrt{t_{kap}}}$ $\left[\frac{kg}{m^2 \sqrt{s}}\right]$

$m = \frac{t_{kap}}{h^2}$ $\left[\frac{s}{m^2}\right]$

Prinsippet for beregning av m og k er vist i figur 426-1. Skjæringspunktet for de to kurvedelene (t_{kap}, Q_{kap}) kan enten bestemmes grafisk eller ved lineær regresjonsanalyse.

$k = \frac{Q_{kap}}{\sqrt{t_{kap}}}$ [kg/m$^2 \sqrt{s}$] $m = \frac{t_{kap}}{h^2}$ [s/m^2]
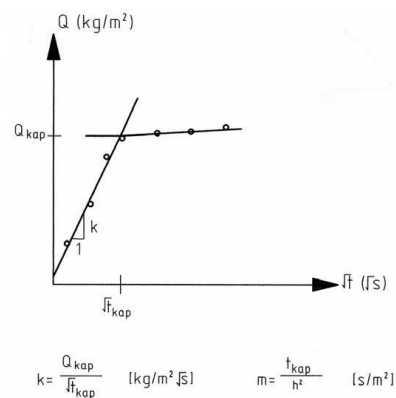
Figur 426-1 Beregning av motstandstall og kapillaritetstall

5.2 Usikkerhet

Full prosedyre:

Pålitelighet av resultatene avhenger blant annet av kvaliteten av regresjonsanalysen. Lokaliseringen av skjæringspunktet mellom kurvedelene, og dermed m og k, avhenger av at måleverdiene plasseres i riktig kurvedel. Korrelasjonskoeffisienten (R^2) fra

Figure C.3: PF-Method page 3

426

regresjonsanalysen kan brukes som kriterium for plassering av målepunktene. Den beste konfigurasjonen gir normalt de største korrelasjonskoeffisientene. Det bør legges størst vekt på å oppnå høye verdier av (R^2) for den steile kurvedelen. Målepunkt nær skjæringspunktet kan eventuelt utelates.

Generelt bør korrelasjonskoeffisienten fra regresjonsanalysen ikke underskride 0,95 for den steile kurvedelen, og 0,90 for den horisontale kurvedelen. Ved avvik forkastes beregningen av m og k, og resultatene presenteres bare i grafisk form. Ved grafisk bestemmelse av skjæringspunktet må kvaliteten på bestemmelsen av m og k vurderes skjønnsmessig.

6. Rapportering

Prøvingsrapporten skal minimum inneholde:

– prøvingslaboratorium (navn og adresse)
– ansvarlig for prøvingen
– dato og rapportidentifikasjon
– prøvingsmetode (denne beskrivelsens nummer og tittel)
– eventuelle avvik fra metodebeskrivelsen
– navn og adresse på oppdragsgiver/anlegg
– navn på prøvetaker og metode for prøveuttak, adresse for prøveuttaket
– navn på produsent/leverandør
– sted for uttak, dato og klokkeslett for prøvetakingen
– grafisk framstilling av sugeforløpet
– tabellarisk oppstilling av beregnede verdier

7. Referanser

SINTEF Bygg og miljøteknikk (1996): Bestemmelse av kapillær sugehastighet og porøsitet. KS 70 110, Utgave 2. Trondheim

E.J. Sellevold: «Herdnet betong: Bestemmelse av luft/makro og gel/kapillær porøsitet samt relativt bindemiddelinnhold», NBI-rapport O1731, Oslo, 1986

S. Smeplass: Kapillærabsorpsjon som kvalitetskriterium. SINTEF rapport STF65 A88028. SINTEF, Trondheim, 1988

E.J. Sellevold and T. Farstad: "The PF-method – A simple way to estimate the w/c-ratio and air content of hardened concrete", ConMat'05 and Mindness Symposium ISBN 0-88865-810-9, Vancouver, Canada, 2005

R.H. Relling: "Coastal Concrete Bridges: Moisture State, Chloride Permeability and Aging Effects", Dr. Thesis at NTNU, 1999

8. Tillegg

Skjemaer for registrering av veiedata. Se figurene 426-2, 426-3 og 426-4.

Figure C.4: PF-Method page 4

Testing pH of Concrete

Need for a standard procedure

BY JENNIFER A. GRUBB, HEMANT S. LIMAYE, AND ASHOK M. KAKADE

Although concrete typically begins its life at a highly basic pH of about 13, the pH values at exposed surfaces soon fall as reactions occur between carbon dioxide from the atmosphere and alkalis in the concrete—a process known as carbonation. Over time, fronts of carbonated concrete, with pH values of about 8.5, advance below exposed surfaces.

It may be necessary to determine the depth of this front, as carbonated concrete can allow corrosion of reinforcing steel. This can be done by spraying a phenolphthalein indicator solution onto a fractured or cut surface of the concrete and noting the location of a color change. In this case, the color change occurs when the solution contacts a material with a pH of 9 to 9.5. The depth of the carbonation front can also be evaluated by using a drill to collect samples at selected depths. In this case, the pH of the powdered samples can be evaluated using the standard test methods described in the following sections.

It may also be necessary to evaluate the pH of a concrete floor surface, as the adhesives used to install vinyl flooring or carpet tiles can be damaged when applied to substrates with pH values exceeding 9 (many flooring manufacturers won't issue a warranty on their installed products unless the pH has been verified to be within acceptable ranges). Although paragraph 5.3 in ASTM F 710-05, "Standard Practice for Preparing Concrete Floors to Receive Resilient Flooring,"[1] indicates a procedure to be used to test concrete floors for alkalinity, we believe the procedure isn't adequate. We therefore propose an alternate standard procedure for testing the pH of concrete.

FUNDAMENTALS OF pH

pH is an approximate measure of acidity or alkalinity of a solution and is defined as the negative logarithm of the hydrogen ion (H^+) concentration. As the pH of a solution increases, the number of free hydrogen ions decreases, and a change in pH of one reflects a tenfold change in the H^+ concentration. For example, there are 10 times as many hydrogen ions available at a pH of 7 than at a pH of 8. The pH scale ranges from 0 to 14, and a pH of 7 is considered to be neutral. Substances with a pH less than 7 are acidic and substances with a pH greater than 7 are basic.

The following are examples showing the relationship between H^+ concentration and pH for various solutions:
- In a hydrogen chloride solution, or hydrochloric acid, the H^+ concentration is 1×10^{-2}, and the pH is 2;
- In water, the H^+ concentration is 1×10^{-7}, and the pH is 7;
- In saturated calcium hydroxide, the H^+ concentration is about $1 \times 10^{-12.4}$, and the pH is about 12.4; and
- In sodium hydroxide solution, the H^+ concentration is 1×10^{-14}, and the pH is 14.

Because pH is a measure of a solution, accurately measuring the pH of a solid substance such as concrete is a challenging task.

Figure C.5: pH of Concrete page 1

TABLE 1:
Reported pH values for concrete-related materials

Category	pH
Fresh cement	›12.5
Low alkali cement	12.7 to 13.1
High alkali cement	13.5 to 13.9
High alumina cement	11.4 to 12.5
Mixing water for concrete	6 to 9
Sea water	7.5 to 8.4
Hardened cement paste with ingress of sea water	12.0
Range of phenolphthalein solution (colorless to red)	8 to 10
Class F fly ash	›13.2
Silica fume slurry (equal mass of water & silica fume)	5.5
Reduction in pH due to 10% silica fume	0.5
Reduction in pH due to 20% silica fume	1.0
pH of silica fume concrete	›12.5

EVALUATION

Our evaluation included a literature survey, an informal survey of professionals and associations, and assessment of test standards and methods, including pH strips, pH pencils, and digital meters. In addition, we also quantified the influence of procedural variables on the measured test results.

Literature survey

Our literature survey revealed that there is plenty of literature available concerning the pH of concrete as it relates to carbonation, embedded steel corrosion, alkali-silica reaction, and the effects of mineral admixtures. There are, however, few published papers related to the measurement of concrete pH, especially with regard to a standard procedure. In addition, most of the literature doesn't indicate the procedures followed to measure the pH. Some of the reported pH values are summarized in Table 1.

Informal survey

We used telephone and e-mail surveys of leading petrographers, various trade associations, and test laboratory personnel to determine the procedures now commonly used to measure concrete pH. Although pH-indicating strips reportedly are the most widely used method, most respondents didn't indicate the use of a specific dilution ratio. Some petrographers did indicate they use the procedure provided in ASTM C 25[2] with a pH probe and digital meter, and personnel at a few testing laboratories reported that they measure concrete pH using a pH pencil.

Standards review

As stated previously, to measure the pH of solid materials such as lime, soil, or concrete, an aqueous solution of the powdered material must be created—this dilutes the concentration of the solid material. A review of various standards and commentaries indicates that dilution ratios vary between 1:9 and 1:20. The following are summaries of the methods used in the publications we reviewed:

■ ASTM C 25, "Standard Test Methods for Chemical Analysis of Limestone, Quicklime, and Hydrated Lime"[2]: Mix 10 g (0.35 oz) of sample with 200 mL (6.8 fl oz) of deionized water. Stir for 30 minutes, and let the solution stand for 30 minutes. Measure pH with a pH probe and meter. Report pH value to four significant figures;

■ ASTM F 710, "Standard Practice for Preparing Floors to Receive Resilient Flooring"[1]: Place several drops of distilled or deionized water on a clean concrete surface to form an approximately 25 mm (1 in.) diameter circle. After 60 ± 5 seconds, measure pH using a pH strip; and

■ ICRI Guideline No. 03740, "Guideline for Inorganic Repair Material Data Sheet Protocol"[3]: Mix 10 g (0.35 oz) of sample passed through the 90 μm (No. 170) sieve with 90 g (3.2 oz) of distilled or deionized water for 1 minute. After settling, measure pH using pH paper or a pH probe and meter.

Influence of variables

We designed our experimental program to observe the effects of major variables such as the type of concrete, sample size, and dilution ratio. We also conducted a limited number of tests for other variables such as soaking or waiting time, sample gradation, and temperature. Our samples were prepared using cement paste; mortar; concrete with 0, 15, and 50% cement replacement by weight with fly ash; or concrete from an old sidewalk. The samples were pulverized using a vibratory micro-mill. Sample sizes of 5, 10, and 20 g (0.18, 0.35, and 0.71 oz) were diluted with distilled water, using dilution ratios of 1:1, 1:2, 1:4, 1:9, 1:20, and 1:50 before testing for pH. The pH readings were obtained using either a pH probe with a digital meter or pH strips. The prepared solution was not stirred during the measurement process.

Figure C.6: pH of Concrete page 2

TEST RESULTS AND DISCUSSION
Type of sample

The measured pH values for various mixtures of cement paste, mortar, and concrete are listed in Table 2. All of the prepared samples were less than 2 months old at the time of testing except for the sample from a 20-year-old exposed concrete sidewalk. The tests were conducted using 5 g (0.18 oz) samples with a dilution ratio of 1:2. The highest pH of 12.71 was obtained for cement paste with a water-cementitious material ratio (w/cm) of 0.40. The lowest pH of 10.45 was obtained for the 20-year-old sidewalk sample.

Amount of sample

For each type of mixture, pH was measured using 5, 10, and 20 g (0.18, 0.35, and 0.71 oz) of material with various dilution ratios. Sample graphs are shown in Fig. 1 to 4. The difference in pH was less than 0.30.

TABLE 2:
MEASURED PH VALUES FOR VARIOUS CONCRETE MATERIALS

Material	Measured pH*
0.4 w/cm cement paste	12.71
0.4 w/cm mortar	12.69
0.4 w/cm concrete	12.62
0.55 w/cm concrete	12.49
Concrete with 15% fly ash (0.45 w/cm)	12.58
Concrete with 50% fly ash (0.45 w/cm)	12.37
Concrete from 20-year-old sidewalk	10.45

*All values are for sample size of 5 g (0.18 oz) and dilution ratio of 1:2.

Fig. 2: Measured pH versus dilution ratio for concrete with a 0.4 w/cm

Fig. 3: Measured pH versus dilution ratio for concrete with 15% cement replacement by weight with fly ash

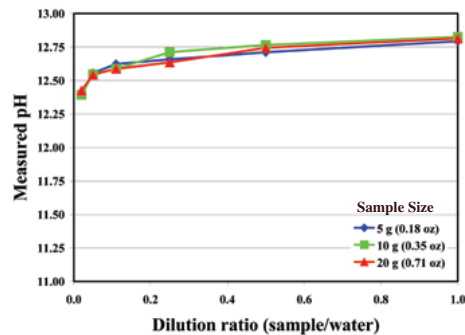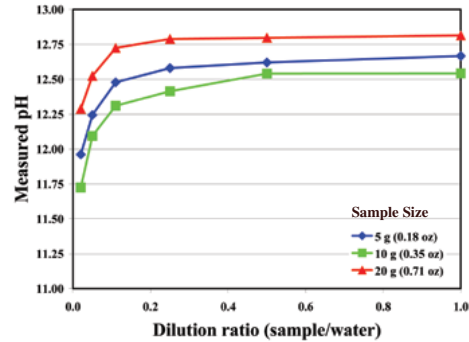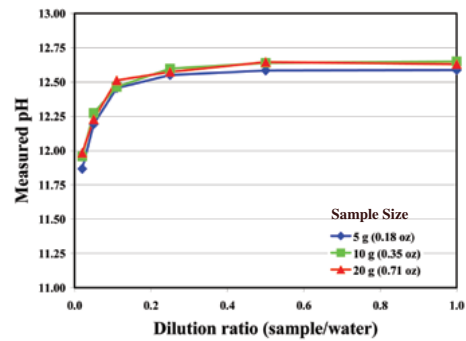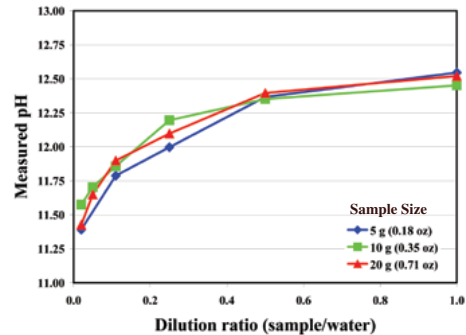
Fig. 1: Measured pH versus dilution ratio for cement paste with a 0.4 w/cm

Fig. 4: Measured pH versus dilution ratio for concrete with 50% cement replacement by weight with fly ash

Figure C.7: pH of Concrete page 3

APPENDIX C. METHODS

Dilution ratio

Figures 1 to 5 also show the effects of dilution ratio on pH values for various materials. The trend of increasing pH as the dilution ratio decreases from 1:50 to 1:1 is similar for all mixtures.
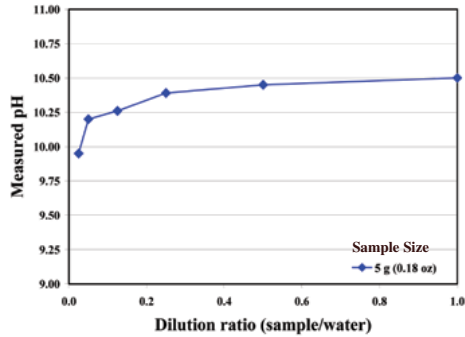

Fig. 5: Measured pH versus dilution ratio for carbonated concrete sample from a 20-year-old sidewalk
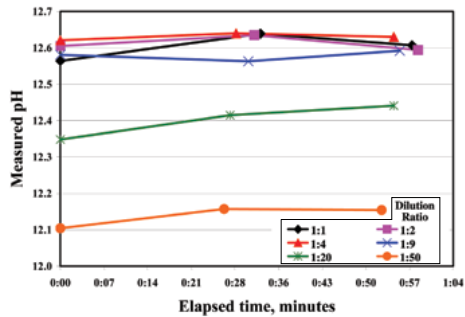

Fig. 6: Measured pH versus elapsed time for concrete with 0.4 *w/cm*

TABLE 3:
Effect of particle size on pH for a 5 g (0.18 oz) sample of concrete with a 0.4 *w/cm* using a 1:2 dilution ratio

Particle size	Distribution, %	Measured pH
Small, passing 850 µm (No. 20) sieve	59.6	12.48
Intermediate, passing 2.00 mm (No. 10) sieve and retained on 850 µm (No. 20) sieve	19.2	11.87
Large, retained on 2.00 mm (No. 10) sieve	21.2	11.55
Combined	100	12.37

Soaking period

The graph in Fig. 6 illustrates the short time (1 hour) effect of soaking time on pH as a function of dilution ratio for a concrete sample. The change in pH was insignificant (less than 0.15) for all dilution ratios.

Sample gradation

Tests were conducted using powdered samples obtained from concrete with a *w/cm* of 0.40 and no fly ash. The pH measurements were conducted on the portion of the sample that was retained on the 2.00 mm (No. 10) sieve (large particles), the portion passing the 2.00 mm (No. 10) sieve and retained on the 850 µm (No. 20) sieve (intermediate particles), and the portion passing the 850 µm (No. 20) sieve (small particles) using a dilution ratio of 1:2. The pH values for the large particle size portion and the small particle size portion were found to be 11.55 and 12.48, respectively. Although the difference in pH was nearly 0.93, the pH of the combined sample was 12.37, indicating that it's not necessary to obtain a sample passing through the 850 µm (No. 20) sieve. The particle size distribution of the sample and measured pH values are shown in Table 3.

Temperature

Raising the temperature of a saturated solution of calcium hydroxide from 0 to 60 °C (32 to 140 °F) has been reported to decrease measured pH from 13.423 to 11.449.[4] The graph in Fig. 7 shows the effect of temperature found in the test program over a narrow temperature range.

COMPARISON OF TEST METHODS

The pH of a concrete slab was measured using a pH pencil, a pH probe with digital meter, and pH strips using the procedure indicated in ASTM F 710. As shown in Table 4, the measured values varied between 10 and 12. Color change obtained using a pH pencil (Fig. 8) was difficult to judge, as it was confusing to distinguish between the color match for pH values of 10 and 13.

To measure the pH of the slab with a pH probe and meter, a 0.3 g (0.011 oz) sample of concrete powder was obtained by sanding the surface, and the sample was mixed with 6 mL (0.2 fl oz) of distilled water. The mixture was contained in a sealed ring on the concrete slab (Fig. 9). With this method, a pH of 11.5 was obtained for a dilution ratio of 1:20.

When the procedure described in ASTM F 710 was used on a clean concrete surface, a pH of 10 was measured (Fig. 10). To improve the accuracy of the ASTM F 710 procedure,

Figure C.8: pH of Concrete page 4

a powdered sample of the concrete was collected by sanding the surface of the slab. The measurement was then taken using a pH strip dipped into the mixture. This procedure resulted in a measured pH of 12 for the same concrete. Even though pH values of 10 and 12 appear to be close, it should be noted that a pH value of 10 could be considered carbonated concrete, while a pH of 12 could be considered non-carbonated concrete.

TABLE 4:
COMPARISON OF TEST METHODS TO MEASURE SURFACE PH OF A CONCRETE SLAB

Method	Measured pH
ASTM F 710	10
Proposed method	12
pH pencil	?*
pH probe and meter	11.5

*Color change obtained using a pH pencil was difficult to judge, as it was confusing to distinguish between the color match for pH values of 10 and 13.
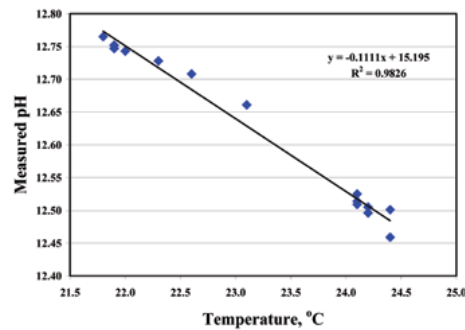

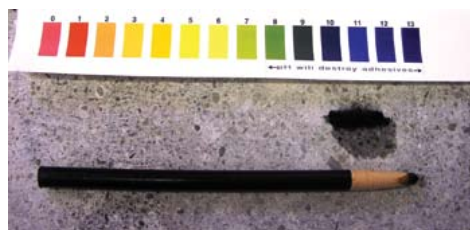Fig. 7: Measured pH versus temperature

Fig. 8: Measuring pH using a pH pencil. It's difficult to distinguish color differences for pH values from 10 to 13

In another field test, the pH of a slab that had been previously tested by others using the ASTM F 710 procedure was found to have a pH of 7. The same slab was found to have a pH of 9 when the slab was sanded to obtain a powdered sample before conducting the ASTM F 710 procedure.

DISCUSSION AND CONCLUSIONS

Based on the test results from this study, dilution ratio and temperature have the greatest effect on measured pH values. All other factors such as particle size, amount of sample, and soaking time have less influence on the measured pH value. The use of a dilution ratio of 1:2 seems practical to make the pH measurement.

The pH measured on a powdered concrete sample of a slab was significantly different than the pH measured using the ASTM F 710 procedure. This shows that placing a few drops of deionized water on an undisturbed concrete surface is not enough to form a solution containing concrete particles. It's therefore our opinion that the procedure

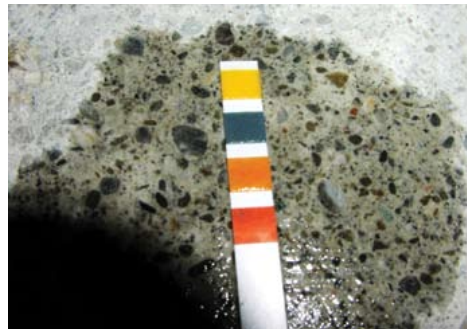Fig. 9: Measuring pH using a pH probe with a digital meter. Here, the pH is shown to be 11.53

Fig. 10: The pH of clean concrete surface is measured using a pH strip and the procedure provided in ASTM F 710. Here, the pH is shown to be 10

Figure C.9: pH of Concrete page 5

provided in ASTM F 710 doesn't provide a true indication of concrete pH, and the procedure should be modified.

The experience gained during our testing program also showed that it's not convenient to measure the pH of the concrete slab with a pH probe with a meter. The probe that we used needs at least 6 mL (0.2 fl oz) of solution to measure pH. At a dilution ratio of 1:2, this requires 3 g (0.11 oz) of powdered sample. Sanding a concrete surface to obtain this much powder is time-consuming and laborious. Therefore, we recommend that the probe and meter be used only in a laboratory with a larger concrete sample.

Because floor adhesive is only in contact with the surface of the concrete slab, flooring industry personnel are only interested in measuring the pH of the concrete surface. To achieve proper adhesion of resilient flooring, most manufacturers recommend abrasive cleaning or bead blasting of the slab to remove surface residue. Therefore, it makes sense to measure pH by sanding the surface of the slab. For carbonation and embedded steel corrosion-related issues, it's necessary to measure the pH of the concrete at various depths with more precision. Therefore, it's our opinion that two different procedures are needed: one for using pH strips to measure the pH of the concrete surface in the field, and one for using a pH probe to measure the pH at various depths within the concrete in the laboratory.

RECOMMENDED TEST PROCEDURES
Field test for pH measurement of a concrete surface
- Clean the surface using a wire brush. Be sure to remove dirt, concrete sealer, and old adhesive residue;
- Gather 0.5 g (0.018 oz) of concrete powder by hand sanding an approximately 50 x 50 mm (2 x 2 in.) area with 50-grit general-purpose sandpaper;
- Thoroughly mix the concrete powder with 10 to 12 drops of fresh distilled water with a small, flat plastic stirrer. Let stand for 60 seconds;
- Insert a pH strip into the mixture. Compare the strip to the color chart to determine the pH; and
- Note the temperature of the concrete surface.

Laboratory test for pH measurement of concrete
- Calibrate the pH probe and meter using the manufacturer's directions and appropriate buffer solutions;
- Collect 5 g (0.18 oz) of concrete powder at the required depth using a drill;
- Use a plastic stirrer to mix the concrete powder with 10 mL (0.34 fl oz) of fresh distilled water at a temperature of 22 ± 1 °C (72 ± 2 °F);
- Filter the mixture using No. 40 filter paper;
- Insert the pH probe into the mixture. Read the pH to one decimal place; and

- Note the temperature of the mixture.

Acknowledgments

References
1. ASTM F 710-05, "Standard Practice for Preparing Concrete Floors to Receive Resilient Flooring," ASTM International, West Conshohocken, PA, 2005, 6 pp.

2. ASTM C 25-06, "Standard Test Methods for Chemical Analysis of Limestone, Quicklime, and Hydrated Lime," ASTM International, West Conshohocken, PA, 2006, 36 pp.

3. Guideline No. 03740, "Guideline for Inorganic Repair Material Data Sheet Protocol," International Concrete Repair Institute, Des Plaines, IL, 2003, 10 pp. (Available at http://www.icri.org/committees/03740DataSheetProtocol_11082004_linenumberedDraft.pdf)

4. Bates, R.G., *Determination of pH—Theory and Practice*, 2nd Edition, John Wiley & Sons, New York, NY, 1973, 479 pp.

Jennifer A. Grubb performed the testing for this research in 2004 while an intern at Concrete Science, Inc., Hayward, CA, and is now an Engineer at Simpson Gumpertz & Heger, Inc., Boston, MA. She received her BS in civil engineering from Cornell University in 2003 and her ME in structural materials from the University of California at Berkeley in 2005.

ACI member **Hemant S. Limaye** is a Principal Engineer with Concrete Science, Inc. He is also a member of the American Society of Mechanical Engineers. His interests include nondestructive methods, sensors, instrumentation, and testing methodologies.

ACI member **Ashok M. Kakade** is a Principal Engineer with Concrete Science, Inc., where he is a professional engineer involved in the evaluation of and repair recommendations for concrete structures. He is also a member of ASTM International, the American Society of Civil Engineers, and the International Concrete Repair Institute.

Figure C.10: pH of Concrete page 6